REMOVAL OF SULFUR DIOXIDE FROM POWER PLANT STACKS BY A MODIFIED CLAUS PROCESS

R. T. Struck, M. D. Kulik, and Everett Gorin

CONSOLIDATION COAL COMPANY
Research Division
Library, Pennsylvania 15129

A large amount of research and development is being conducted both by government and industry to develop processes for removal of SO_2 from power plant stack gases. These efforts have been stimulated by the activity of the Federal Government in suggesting to local, state and interstate air pollution control agencies that stringent standards be set up on the maximum permissible ground level concentration of SO_2. The suggested criterion[1] calls, for example, for a maximum ground level concentration over a 24-hour period of 0.1 ppm of SO_2. It is difficult to relate this criterion to a maximum permissible level of SO_2 in a typical power plant stack since this depends on many factors such as stack height, presence of other pollution sources, metereological conditions, etc. However, in many instances this would require reduction of the SO_2 content in the stack to a level corresponding to the combustion of a fuel containing much less than 1% sulfur.

There is no doubt that wherever such stringent air quality standards may become legally required, power plant operators will be forced either to install SO_2-removal equipment or to switch to low-sulfur fuels (if such should be available).

The situation is of particular concern to the coal industry, since over 50% of its production is used for power generation and only a small fraction of the coal produced in the Eastern United States is low enough in sulfur to meet the stringent standards mentioned above.

The most feasible solution to the problem for a coal burning utility at the present time is the installation of SO_2-scrubbing facilities since removal of sulfur from the coal to the level required is a much more difficult task.

The first system for flue gas cleanup to undergo trial operation on a full commercial-scale is the combined limestone injection and wet scrubbing process offered by Combustion Engineering.[2] The above system does not produce any valuable by-products and incurs a cost debit for limestone purchase and spent calcium sulfate slurry disposal.

A number of developments is in progress aimed at reducing the net cost of SO_2 scrubbing by sale of by-products, usually either sulfuric acid or sulfur. Some processes are also aimed at the production of either $(NH_4)_2SO_4$ or liquid SO_2 as by-products, but these are not of general interest because of restricted markets.

The production of sulfuric acid has a somewhat broader market potential. Two processes are being offered for commercial use, i.e., Monsanto's[3] Cat-Ox process and Lurgi's Sulfacid process.[4] The high cost of shipping sulfuric acid to consuming points, however, also restricts the number of plants to which this approach is applicable.

The production of elemental sulfur on the other hand, considerably broadens the market potential due to its low cost of shipping relative to sulfuric acid. Considerable research and development is underway, therefore, directed at SO_2 scrubbing processes which yield elemental sulfur as a by-product. None of these, however, is as yet available for commercial use.

Most of these processes are based on the use of an "alkaline type" absorbent either in form of an aqueous[5] or molten carbonate[6] or an alkalized solid support such as alkalized alumina.[7] The absorption process is associated with unavoidable oxidation, if it is conducted at high temperatures, such that large amounts of alkali sulfate are generally formed. The regeneration system, in general, involves reduction of the alkali sulfate with CO and H_2 mixtures, and recovery of the sulfur as H_2S which is subsequently converted to sulfur in a conventional Claus plant.

This type of process requires more than 3 and as many as 4 mols of CO plus H_2 reductant per mol of sulfur recovered, as typified by the equation below describing the overall process,

$$SO_2 + 1/2\ O_2 + 4\ H_2 = 3\ H_2O + H_2S.$$

The most convenient way of generating the CO plus H_2 reductant is by way of steam-methane reforming. The thermal efficiency of such plants may be taken as equal to about 70%, based on natural gas feed. It is readily computed on the above basis that the natural gas requirement, where 4 mols of CO + H_2 reductant are required per mol of elemental sulfur recovered, amounts to 48 MM Btu/long ton of sulfur. Present prices for natural gas at most locations in north eastern United States, i.e., in the range of 35-45¢/MM Btu, are such that the reductant cost ($17-21/long ton of sulfur for a 4/1 mol ratio) places a very high economic burden on such a process even without considering the capital and other significant operating costs of the gas generation and reagent regeneration processes.

It is clear, therefore, that a very large incentive exists to reduce the reductant cost to the theoretical minimum of 2 mols/mol of sulfur recovered as typified by the overall reaction,

$$2\ H_2 + SO_2 = S + 2\ H_2O$$

or roughly half, as compared with the schemes discussed above.

One method that has been proposed which accomplishes this objective is to inject H_2S into the flue gas and reduce the SO_2 in situ, to produce sulfur by a Claus type process, i.e.,

$$2\ H_2S + SO_2 = 3\ S + 2\ H_2O.$$

Two thirds of the recovered sulfur are reduced to H_2S and reinjected into the flue gas. This process, in principle, then produces sulfur with a consumption of only 2 mols of reductant/mol of sulfur produced.

The conventional Claus process is usually operated with concentrated gases using an alumina catalyst at sufficiently high temperatures, usually 400-450°F, such that the sulfur vapor produced does not condense on the catalyst.

Thermodynamic limitations in the case of flue gas, however, preclude such a type of operation. This is illustrated by the equilibrium calculations for a typical flue gas to which 2 mols H_2S/mol SO_2 have been added as illustrated in Figure 1. These calculations were made utilizing the most modern available thermodynamic data.[8] Data are also shown, for an artificial case, where water is removed from the flue gas to illustrate the adverse effect of water vapor on the equilibrium.

It is seen from Figure 1 that efficient removal of SO_2 from flue gas by the modified Claus technique requires operation at temperatures well below those utilized in the standard Claus process. This is necessitated to a large degree, as shown in Figure 1, by the adverse effect of water vapor on the equilibrium. It should be remembered also, that because of the more noticeable odor of H_2S, the permissible level

of sulfur compounds in the stack should probably be held to a level well under that for SO_2 alone. Thus, operation at very low temperature, i.e., below about 240°F is indicated. Under these conditions, more than 98.5% of the sulfur produced will condense on the catalyst. It is clear, therefore, that either a cyclic or moving-burden process is required to periodically remove the deposited sulfur from the catalyst.

The first attempt to apply such a process to gas purification was made to coke oven gas by Audas.[9] In this case, the process was applied in reverse, i.e., SO_2 was added to the H_2S-containing gas, and the modified low temperature Claus process was conducted with condensation of the sulfur on the alumina catalyst and its subsequent regeneration.

Application of the concept to flue gas treating was proposed by Kerr[10] in a patent assigned to Peter Spence, Ltd. In both the Audas and Kerr processes, the sulfur-fouled catalyst is cycled through a thermal regeneration step where the sulfur is removed by distillation at about 900-950°F.

More recently, Princeton Research has undertaken work to develop this type of process[11] under the auspices of the National Air Pollution Control Administration. Little information is available, however, about the results of their work at this time.

The Consolidation Coal Company undertook evaluation of the "modified Claus Process" in its laboratories since it appears to be potentially one of the most attractive processes for treating flue gas. The work soon showed that the alumina catalyst was rapidly poisoned on cycling through the process, largely due to formation of aluminum sulfate.

A two-step regeneration process now under development is described herein which removes this poison and recovers 93% of the sulfur as elementary sulfur and 7% as ammonium sulfate. The tail gas from the process contains less than 50 ppm of H_2S and SO_2.

EXPERIMENTAL

The apparatus used is shown in Figure 2. A fixed bed of catalyst is supported on quartz chips in a heated tube through which the simulated stack gas flows. The gases are preheated by passage through Pyrex wool and quartz chips. A central thermocouple well with adjustable couple position is used to measure the bed temperature. The controlled temperature is taken as the hotest spot in the bed. Water is added to the incoming gases by bubbling one of the gas streams through a water bath held at the proper temperature. Under the conditions used here, elemental sulfur remains on the catalyst and the tail gases pass out through a soda lime trap before being metered. At regular intervals, part of the tail gas is diverted through an iodine scrubber to analyze for H_2S and SO_2. Catalyst bed depths of one and three inches were used, and a reactor pressure of 810 mm Hg absolute.

Thermal regeneration of the catalyst is carried out by passing nitrogen at 1 to 4 SCFH over the catalyst as it is heated above the boiling point of sulfur to distill off sulfur. The exit gases pass through a sulfur trap (dotted line on Figure 1) and then through the iodine scrubber to analyze for H_2S and SO_2 liberated during stripping. The analysis for H_2S and SO_2 is based on their reactions with iodine as was previously described by Doumani.[12]

Three different aluminas were used as catalysts in these tests. Catalyst A is a commercial dessicant alumina which contains 1.6% alkali and 2.0% silica. The others are purer, more expensive aluminas with properties given in Table I.

DISCUSSION OF RESULTS

Table II shows the results of short term tests at 300°F (149°C) feeding the stoichometric ratio: $H_2S/SO_2 = 2$. With neither oxygen or water vapor present, the reaction goes nearly to completion and reaches the thermodynamic equilibrium predicted by Figure 1. With added oxygen, results are nearly equivalent. The presence of both steam and oxygen gives much poorer results (last line, Table II). The thermodynamic equilibrium values of Figure 1 were not approached indicating that the presence of steam has an adverse effect on both the kinetics and equilibrium in the Claus reaction. Results of similar experiments to test the effect of oxygen and steam at higher temperatures, i.e., 360°F, can be seen in Figure 3. The right hand figure gives the results in the absence of oxygen, showing that at this temperature, the reaction, after an initial induction period, gives a tail gas having an even lower content of $H_2S + SO_2$ (900 ppm) than the predicted thermodynamic equilibrium value of 1100 ppm in Figure 1. The low initial SO_2 content of the tail gas is probably due to absorption of SO_2 on the catalyst. When free oxygen is present (as it always is in power plant stacks), the results shown in the left hand half of Figure 3 are obtained. Although the SO_2 concentration was erratic, the rapidly increasing level of H_2S shows how the catalyst became quickly poisoned. Following this test, an appreciable amount of sulfate was found on the catalyst. It is thus clear that undesirable oxidation of SO_2 is taking place.

The next tests were made at the lower temperatures of 212°F (100°C) in an attempt to minimize sulfate formation and to improve the completeness of the reaction. The first cycle of this test (Figure 4) showed surprisingly that the reaction was very fast at this low temperature and that nearly sulfur-free tail gas could be obtained at this temperature as predicted by the equilibrium curve of Figure 1. Some H_2S breakthrough occurred in the early part of the run and both gases broke through due to filling of pores with product sulfur after about 60 grams of sulfur had been fed per 100 grams of catalyst. During the early period when considerable H_2S breakthrough was observed, it is noted again that no SO_2 broke through. This again is likely due to adsorption of SO_2 by the alumina catalyst.[13] The adsorptive capacity of alumina for SO_2 is taken advantage of in the Audas[9] process previously cited. After this "breakout," the run was stopped and the catalyst heated to 950°F in a stream of nitrogen to remove sulfur. The simulated stack gas was then fed over the catalyst again and the process repeated through four cycles. Results from the last cycle (right half of Figure 4) show that the capacity to completely remove SO_2 had been reduced from 60 to less than 10 grams of sulfur fed per 100 grams of catalyst. This loss of capacity was found again to be due to formation of sulfate poisons even at the low temperature of 212°F. The origin of the sulfate is not wholly clear at the present time as it was found that some sulfate is formed at 212°F even when oxygen is excluded from the flue gas. This problem is being investigated further at this time.

Several attempts were made to remove sulfur from the catalyst by means of organic solvents, such as toluene and carbon disulfide, in order to avoid the thermal stripping. Other aqueous solvents, such as ammonium hydrosulfide solutions, with the potential of removing both sulfates and sulfur, also were tested. With all of these solvents the catalyst particles were disintegrated or weakened so that mechanical handling would be impossible.

The final regeneration process which was successful in maintaining activity consists of two stages: 1) heat the sulfur-laden catalyst to strip off sulfur, and 2) treat the stripped catalyst with aqueous ammonium hydroxide to remove sulfates and regenerate an active alumina surface.

The second stage was accomplished by dropping the cooled catalyst (after stripping) into about 50 times its weight of 2% NH_4OH at 75°F. After soaking 15 minutes, the catalyst was removed and rinsed four times with distilled water. After air drying, the catalyst was recharged to the reactor and heated to 400°F in nitrogen to remove ammonia.

Figure 5 shows the results of the first and fifth cycles using the new two-stage catalyst regeneration. Although results of the first cycle are erratic (the SO_2 breakthrough suggests that the feed ratio probably was not exactly at the stoichiometric ratio) it is clear that after five cycles there had been no deterioration. In addition, the initial break-in period with high H_2S values had been eliminated, so that right from the start there was no detectable H_2S or SO_2 until breakthrough at 24 grams of sulfur fed per 100 grams of catalyst. The uneven results thereafter represent attempts to explore the effects of changing the H_2S/SO_2 feed ratio slightly on both sides of 2.0.

No change in catalyst size or weight was detectable after five cycles. After stripping off sulfur, the cooled catalyst was tested for hardness in the Hardgrove Grindability Machine (A.S.T.M. Method D-409). The used catalyst was slightly stronger than fresh catalyst.

Figure 6 shows how the two-stage regeneration has eliminated the poisoning problem. The upper graph shows how the catalyst capacity dropped rapidly when only thermal removal of sulfur was used. The lower graph shows that capacity gradually increased through five cycles with the two-stage regeneration. This may be attributable to precipitation of fresh alumina in the ammonia wash. The overall lower capacity shown by the lower graph is a function of the catalyst used. The catalyst, H, has a pore volume of 0.77 versus 0.55 cc/g for catalyst A. It is also noteworthy that the percentage of sulfur in the products which was recovered as elemental sulfur also gradually increased from cycle to cycle: from 92.2 in Cycle 1 to 95.0 in Cycle 5.

Based on results of Cycle 5, the steady-state sulfur balance for the process would be as follows:

In (As Gases)	Percent of Sulfur Fed to Reactors	
SO_2 in Stack Gas	31.8	
SO_2 Recycled from Stripping	1.5	
H_2S Recycled from Stripping	1.5	
H_2S Made from S Produced	65.2	
	100.0	
Out (On Catalyst)		
Elemental Sulfur	95.0	
Sulfate	2.0	
H_2S	1.5	
SO_2	1.5	
	100.0	
Net Products		Percent of Sulfur Fed in Stack Gas
Elemental Sulfur	29.8	93.7
Sulfate	2.0	6.3
	31.8	100.0

It should be noted that the process also would handle the small amount of SO_3 present in stack gases, giving a slightly higher yield of sulfate.

The authors would like to express their appreciation to Consolidation Coal Company for permission to publish this work.

REFERENCES

(1) Chem. & Eng. News, 45, No. 15, p 20 (April 3, 1967).
Chem. Eng., 70, No. 4, p 38 (February 24, 1969).
(2) Miller, P. M. and Jonakin, J. - Electrical World, 169, No. 35 (March, 1968).
(3) Remirez, Raul - Chem. Eng., 76, No. 9, p 86 (April 21, 1969).
(4) Scheidel, C. F. - Preprint 6E of Paper Presented at 61st Annual Meeting AIChE, Los Angeles (December 1 - 5, 1968).
(5) Pollock, W. A., Tomany, J. P. and Frieling, Garry - Preprint of Paper Presented Before ASME Meeting, New York, N. Y. (November 27 - December 1, 1966).
Galeono, S. F. and Harding, C. I. - Jour. Air Pollution Control Assoc'n., 17, No. 8, p 536 (1937).
(6) Oldenkamp, R. A. - Paper Presented Before 65th Annual Meeting AIChE (May 5, 1969).
Heredy, L. A., McKenzie, D. E. and Yosim, S. J. - U.S. Patent 3,483,722 (May 15, 1967).
(7) Bienstock, D., Field, J. H., Katell, S. and Plants, K. D. - Jour. Air Pollution Control Assoc'n., 15, 459 (October, 1965).
(8) "Janaf Thermochemical Tables" - Dow Chemical Company, PB 168370 (August, 1968).
(9) Audas, F. G. - Coke and Gas, 13, p 229 (July, 1951).
(10) Kerr, John - Brit. Patent 1,097,306 (January 3, 1968).
(11) Chem. & Eng. News, 46, No. 39, p 22 (September 9, 1968).
(12) Doumani, T. F., Deery, R. F. and Bradley, W. E. - Ind. Eng. Chem., 36, 329 (1944).
(13) Munro, L. A. and Johnson, F. M. G. - Ind. Eng. Chem., 17, 99 (1925).

TABLE I

Catalyst Analyses

Catalyst Composition, ppm	A	C	H
Na	11,900(1)	5	180
Si	9,300(1)	< 100	560
Fe	840	40	280
Ca	--	37	9,100
Al	Balance	Balance	Balance
Surface Area m^2/g	390	200	218
Pore Volume, cc/g	0.55	0.42	0.77
Bulk Density, Lb/CF	54	--	32

(1) This corresponds to 2% SiO_2 and 1.6% Na_2O.

TABLE II

The Effect of Water and Oxygen on Reaction Efficiency

Conditions: Catalyst C VHSV = 4200
Temperature 300°F Bed Height = 1 Inch

Feed Gas Composition, Vol %				Tail Gas Composition, ppm	
SO_2	H_2S	O_2	H_2O	SO_2	H_2S
0.163	0.325	0	0	< 50	< 50
0.159	0.317	1.23	0	< 50	50
0.307	0.614	2.40	6.0	700	1400

Figure 1

EQUILIBRIUM CONCENTRATION IN TAIL GAS AND PERCENT OF SULFUR FORMED WHICH CONDENSES vs OPERATING TEMPERATURE

VOL.%	NORMAL -o- WET FEED	DRY FEED -Δ-
H_2S	0.6	0.6
SO_2	0.3	0.3
H_2O	6.0	0.0
OTHER	93.1	99.1

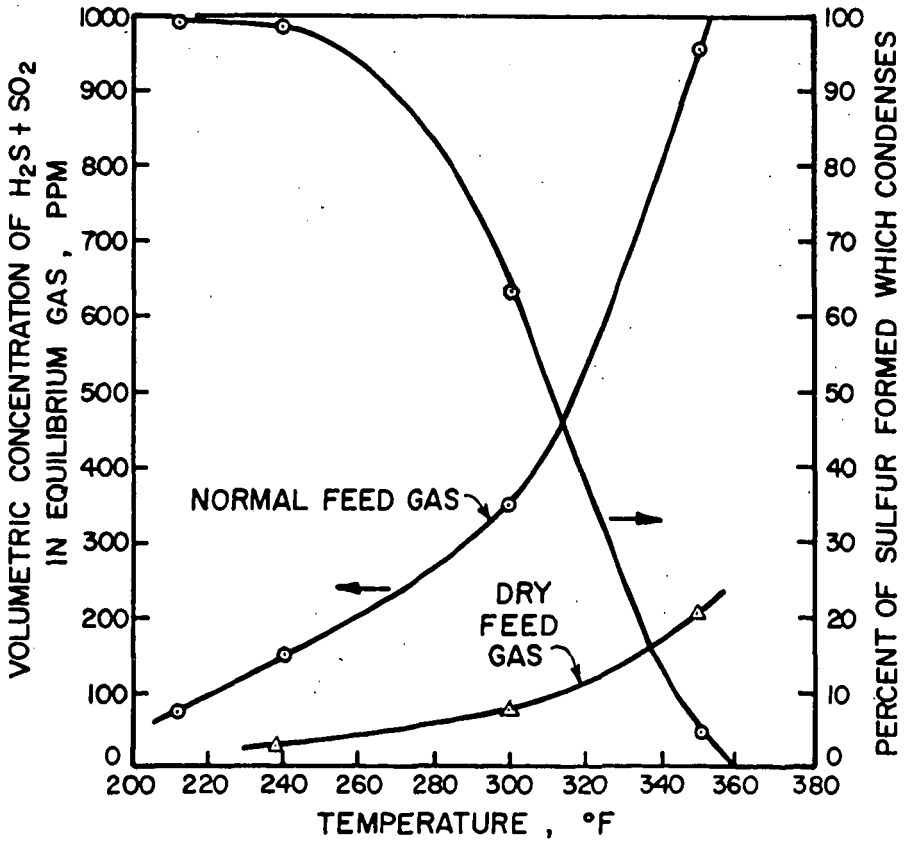

Figure 2

EXPERIMENTAL APPARATUS

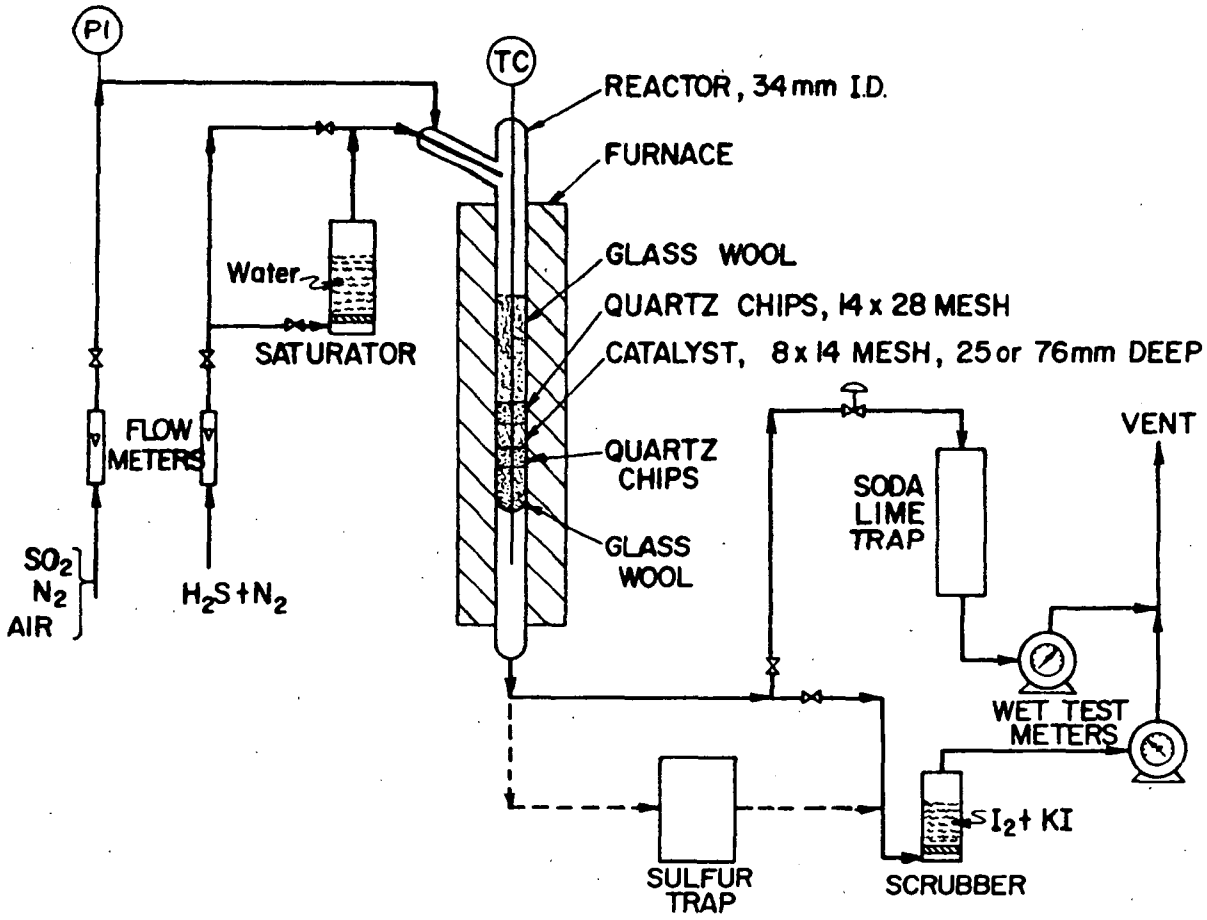

Figure 3

THE EFFECTS OF OXYGEN AT 360°F

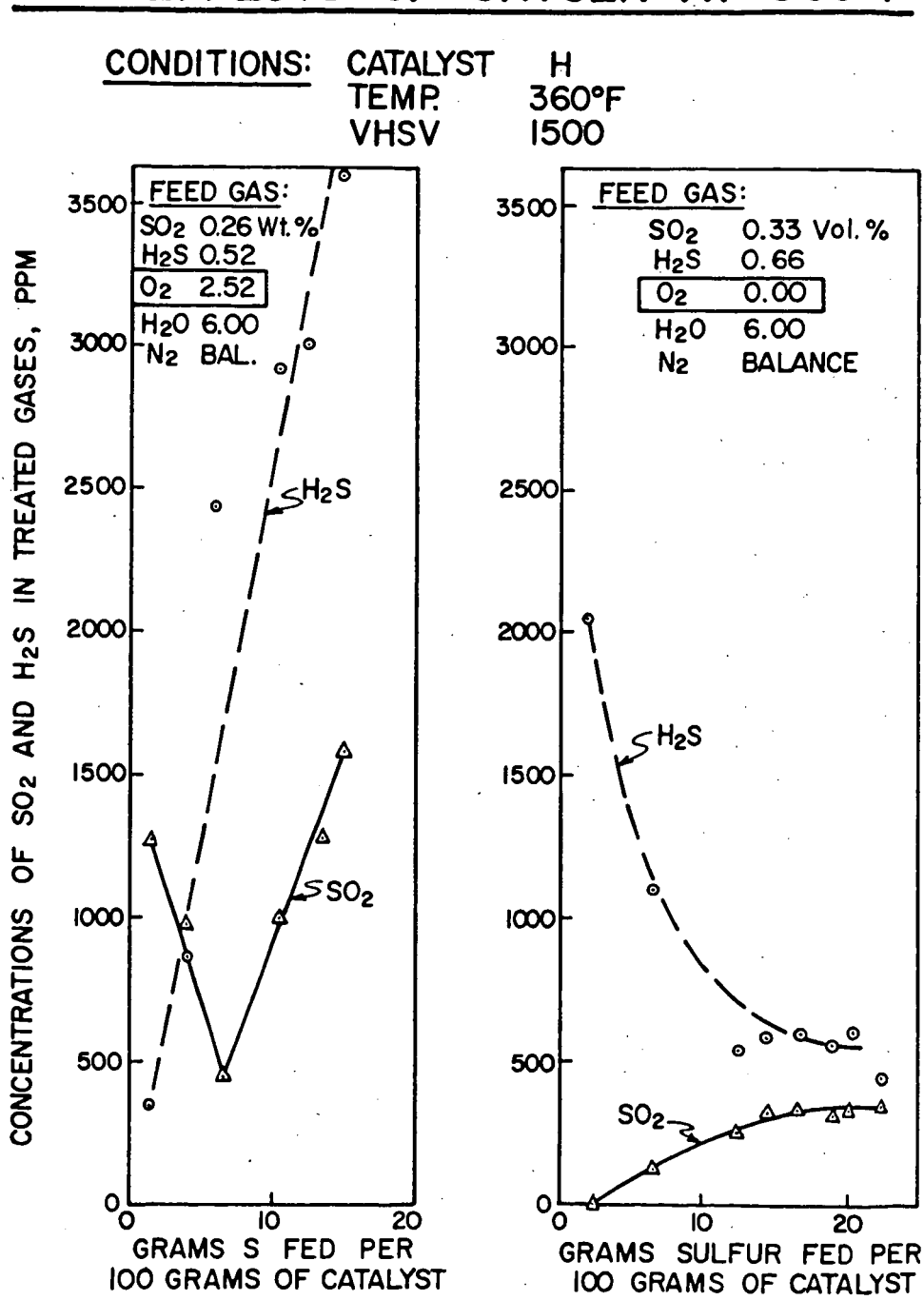

Figure 4

DECREASE IN CATALYST ACTIVITY USING SINGLE-STAGE THERMAL REGENERATION

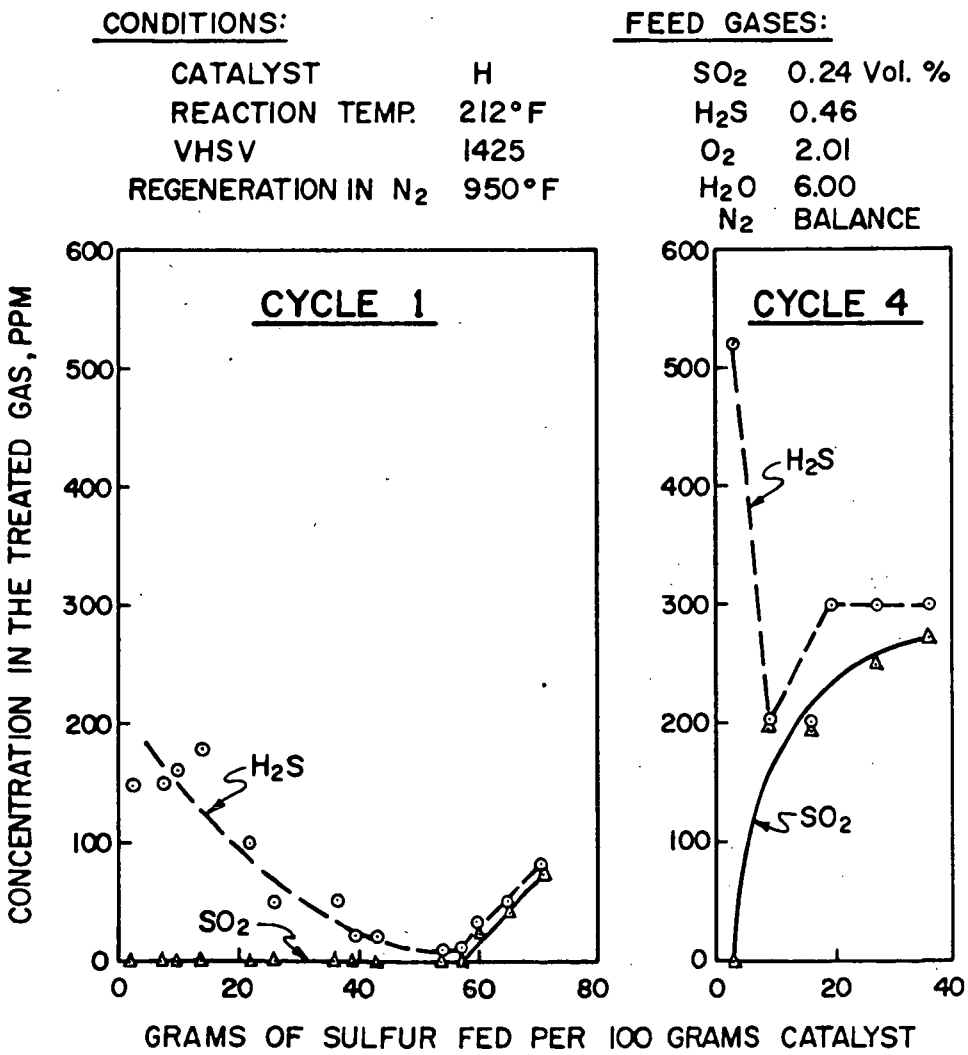

Figure 5

CATALYST ACTIVITY USING THE CONSOL TWO-STAGE REGENERATION

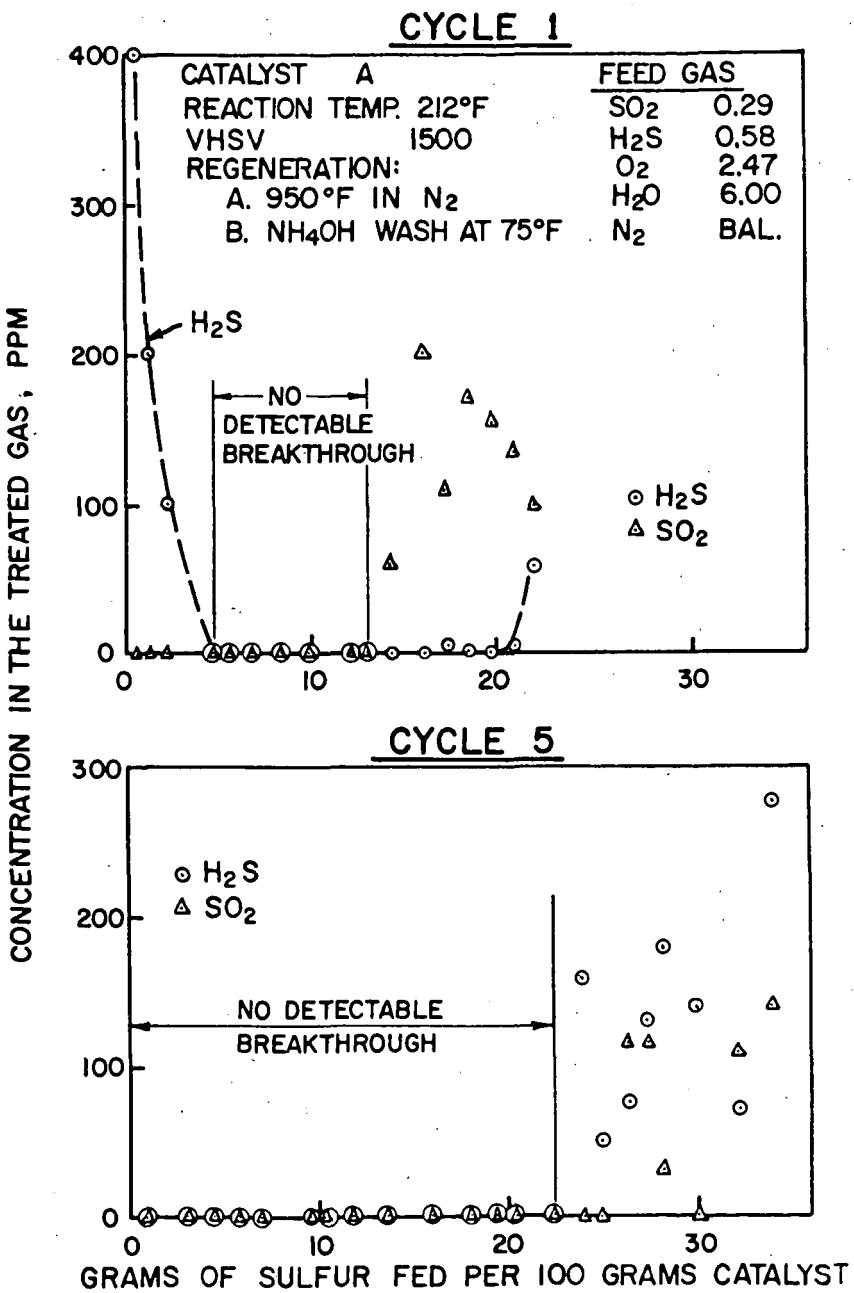

Figure 6

AMOUNT OF STACK GAS FED PRIOR TO SULFUR DIOXIDE BREAKTHROUGH

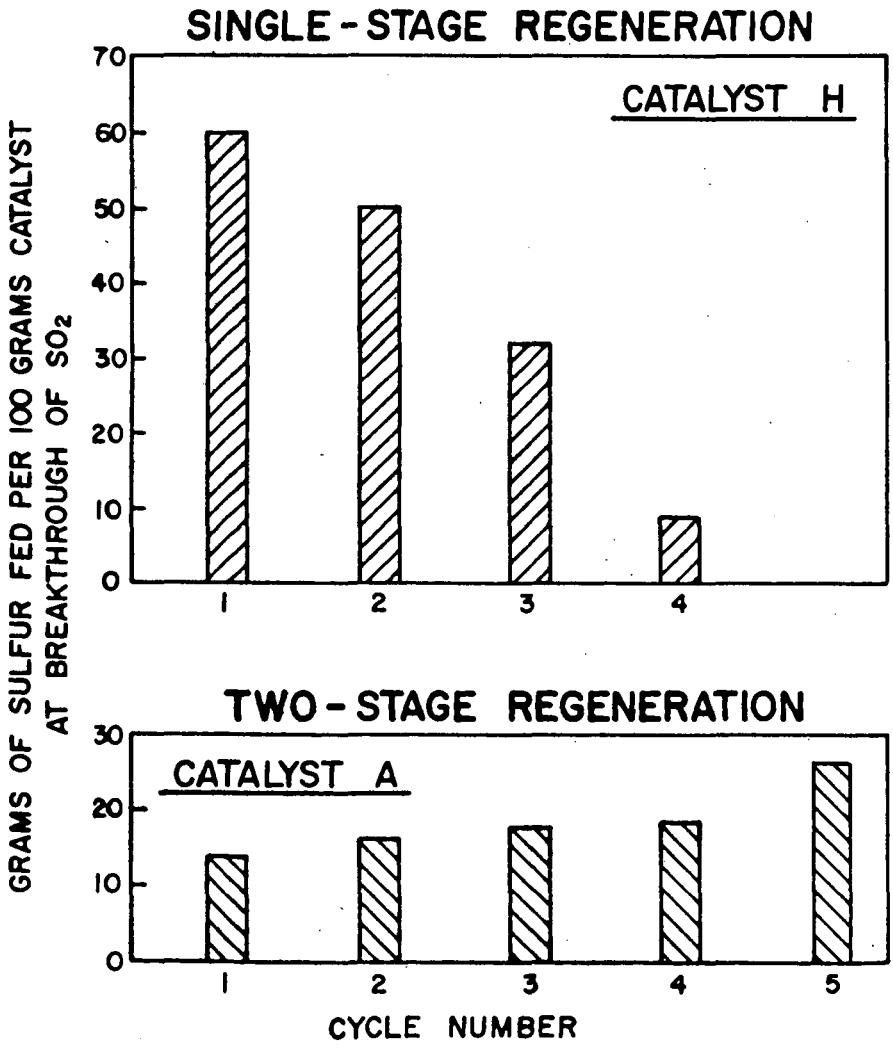

SULFUR REMOVAL DURING COMBUSTION OF SOLID FUELS IN A FLUIDIZED BED OF DOLOMITE

C. W. Zielke, H. E. Lebowitz, R. T. Struck, and E. Gorin

Research Division
Consolidation Coal Company
Library, Pennsylvania 15129

INTRODUCTION

The national concern over atmospheric pollution has led to extensive research and development on removal of sulfur oxide pollutants from flue gases. There has been considerable effort in this regard using limestone or dolomite to react with the sulfur oxides in dry, high-temperature processes. In these processes, SO_2 in the gases produced during combustion is fixed as $CaSO_4$ by reaction with CaO:

$$CaO + SO_2 + \tfrac{1}{2}O_2 = CaSO_4 \qquad (1)$$

Usually the raw stone (dolomite or limestone) is fed to the process and calcination immediately takes place by the following reaction:

$$CaCO_3 = CaO + CO_2 \qquad (2)$$

One method of operation has involved removal of sulfur oxides by direct injection of limestone dust above the burners of power plant boilers. A system such as this requires a minimum of new facilities and is readily adaptable to existing plants. However, the removal of sulfur in this case is carried out in a relatively inefficient and uncontrolled manner. Hence, utilization of limestone is poor and sulfur removal does not exceed 50 to 60%. An excellent article by the Tennessee Valley Authority reviews work done along this line.[1]

More efficient contact between gases and solid, as well as excellent temperature control, can be obtained by passing the combustion gases through a fluidized bed of lime or dolomite. The research reported here was aimed at the ultimate combination along this line: combustion of the fuel within a fluidized bed of lime or dolomite, which, in addition to pollution control, has great potential for reducing boiler size and cost by locating boiler tubes within the fluidized bed.[2,3,4,9]

EXPERIMENTAL

The experimental unit consists of a continuous fluidized combustor, four inches in diameter, with a fluidized bed depth of 36 inches. The bed is supported on a perforated plate above a plenum chamber through which fluidizing gas is fed. Figure 1 shows the arrangement of equipment for feeding and recovering products. The combustor fits within an electric furnace for startup, and thereafter, cooling is provided by an air flow between reactor and furnace. The cyclone to recover coal ash and dolomite fines is operated at 350°F, and the filter at 150 to 200°F. The dolomite overflowing the bed via the weir is substantially free of ash. Argon is used for purges to facilitate accurate analysis of off-gases. Operating pressure was 8 psig, the pressure required to force the gases through the recovery train and give adequate control. All runs were preceded by a line-out period at conditions involving at least 3 changes of bed inventory.

In addition to combustion studies under various conditions with once-through use of dolomite, the re-use of dolomite was explored using $6\frac{1}{2}$ cycles of alternate regeneration and SO_2-absorption.

The SO_2 absorption runs were conducted in a manner similar to the normal combustion runs except that SO_2 gas was added with the fluidizing air as a major source of sulfur; coal was burned to supply heat and supply a minor amount of sulfur. The purpose of adding SO_2 was to produce large amounts of highly sulfated dolomite in a relatively short time. The activity of the regenerated product was measured in these runs by determining the CaO-to-S mol feed ratio required to produce a 20% sulfur breakthrough in the exit gas. The required ratio was reached by adjusting the amount of feed SO_2; the dolomite residence time was held essentially constant in all cycles. When the desired Ca-to-S ratio was reached, conditions were maintained constant and the usual line-out and balance were made.

The regeneration portion of each cycle was conducted at 1950°F with CO as the reducing gas according to the overall reaction

$$CO + CaSO_4 = CaO + SO_2 + CO_2 \qquad (3)$$

No solid fuel was used in the regeneration runs. However, excess CO, over that required to carry out the reduction reaction, was burned with air to supply the heat. The gas flows were first established with nitrogen being substituted for the CO carrier gas. A bed of dolomite was established with the bed held at about 1400°F. Sufficient CO was then substituted in place of an equal amount of N_2 such that the bed was heated to 1925°F under a slightly oxidizing atmosphere. The remaining CO was then introduced, the used dolomite feed restarted and the unit lined out at 1950°F. Frequent analyses of the off-gas were made by gas chromatography to determine the CO/CO_2 ratio. Frequent analyses of the SO_2 content of the gas were made by determining the sulfate obtained in hydrogen peroxide scrubbers.

Feedstocks

The solid fuels tested in the combustor were Ireland Mine Coal, Disco Char, and Cresap Char. Analyses of these feeds are given in Table I. Ireland mine coal is a highly caking, high volatile, bituminous coal from the Pittsburgh seam. It is typical of the product sold to power stations. Both chars are from low temperature carbonization processes. The Disco char was produced in a rotary kiln from a Pittsburgh seam coal. The Cresap char was derived from Ireland mine coal. It was produced by fluidized low temperature carbonization of the residue remaining after solvent extraction of the coal in the "Project Gasoline" pilot plant operated by Consol for the U. S. Office of Coal Research at Cresap, West Virginia.

The dolomite used is from the Tymochtee formation in western Ohio. This stone was chosen because it had shown good physical strength and good resistance to chemical deactivation in CO_2 acceptor gasification studies.[6] Its analyses are given in Table II. The dolomite typically contained 0.05 to 0.10 weight percent moisture as it was fed to the unit.

RESULTS AND DISCUSSION

A. Runs Using Dolomite On a Once-Through Basis

Table III gives results using Disco char and Cresap char. Disco char was used in the initial runs because it is non-caking, thus precluding the possibility of operability problems due to coking. Cresap char was of interest because of its unusually high sulfur and ash content. Table IV gives results with Ireland coal. Superficial velocity is defined as the velocity of the air feed at process conditions based on the empty reactor. Superficial residence time is based on the superficial velocity and fluidized bed depth. Stoichiometric air is defined as that required to completely burn carbon to CO_2, hydrogen to water, and sulfur to SO_2.

1. Sulfur Removal

Runs 1 through 4 of Table III using Disco char explored the effect of temperature in the range of 1700-1900°F and the effect of residence times of one and two seconds. A large excess of acceptor was used in these runs (Ca/S mol feed ratio of 7.3 to 8.3) while holding the air input substantially constant at 120±5% of stoichiometric. Neither the temperature nor time variation had a significant effect on sulfur absorption which was nearly complete in all runs.

Runs 5 and 6 of Table III with Cresap char and Runs 7 through 10 of Table IV with Ireland coal explored the effect of Ca/S mol feed ratio at a constant temperature of 1800°F, one second gas residence time, and about 120% of stoichiometric air. Figure 2 shows the sulfur removal data for these runs plotted as a function of Ca/S mol feed ratio. Sulfur removal efficiency appears to be independent of the feed sulfur concentration which indicates the absorption reaction is first order with respect to SO_2 at a given Ca/S ratio. There is further evidence of this in the life study data which will be discussed later. Therefore, the data with Disco char were also plotted on Figure 2, although its sulfur content was lower than either the Cresap char or Ireland coal. It is apparent from Figure 2 that a desulfurization efficiency exceeding 90% can be achieved at Ca-to-S ratios of 2 or higher; at a Ca-to-S ratio of 1.0, sulfur removal efficiency was about 78%.

In general, these results with low Ca-to-S ratios (1.0 to 1.5) are superior to those reported in the literature by others for such a coarse dolomite (16 x 28 mesh). In scrubbing SO_2 from flue gases in a fluidized bed of dolomite at 1600°F, Skopp[4] found that a high CaO utilization of 75% or more required that the dolomite size be finer than 100 mesh; his results indicate CaO utilization of only 50% or less with 16 x 28 mesh material. Williams, of the National Coal Board of England, ground his limestone to -120 mesh before he got close to 100% sulfur removal at 1.5 Ca-to-S mol ratio. These results are some of the best reported.

Possible reasons for the superior results of this work would be the type of stone, the rapid, but controlled high temperature calcination, sufficient residence time, and good contacting of gas with the absorbent. The importance of good contact and good dispersion can be seen by comparing Run 7 of Table IV with Run 11. The baffle mounted above the feed port, shown in Figure 1, was employed in Run 11 but not in Run 7. With the baffle in place, 93.6% sulfur removal was achieved, but without it, only 66.5% sulfur removal was achieved.

Most workers blame the poor CaO utilization using coarse acceptor on an impervious shell of $CaSO_4$ which acts as a diffusion barrier preventing utilization of most of the CaO. Our results indicate that, under some conditions, the shell can be permeated reasonably well. For example, with 77% CaO utilization, penetration is at least 39% of the radius assuming spherical particles.

In all of this work, only the CaO fraction of the dolomite has been assumed to be active as a sulfur acceptor; the MgO has been assumed to have no ability for SO_2 removal because of equilibrium limitations.

2. Carbon Burnout

Carbon burnout efficiency at 1800°F with one second residence time using coal feed was 97%, as the data of Table IV show. The chars were somewhat less reactive, as would be expected. At conditions similar to the coal runs, Cresap char burnout was 93-94% (Runs 5 and 6 of Table III) and Disco char burnout was 94% (Run 3 of Table III). Increasing the temperature from 1800 to 1900°F, or increasing the residence time from one to two seconds at 1800°F, raised the burnout of Disco char from 94 to 98 or 97%, respectively.

3. Dolomite Fines Formation

A substantial amount of the feed dolomite is degraded to fines under some conditions. These fines are elutriated from the bed along with the large majority of the ash and unburned carbon. Figure 3 shows the rate of fines formation as a function of the Ca-to-S ratio in the bed. The ordinate of Figure 3 is defined as follows:

$$\text{Attrition Rate \%/hr} = \frac{\text{lbs(Ca + Mg) in Overhead Fines from Dolomite x 100}}{\text{lbs(Ca + Mg) in Dolomite Feed x Dolomite Res. Time in hrs.}}$$

It is apparent that the highly sulfated dolomite is much more resistant to size degradation than the lightly sulfated dolomite. At low Ca-to-S ratios, the rate of degradation is very low, that is, about 0.5% per hour. The rate of fines formation is also much higher using coal feed than with char feed for some unknown reason. Perhaps the higher reactivity of the coal causes greater thermal stresses in the particles.

4. Nitrogen Oxides in the Gases

The nitrogen oxides content of the gases vary considerably from run to run, i.e., 60 to 340 ppm. There is no apparent pattern to the variation. Perhaps this is due to variation in the rate of quenching of the off-gases which was not carefully controlled.

B. Dolomite Life Study

Potentially, the amount of new acceptor required per ton of coal can be reduced substantially by regenerating the acceptor and recycling the used acceptor back to the combustion process. One advantage of combustion in a bed of coarse acceptor is that the ash and fines are separated naturally by elutriation during combustion leaving substantially pure acceptor for regeneration treatment. To help assess the possibilities of regeneration, a series of cyclical combustion-regeneration runs was made. Results of the combustion runs with sulfur absorption are given in Table V; results of the regeneration runs are given in Table VI.

1. Regeneration

Regeneration comprises converting the $CaSO_4$ in the acceptor to CaO. In the present work, this was done using CO as the reducing gas at 1950°F. It is first of all necessary to reduce a portion of the $CaSO_4$ to CaS by the reaction

$$1/4\ CaSO_4 + CO = 1/4\ CaS + CO_2 \qquad (4)$$

The ratio of CO_2 to CO in the exit gas needs to be near that which corresponds to equilibrium for the above reaction so as to provide for the co-existence of $CaSO_4$ and CaS. The concentration of SO_2 in the off-gas from regeneration in cycle 1 was about 23 times greater than that in a flue gas from burning a 4% sulfur fuel, making its recovery much easier. Sulfur rejection then occurs by the reaction

$$1/4\ CaS + 3/4\ CaSO_4 = CaO + SO_2 \qquad (5)$$

The overall reaction can be represented by the equation

$$CaSO_4 + CO = CaO + CO_2 + SO_2 \qquad (6)$$

$$\Delta H = +59.2\ \text{Kcal/mol}$$

Since the overall reaction is endothermic, excess CO over that required to carry out the reduction of $CaSO_4$ was burned to provide the heat to conduct the regeneration at

1950°F. At 1950°F and 1.5 atmospheric pressure, the equilibrium concentration of SO_2 in the gas is 12 mol %. This provided adequate driving force since the maximum concentration of SO_2 in the gases produced was 7.10%.

It was found that best results were obtained with the effluent gas slightly richer in CO than the equilibrium CO_2-to-CO ratio of 46, i.e., 23 to 30. Higher or lower ratios gave lower sulfur rejection. When the appropriate CO_2/CO ratio was established, rejection of 93% or more of the sulfur was achieved. In Runs 3 and 4, an erroneously low CO concentration was used and sulfur rejection was poorer.

A small amount of COS is produced as shown in the gas analyses. The concentration corresponds roughly to that at equilibrium for the reaction

$$CaS + CO_2 = CaO + COS \qquad (7)$$

$$Kp = \frac{(COS)}{(CO_2)} = .00037 \text{ at } 1950°F^{(6)}$$

In principle, the regeneration could be carried out in a similar fashion in a single stage by burning coal or char with a deficiency of air according to the overall equation

$$CaSO_4 + C + \tfrac{1}{2}O_2 = CaO + SO_2 + CO_2 \qquad (8)$$

Fusion of ash, of course, may be a problem if the reaction is to be carried out at 1900°F or more since the ash fusion temperature is lowered under the reducing conditions necessary to carry out the sulfur rejection.

2. Sulfation

The results of the sulfation (SO_2 absorption) runs are given in Table V. These runs were conducted in much the same way as the once-through combustion runs except that SO_2 gas was added in order to rapidly produce large amounts of treated dolomite for the cyclical life study. The SO_2 content of the gas was adjusted to give 20% breakthrough of sulfur in the gas, i.e., 80% absorption. The Ca/S ratio obtained then was the measure of dolomite activity. It is apparent from the results that ~80% absorption was obtained in all cycles. In cycle 1, with fresh dolomite, a 0.95 Ca/S mol feed ratio gave 79% sulfur absorption. This point falls approximately on the curve of Figure 2, again showing that the absorption reaction is first order.

The acceptor activity as listed is based only on the CaO in the feed and not the $CaSO_4$ since, in cycles 3 and 4, regeneration wasn't as complete as desired.

3. Dolomite Life

The activity, a, of the dolomite sulfur-acceptor from cycle to cycle was measured as the fraction of available calcium which would absorb sulfur while maintaining 20% breakthrough of SO_2. This is calculated from the spent acceptor analysis on a mol basis: $CaSO_4/(CaO + CaSO_4)$. Figure 4 shows how the capacity (activity) of the dolomite decreased with the number of cycles, n, of absorption and regeneration.

Using the composite activity for a perfectly-mixed bed as described by Curran,[6] the effect of recycling dolomite has been calculated as a function of the rate of recirculation. Figure 5 shows this relationship. The ordinate of Figure 5 is the ratio of the pounds of fresh dolomite feed in the once-through process to that in the regenerative process, with the amount and efficiency of sulfur dioxide pick-up held constant. By going to high recirculation rates of regenerated acceptor, the makeup rate of fresh acceptor can be kept quite low.

Fresh dolomite makeup rate is usually controlled by activity loss since decrepitation loss is generally small. Total loss as fines overhead in 6½ cycles was 9.43% or about 1.5% per cycle. The average rate of decrepitation was 0.39%/hr during regeneration and 0.67%/hr during combustion. Discarding the attrition results from cycles 3 and 4, which look erroneously high, the rate during combustion was 0.42%/hr. Thus, it is apparent that makeup requirements due to attrition are probably not more than 1%/cycle.

COMMERCIAL IMPLICATIONS

The results of this work suggest two basic processes: 1) a process where dolomite is used on a once-through basis and discarded, or 2) a process in which the dolomite is regenerated and reused. The first process would require at least 0.25 ton of dolomite/ton of coal feed of 4% S. The second process could require 0.05 ton or less of dolomite per ton of coal feed. The cost of regeneration could be partially offset by recovering elementary sulfur from the sulfur-rich regeneration off-gas. If a relatively pure limestone could be found that has the same activity as the dolomite, the stone requirements could be cut substantially because of the greater CaO content in a limestone as compared with a dolomite.

REFERENCES

(1) "Sulfur Oxide Removal from Power Plant Stack Gas", PB-178972, Tennessee Valley Authority, 1968.

(2) Bishop, J.W., Robinson, E.B., Ehrlich, Shelton, Jain, A.K., Chen, P.M., "Status of the Direct Contact Heat Transferring Fluidized Bed Boiler", ASME Publication 68-WA/FU-4, 1968.

(3) Moss, G., Paper presented at the "First International Conference on Fluidized Bed Combustion" at Hueston Woods State Park, Oxford, Ohio, Nov. 18-22, 1968.

(4) Skopp, A.P., Work published in the "Proceedings of the First International Conference on Fluidized Bed Combustion" at Hueston Woods State Park, Oxford, Ohio, Nov. 18-22, 1968.

(5) Kruel, M., and Juntgen, H., Chemie-Ingenieur-Technik 39, No. 9/10, 607, 1967.

(6) Curran, G.P., Fink, C.E., and Gorin, E., Fuel Gasification, Advances in Chemistry Series, 69, 141, 1967.

(7) Barney, J.C. and Bertolacini, Anal. Chem., 29, 283, 1957.

(8) Standard Methods for the Examination of Water and Waste Water; American Public Health Association, Inc., 11th ed. 175, 1960.

(9) Williams, D.F., Work published in the "Proceedings of the First International Conference on Fluidized Combustion" at Hueston Woods State Park, Oxford, Ohio, Nov. 18-22, 1968.

(10) Zawadski, J., Ztschr. Anorg. Chem., 205, 180, 1932.

(11) Marchal, G., Compt. rend., 175, 270, 1922.

TABLE I

ANALYSES OF CHAR AND COAL FEEDS

	Disco Char	Cresap Char	Ireland Coal
Moisture, Wt.%	3.65	1.15	1.30
Proximate Analysis, Dry Basis, Wt.%			
Volatile Matter	20.77	14.34	39.84
Fixed Carbon	66.24	60.99	52.60
Ash (Ex. mineral sulfur)	12.99	24.67	12.67
Elemental Analysis, Dry Basis, Wt.%			
H	3.28	1.65	4.81
C	70.81	63.08	69.25
N	1.42	1.55	1.37
O (Diff.)	10.53	4.60	8.94
S	1.72	6.20	4.15
Btu/lb MF Fuel, Net	11845	10350	12840
Ash Fusion Temp., °F (Oxid. Atm.)			
Initial Deformation	2040	1920	1950
Softening	2120	2020	2020
Hemispheric	2270	2200	2140
Fluid	2360	2360	2320
Screen Size, Tyler Mesh	28 x 150	28 x 200	28 x 150

TABLE II

ANALYSIS OF TYMOCHTEE FEED DOLOMITE

	Weight, %
CaO	27.93
MgO	18.56
Fe_2O_3	.41
SiO_2	1.40
Al_2O_3	1.64
CO_2	44.87
Unaccounted for	5.19

SCREEN ANALYSIS, TYLER MESH

On 14	0
16	1.0
20	39.1
24	33.9
28	24.7
35	1.2
-35	0.1

Raw dry stone/fully calcined stone, wt. ratio = 1.814

Ca/Mg, mol ratio - 1.08

TABLE III

RESULTS WITH CHAR FEEDSTOCKS
AND ONCE-THROUGH DOLOMITE

Acceptor: 16 x 28 mesh raw Tymochtee dolomite
Inlet Gas: 100% air
Pressure 8 psig.

Run No.	1	2	3	4	5	6
Fuel	←Disco Char→				←Cresap Char→	
Bed Temperature, °F	1700	1800	1800	1900	1800	1800
Ca/S mol feed ratio	7.3	7.9	8.3	8.0	4.2	2.0
Superficial velocity, fps	1.5	1.5	←	3.0	→	
Stoichiometric air, %	116	118	120	121	125	118
Fuel feed rate, lb/hr	1.27	1.19	2.34	2.23	2.46	2.62
Raw dolomite feed rate, lb/hr	1.00	1.01	2.09	1.90	4.05	1.99
Run length, hr.	30	28	32	29	38	33
Gas residence time, sec.	2.0	2.0	←	1.0	→	
Results						
Feed sulfur removed, %	100.0	97.9	98.2	99.0	94.5	90.7
Sulfur in effluent acceptor, Wt.%	3.12	2.70	2.51	3.39	5.27	9.40
Carbon burnout, %	95.8	98.3	94.4	97.1	93.8	93.2
Lb. dust overhead/lb. fuel fed	0.165	0.159	0.284	0.267	0.304	0.278
Dolomite overhead as dust, %	7.3	9.4	23.6	24.5	3.8	1.8
Dry Exit Gas, Mol %						
CO_2	16.3	16.8	19.2	20.6	16.5	16.1
CO	0.00	0.00	0.00	0.00	0.01	0.01
O_2	4.1	3.7	5.0	4.1	5.2	4.7
N_2 + A	79.6	79.5	75.8	75.3	78.3	79.1
SO_2	0.0000	0.0031	0.0026	0.0015	0.0290	0.0536
NO_x	0.024	0.027	0.013	0.027	0.0060	0.0103

TABLE IV

RESULTS WITH COAL FEEDSTOCKS AND ONCE-THROUGH DOLOMITE

Acceptor:	16 x 28 mesh raw Tymochtee dolomite
Inlet Gas	100% air
Pressure, psig	8.0
Superficial velocity, fps	3.0
Temperature, °F	1800
Superficial gas residence time, sec.	1.0

Run No.	7	8	9	10	11
Ca/S, mol feed ratio	4.03	1.89	1.45	.95	3.68
Stoichiometric air, %	122	115	119	120	120
Coal feed rate, lb/hr	2.15	2.27	2.20	2.18	2.19
Raw dolomite feed rate, lb/hr	2.25	.94	.70	.46	2.09
Run length, hr	36	53	85	113	38
Results					
Feed sulfur removed, %	93.6	88.5	87.0	74.1	66.5
Sulfur in effluent acceptor, wt.%	5.00	8.62	10.93	12.59	2.99
Carbon burnout, %	97.5	96.7	96.9	97.1	97.5
Lb total dust overhead/lb feed coal	.254	.162	.157	.136	.258
Dolomite overhead as dust, %	20.9	21.6	14.7	11.4	17.6
Dry Exit Gas, Mol %					
CO_2	15.5	14.8	13.9	14.2	14.8
CO	.02	.01	.00	.00	.08
O_2	4.3	4.0	4.7	4.6	4.3
N_2 + A	80.2	81.2	81.4	81.1	80.7
SO_2	.0205	.0334	.0370	.0726	.110
NO_x	.0116	.0044	.0152	.0090	.034

TABLE V

CONDITIONS AND RESULTS
OF COMBUSTION RUNS WITH SO_2 ABSORPTION
IN DOLOMITE LIFE STUDY

Bed temperature, °F	1800
Pressure, psig	8
Fuel	-28 mesh Ireland coal
Fuel feed rate, lb/hr	1.79
Dolomite feed	To first cycle: raw, 16 x 28 mesh To succeeding cycles: regenerated material from previous cycle
Superficial inlet gas velocity, fps	3.0
Superficial gas residence time, sec.	1.0
Nominal percent of stoichiometric air	120

Cycle Number	1	2	3	4	5	6	7
Dolomite feed rate, lb/hr	10.2	5.8	5.7	6.0	6.0	5.7	5.6
Dolomite residence time, hr	1.09	1.15	1.14	1.11	1.25	1.21	1.11
Inlet gas composition							
Air, SCFH				3.34			
SO_2, lb/hr	3.29	2.19	1.56	1.56	1.24	1.26	1.08
CaO/S mol feed ratio	.953	1.38	1.86	1.86	2.25	2.27	2.62
Results							
Feed S absorbed, %	79.3	80.4	80.2	78.7	77.6	79.3	80.6
S in effluent acceptor, Wt.%	14.27	11.41	9.02	9.70	8.43	7.64	7.13
Carbon burnout, %	97.1	97.5	96.4	97.1	96.4	96.4	97.0
Acceptor activity, $CaSO_4/(CaO+ CaSO_4)$	.770	.540	.382	.400	.306	.313	.284
Feed dolomite overhead as dust, %	1.02	.71	1.50	1.42	.25	.25	.21
Dry Exit Gas, Mol%							
CO_2	18.4	12.6	12.7	12.5	12.2	12.3	13.1
CO	0.40	.16	.29	.35	.10	.14	.18
O_2	4.4	5.0	5.6	5.7	5.9	5.8	5.2
N_2 + A	75.7	81.2	81.1	80.9	81.2	81.2	81.1
SO_2	1.21	.89	.66	.70	.61	.57	.44
Balance Closures							
Mass	96.7	97.2	97.2	96.6	97.2	96.6	98.4
S	95.5	94.3	92.0	91.1	93.3	95.6	96.2
CaO	109.0	100.0	102.5	103.2	116.6	104.7	109.5

TABLE VI

CONDITIONS AND RESULTS OF REGENERATION RUNS IN DOLOMITE LIFE STUDY

Bed temperature, °F	1950
Pressure, psig	8
Superficial inlet gas velocity, fps	2
Superficial gas residence time, sec.	1.5

Cycle Number	1	2	3	4	5	6
Spent dolomite feed rate, lb/hr	8.82	8.20	7.23	6.83	6.98	7.12
Dolomite bed residence time, hr	1.62	1.70	1.78	1.79	1.83	1.78
Inlet gas composition, mol %						
Air	44.6	44.6	44.2	44.2	44.2	44.2
Added N_2	30.3	31.6	34.3	35.2	34.0	33.9
CO	25.1	23.8	21.5	20.6	21.8	21.9
Excess CO after combustion, mol ratio						
Feed S	.98	.94	.75	.58	.97	1.08
Results						
Fraction of $CaSO_4$ converted to CaO	.966	.932	.816	.695	.932	.940
Sulfate S in effluent acceptor, Wt.%	.95	.68	2.28	3.53	.56	.51
Sulfide S in effluent acceptor, Wt.%	.03	.40	.00	.00	.20	.07
Feed dolomite overhead as dust, Wt.%	1.86	.75	.33	.25	.38	.50
Dry Exit Gas, Mol %						
CO_2	23.4	22.2	20.5	19.9	20.9	21.0
CO	.78	.78	.56	.50	.91	.90
O_2	.09	.13	.15	.42	.27	.33
N_2 + A	68.6	71.6	75.0	76.4	74.3	74.7
SO_2	7.10	5.12	3.78	2.84	3.53	3.03
COS	.02	.03	.01	.01	.03	.03
Balance Closures, (Out)(100)/In						
Mass	98.1	98.8	99.9	100.1	96.3	101.2
S	104.4	97.5	108.9	105.3	102.2	98.5
CaO	97.6	91.6	100.2	95.0	95.3	99.0

FIGURE 1

SIMPLIFIED FLOW DIAGRAM OF CONTINUOUS FLUIDIZED COMBUSTOR

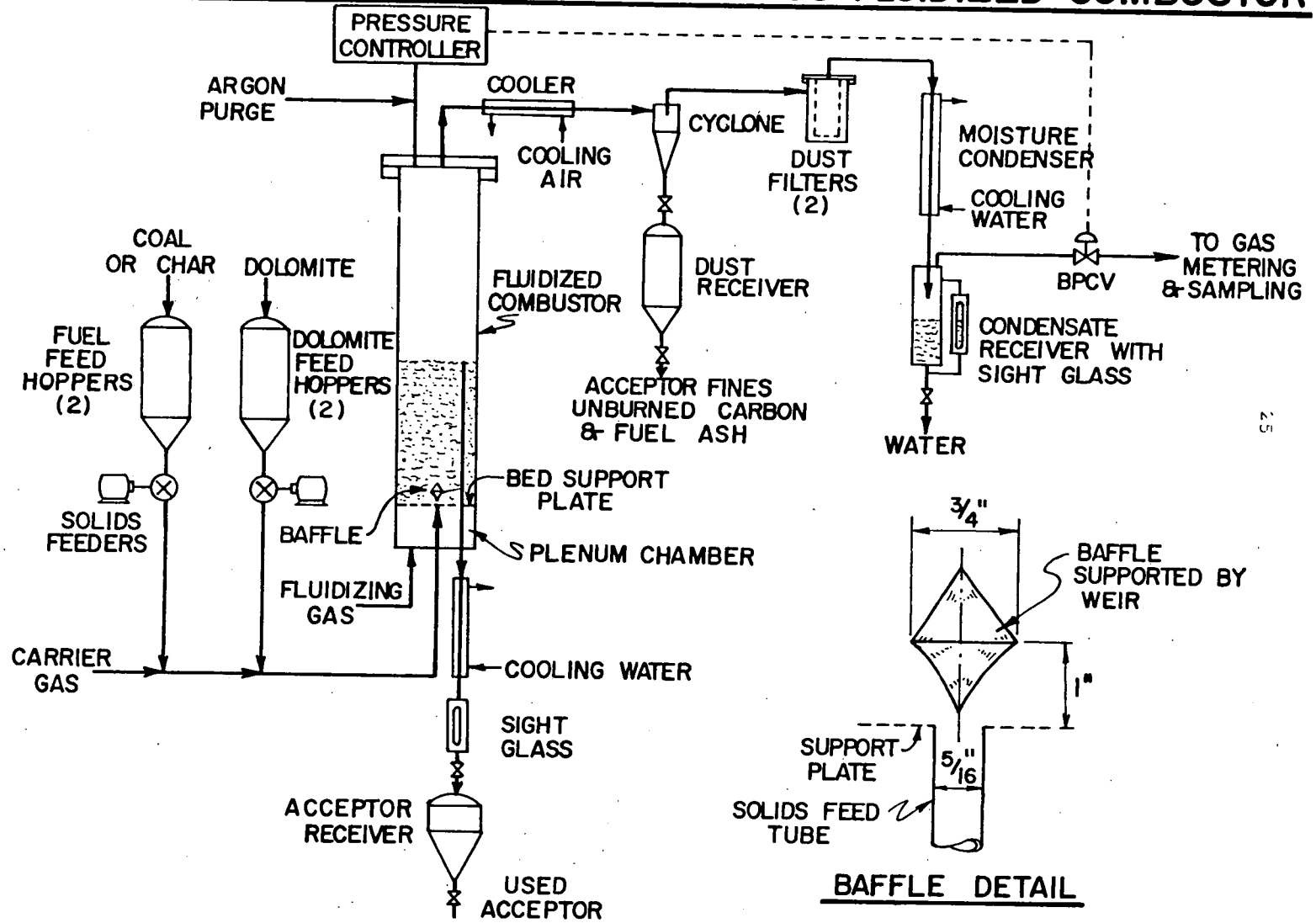

FIGURE 2

SULFUR REMOVAL EFFICIENCY vs Ca/S MOL FEED RATIO

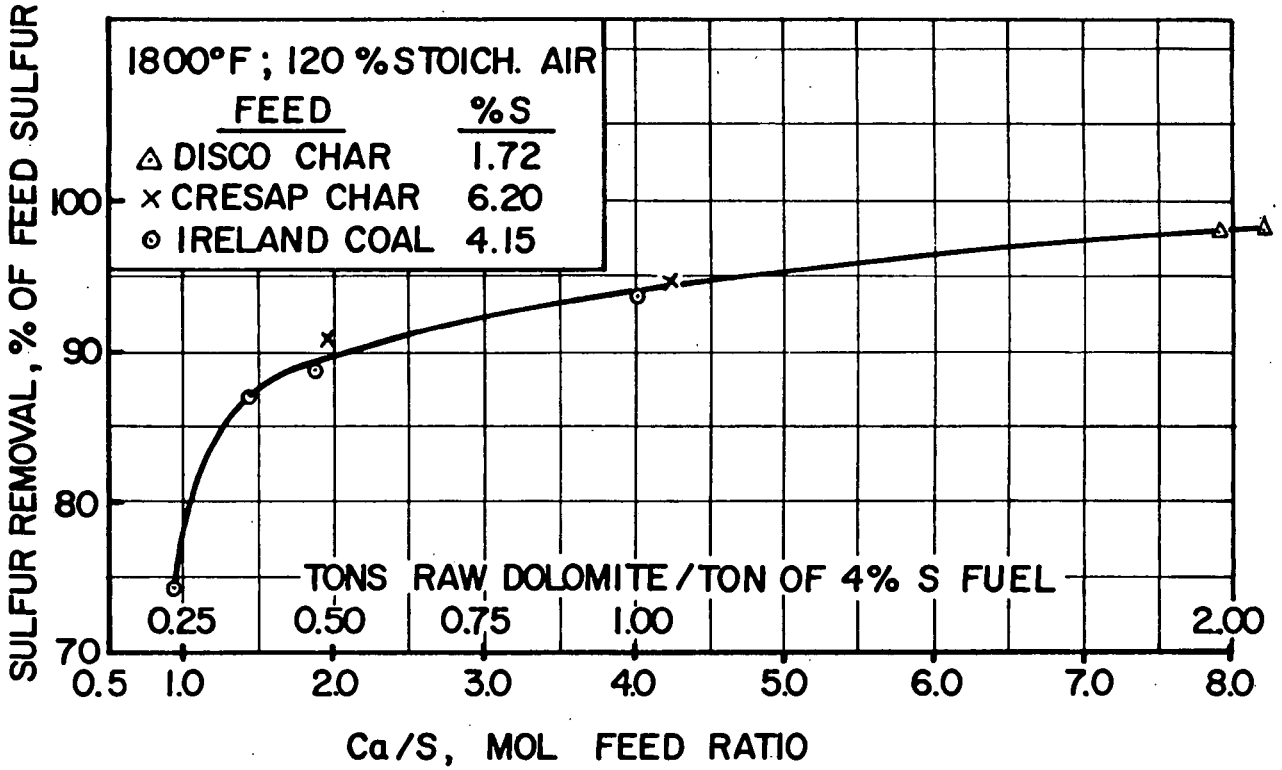

FIGURE 3

DOLOMITE ATTRITION RATE vs SULFUR CONTENT OF EFFLUENT ACCEPTOR

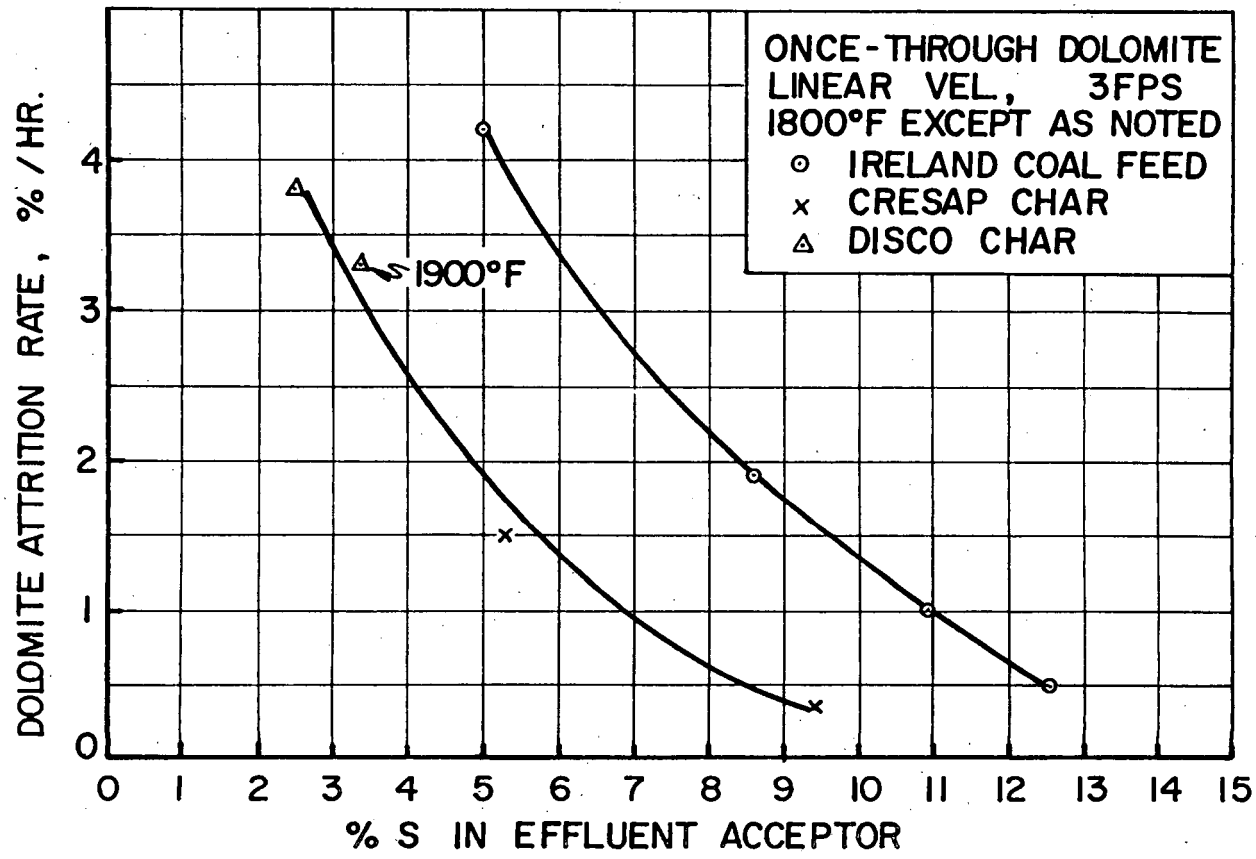

FIGURE 4

ACTIVITY OF REGENERATED ACCEPTOR

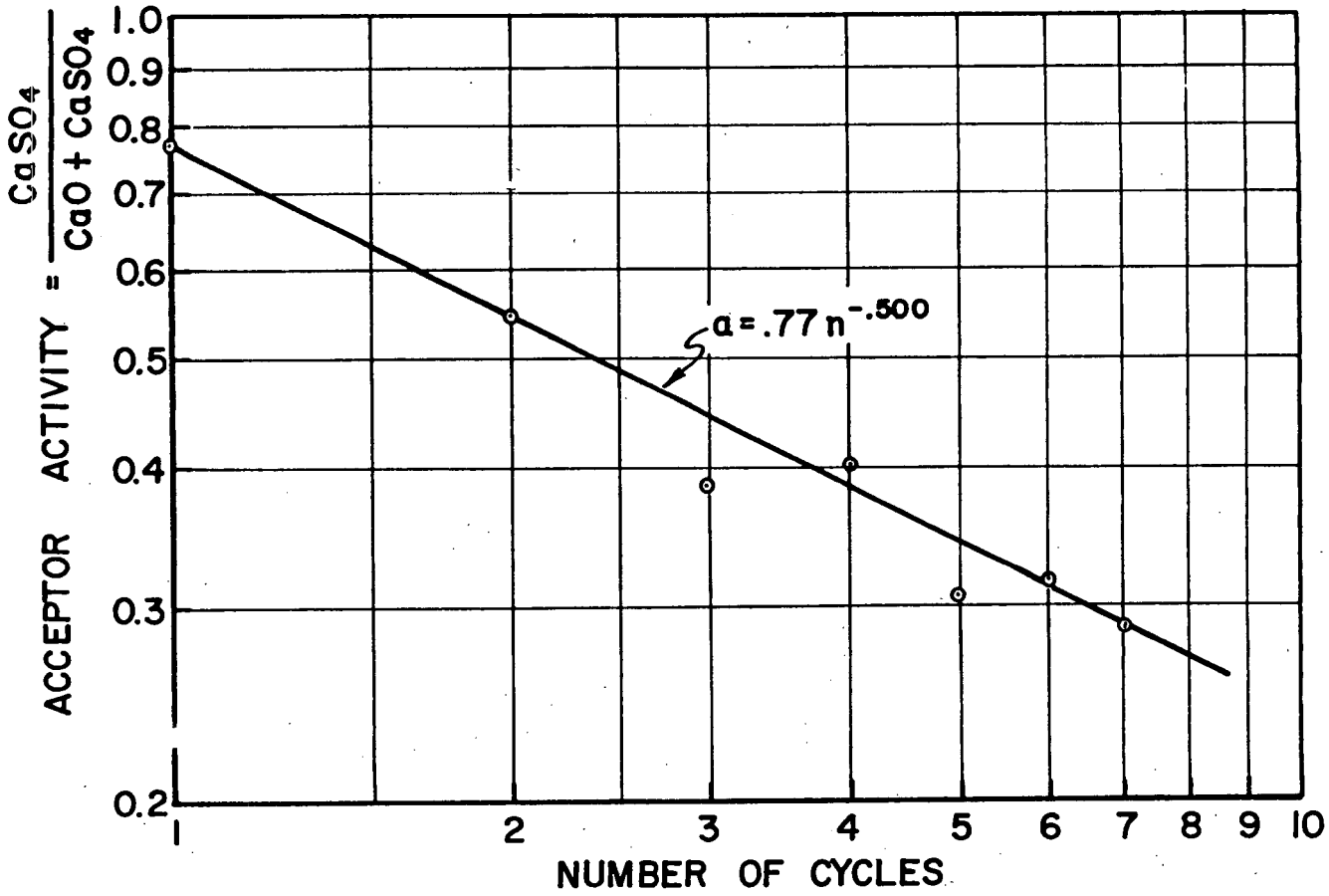

FIGURE 5

ACCEPTOR LIFETIME IN A CONTINUOUS REGENERATING SYSTEM

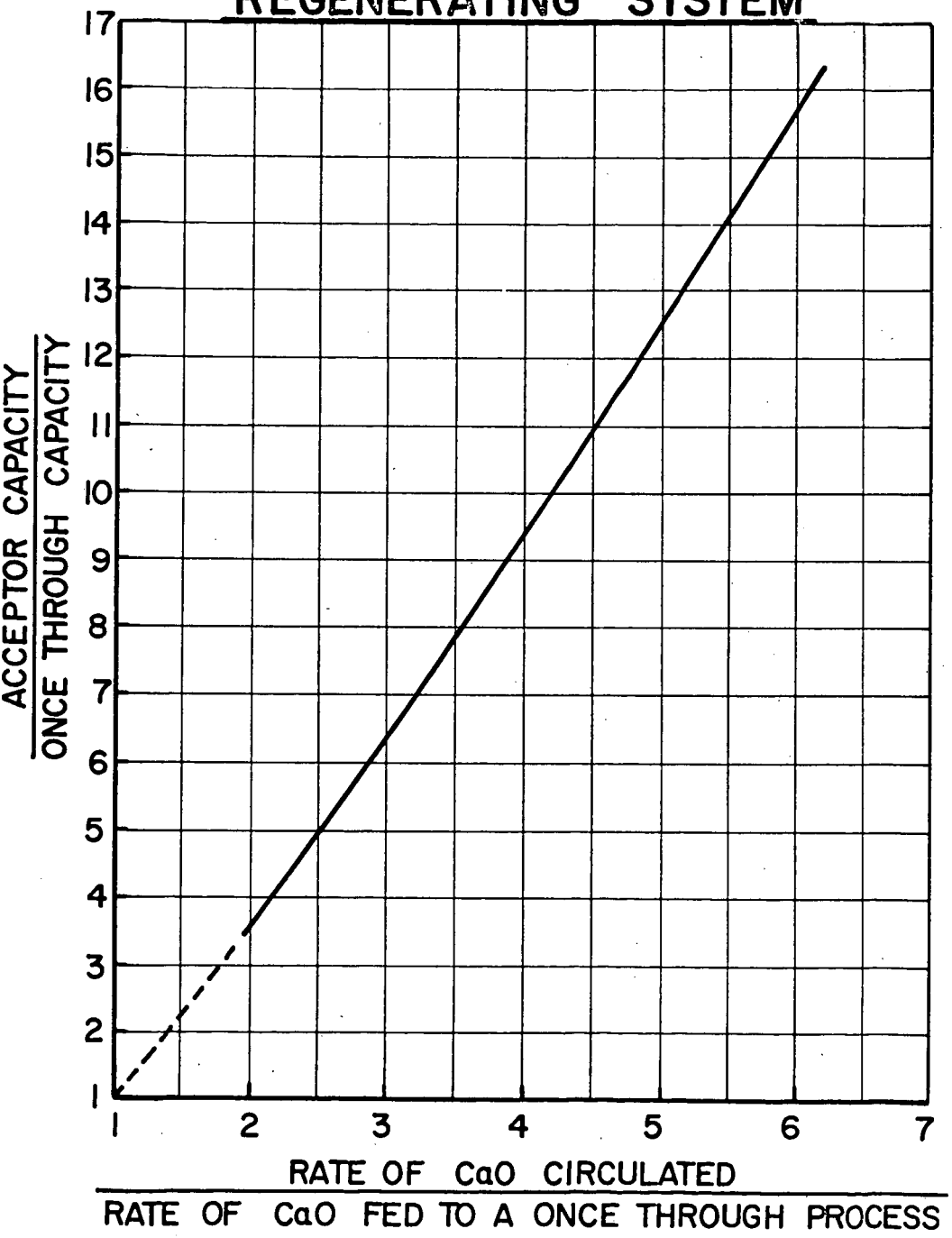

HYDROGEN SULFIDE REMOVAL FROM HOT PRODUCER GAS WITH SINTERED ABSORBENTS

Forrest G. Shultz and John S. Berber

U. S. Department of the Interior, Bureau of Mines,
Morgantown Coal Research Center, Morgantown, W. Va. 26505

Gas producers have been receiving attention in recent years as a potential source of clean, pressurized gas for a variety of industrial purposes. Removal of H_2S (hydrogen sulfide) from the hot producer gas is of interest because hydrogen sulfide is an air pollutant, deteriorates equipment, and removal while still hot should be less costly.

Temperature of the producer gas to be treated for H_2S removal ranges from 1,000° to 1,500° F. To economically utilize the sensible heat of producer gas for power generation, the H_2S must be removed near the generation temperature of the gas. This precludes the use of liquid absorbents and limits the process to the use of solid absorbents that can react with H_2S at elevated temperatures. The material should also be regenerable for reuse through several cycles of H_2S absorption followed by air regeneration.

Literature on producer gas cleanup in the 1,000° to 1,500° F range is quite limited. Information is available on the desulfurization of industrial gases between 68° and 1,292° F with -16 + 100 mesh iron oxide, including data on static and fluidized beds between 617° and 752° F (3). Static beds were tested at a space velocity (gas volume per absorbent volume per hour) of 100 and fluidized beds at 3,000 vol/vol/hr. An absorption capacity of 30% by weight of sulfur per unit weight of absorbent was obtained at higher temperatures and H_2S removal efficiency was 95 to 99.9%. A full-scale operating plant was built with a capacity for treating 32 million cubic feet of coke oven gas per day (2). Iron oxide was the absorbent in a fluidized bed operating at 680° to 752° F. Although overall operation of the plant was satisfactory, troublesome accumulations of fine oxide dust reportedly were experienced in various parts of the plant.

This paper gives results of a Bureau of Mines investigation of prepared solids for their capacity to remove H_2S from hot producer gas. Solids utilized were (1) a sintered mixture of ferric oxide (Fe_2O_3) plus fly ash; (2) pumice stone coated with fused ferric oxide (Fe_2O_3); and (3) sintered pellets prepared from red and brown muds--aluminum refining residues that contain large amounts of Fe_2O_3.

APPARATUS AND PROCEDURE

Bench-scale apparatus utilized in this study is shown in Figure 1. Gases from cylinders of nitrogen, hydrogen, hydrogen sulfide, carbon monoxide, and carbon dioxide were metered to form a stream of simulated producer gas devoid of ash and tars and containing approximately 1.5 volume percent H_2S. The percentage of other constituents is listed on the flowsheet (fig. 1).

Simulated producer gas was passed through a bed of the test absorbent contained in an electrically heated section of 1-inch diameter by 5-feet long, schedule 40 stainless-steel pipe. Alumina spheres in the bottom 22 inches of the pipe extended 10 inches into the hot zone of the furnace. These spheres supported the absorbent bed and preheated the gas. Regeneration facilities, shown in the center right portion of the flow sheet, consisted of an air supply with pressure regulator and flow meter. Purified producer gas and the regeneration gas were vented through a common system. Fifteen-inch depths of absorbent were subjected to a gas flow rate of 15 scfh (7.08 liters per minute), which is equal to a space velocity of 2,000. Hydrogen sulfide concentration in the simulated producer gas was controlled to equal 20.6 to 22.9 mg/l (mg/l x 43.7 = grams/100 cu ft). Experiments were conducted at 1,000°, 1,250°, and 1,500° F. The runs were terminated when the H_2S concentration in the effluent gas stream of the test bed, originally near zero, reached 2.3 mg/l. Sulfur capacities of the absorbent were calculated from the product of H_2S concentration, flow rate, and time duration of the test.

ANALYTICAL METHODS

Hydrogen sulfide concentration of the gas stream was determined by the Tutwiler method (1) and verified by chemical detection tubes and gas chromatography. Reasonable agreement was found between the different methods. Absorbent was regenerated by passing an air stream through the tube at 1,000° to 1,500° F. During the first several tests, SO_2 liberated during regeneration was absorbed in 2.5 N caustic soda solution, an aliquot was acidified with HCL, and titrated to a starch end point with iodine. The weight of sulfur regenerated was calculated and compared with the calculated weight of sulfur absorbed to determine the error in the sulfur balance. These balances usually checked within 20%. Part of this variance is explained by the fact that during regeneration some of the sulfur was evolved in elemental form and collected in the filter at the effluent end of the reaction tube, and thus was not measurable. Later, SO_2 concentrations were measured by means of impregnated silica gel detection tubes.

ABSORBENTS

Several commercial absorbents were tested first, but they did not give satisfactory results, all of them disintegrating in the temperature range used. Included among these were chromium-promoted iron oxide, calcined pellets of dolomite, and alkalized alumina pellets. Seeking more satisfactory absorbents, several other materials were prepared for investigation. The first material consisted of a mixture of fly ash (-4 + 6 mesh) from a bituminous coal-burning power plant (Table 1) and pure Fe_2O_3. Fly ash and oxide were thoroughly mixed, water was added, and pellets were formed and sintered at about 1,800° F. Tests were also made with sintered taconite and sintered (pure) Fe_2O_3.

The second prepared absorbent consisted of granular pumice stone (-4 + 8 mesh, Table 2) impregnated with 99+% pure Fe_2O_3. Pumice stone granules were coated with the oxide as follows: moistened granules were placed in a tumbler, dry oxide was added and the mixer was operated until a fairly uniform coating of the granules was observed. These were then heated at 1,500° F for 2 hours to bond the two materials. Some shrinkage occurred during the heating, but the

granules remained porous and the oxide adhered well to the pumice stone. Excessive shrinkage and loss of porosity occurred when the absorbent was heated at 1,900° F.

The third material consisted of red or brown mud residues from aluminum refining. They were received in powder or lump form, the latter being reduced to powder before use. The powder was moistened with enough water to form a putty-like material that was formed into 1/4-inch spheres, predried at 500° F, then heated at 2,000° F for 10 to 20 minutes to produce a hard pellet. Chemical analyses of the muds are given in Table 3.

ABSORPTION TESTS

Results of tests with these materials are given in Table 4. The fly ash (75%) and Fe_2O_3 (25%) formed a pellet with high sulfur-absorption capacity that did not disintegrate at the test conditions. Tests 1 through 10 give the absorptive capacity of this fly ash-Fe_2O_3 mixture through nine H_2S absorption-air regeneration cycles. The data show that there is no loss in absorptive capacity nor any attrition of the pellets. Absorbents with more than 37% Fe_2O_3 were difficult to test because the pellets either disintegrated or the materials fused.

Compositions and results obtained with pumice stone coated with ferric oxide are listed in Table 5 and Figure 2. This material did not exhibit any tendency to disintegrate, and showed some tendency to fuse into larger particles.

Results obtained with the muds are listed in Table 6. Red mud No. 1 formed a very durable pellet and had the highest capacity of any material tested.

Figure 3 shows sulfur capacities of the materials that did not disintegrate or fuse and appeared suitable as H_2S absorbents.

REGENERATION OF ABSORBENTS

During regeneration of absorbents, all at space velocities of 2,000 calculated at standard conditions (68° F and 1 atmosphere pressure), instantaneous SO_2 concentrations were measured by chemical detection tubes. Error in the sulfur balance amounted to about 15% or less when the regeneration temperature was 1,000° or 1,250° F. When regeneration was attempted at 1,500° F, the material fused into a mass that could not be regenerated. About 1,000° appeared to be the optimum temperature for regeneration of these types of absorbents. Release of heat from the exothermic regeneration reaction is sufficient to increase the bed temperature about 400° F.

Complete regeneration of absorbents appears impractical; a few parts per million of SO_2 were measurable even after 80 hours of regeneration. Regeneration proceeds at a high rate (6 to 10 volume percent SO_2) for the first 30 to 50 minutes of regeneration, drops to about 1% by volume after 1 hour, then rapidly decreases and slowly approaches zero. Figure 4 is a plot of SO_2 concentrations versus time for tests in which the absorption temperatures were 1,000°, 1,250°, and 1,500° F, and the regeneration temperature was 1,000° F. The weight of sulfur regenerated in any of these three tests during the first hour was at least 80% of the total that was regenerated. Tests 18 and 19 (Table 4) were conducted

with a regeneration temperature of 800° F. This temperature was adequate to rapidly regenerate the pellets of test 18 with a low sulfur content of 8.1 wt-pct, but did not achieve a fast regeneration in test 19 in which the pellets had a high sulfur content, 34%. Pellets with a low sulfur content (10% or less) appeared to regenerate more quickly than pellets with a sulfur content of 30% or more, indicating that regeneration should be started before the absorption capacity limit is attained.

DISCUSSION

Mixtures of 75% fly ash-25% Fe_2O_3 gave absorption capacities ranging from 8.1% by weight of sulfur at 1,000° F to 42.7% at 1,500° F. Pellets containing 40% pumice and 60% Fe_2O_3 showed sulfur capacities of 23.3% at 1,000° F to 30.6% at 1,500° F. The most effective absorbent was a red mud having capacities ranging from 16.0% at 1,000° F to 45.1% at 1,500° F.

Spectrographic analysis of reaction products revealed the formation of troilite (FeS). Stoichiometric calculations indicate the formation of ferric sulfide (Fe_2S_3) and pyrite (FeS_2) as products of the reaction. No attempt was made to define precisely the stoichiometry because of the numerous forms in which iron sulfide can occur. The reaction is complicated further by the existence of other metal oxides in the absorbent that may or may not absorb H_2S under the test conditions investigated.

Possible methods of recovering the sulfur contained in the SO_2 during regeneration are the catalytic conversion to SO_3 with subsequent production of sulfuric acid, or the reaction of the SO_2 with some of the producer gas over a suitable catalyst to form elemental sulfur.

Gas chromatographic analyses of both influent and effluent gas streams were made (when using sintered fly ash-ferric oxide) to determine if rearrangement of the gas composition occurs and to determine if gaseous sulfur compounds are formed which are not detected by titration for H_2S. At 1,500° F, water vapor and a small concentration of methane (0.4%) were formed, but no other gases were detected that were not present in the influent gas. The influent gas contained the impurities SO_2 and methyl mercaptan in low concentrations (45 and 16 ppm, respectively), but these are not found in the effluent.

CONCLUSIONS

Hydrogen sulfide can be removed from hot producer gas in the 1,000° to 1,500° F temperature range by reaction with a metallic oxide, such as Fe_2O_3 (a material which has long been used to absorb H_2S from producer-type gases at low temperatures), but the material must be incorporated into a semifused porous matrix of other metallic oxides to prevent dust formation and loss of absorption material. This research shows that such a material can be made by mixing Fe_2O_3 with fly ash and sintering the mixture, or by sintering red mud residues from aluminum refining. In all cases, the mixture contains alumina and silica, which may act as matrix formers, and alkali metal oxides which could act as fluxes to reduce temperature required to sinter the materials.

Absorbents were regenerated to an essentially fresh condition by passing air through the bed at a temperature of 1,000° to 1,200° F. Sulfur dioxide was liberated and the reactive metallic oxides were re-formed. Small quantities of elemental sulfur and sulfuric acid were formed during regeneration.

LITERATURE CITED

1. Altieri, V. J., "Gas Analysis and Testing of Gaseous Materials," American Gas Association, Inc., New York, 1945, pp. 339-342.

2. Bureau, A. C., Olden, M. J. F., Chem. Eng. 49, CE55 (1967).

3. Reeve, L., J. Inst. Fuel 31, 319 (1958).

Table 1. - Chemical composition of sintered fly ash used for H_2S absorption

Constituent	Percent
SiO_2	47.9
Al_2O_3	23.8
F_2O_3	15.7
P_2O_5	0.6
TiO_2	2.8
CaO	3.6
MgO	1.5
Na_2O	1.9
K_2O	2.2

Table 2. - Chemical composition of the granular pumice stone

Constituent	Percent
SiO_2	72.49
Al_2O_3	13.55
Fe_2O_3	1.51
Na_2O and K_2O	8.06
CaO and MgO	2.93

Table 3. - Chemical analyses of muds

Mud No.	L. O. I. [1]	Fe_2O_3	SiO_2	TiO_2	Al_2O_3	CaO	Na_2O
1[2]	11.2	42.4	8.1	4.4	18.8	5.3	5.6
2[3]	5.6	7.5	23.3	3.7	6.9	46.4	3.5
3[4]	11.5	53.2	3.6	7.2	12.8	7.3	2.1
4[5]	11.2	34.7	13.9	9.0	19.4	5.8	6.0

[1] Loss on ignition at 1,100° C.
[2] Red mud from Alcoa's Point Comfort operations.
[3] Brown mud from Alcoa's Arkansas operations.
[4] Field dried red mud from Reynolds Metals Co. Sherwin plant.
[5] Mobile red mud from Alcoa.

Table 4. - H_2S absorbing capacities of sintered materials at 2,000 space velocity

Test No.	Absorption temp., ° F	Capacity, g sulfur/100 g material
75% Fly ash - 25% Fe_2O_3		
1	1,000	8.7
2	1,000	8.2
3	1,000	8.1
4	1,250	16.4
5	1,250	21.1
6	1,250	16.5
7	1,250	13.3
8	1,250	15.8
9	1,500	41.1
10	1,500	42.7
Taconite		
11	1,000	3.5
12	1,250	4.8
13	1,500	Disintegrated
Fe_2O_3		
14	1,000	22.0
15	1,250	20.0
16	1,500	Disintegrated
63% Fly ash - 37% Fe_2O_3		
17	1,000	6.1
18	1,250	8.1
19	1,500	34.0
20	1,500	26.0
87% Fly ash - 13% Fe_2O_3		
21	1,000	4.4
22	1,250	9.8
23	1,500	22.0

Table 5. - H_2S absorbing capacities of sintered pumice stone

Test No.	Temp., °F	Capacity, g sulfur 100 g absorbent
Pumice, granular, -4 + 8 mesh		
24	1,000	0
25	1,250	1.4
26	1,500	3.7
87% Pumice, 13% Fe_2O_3		
27	1,000	4.7
28	1,250	6.3
29	1,500	8.5
66% Pumice - 34% Fe_2O_3		
30	1,000	7.2
31	1,250	8.4
32	1,500	12.3
33	1,500	13.3
40% Pumice - 60% Fe_2O_3		
34	1,000	23.3
35	1,000	20.4
36	1,250	26.8
37	1,500	27.6
38	1,500	30.6

Table 6. - H_2S absorbing capacities of brown and red mud

Test No.	Temp., °F	g of sulfur 100 g absorbent: Capacity from quantity H_2S absorbed	g of sulfur 100 g absorbent: from quantity SO_2 evolved	Percent error in sulfur balance
Mud No. 1				
39	1,000	16.2	16.0	1.2
40	1,250	25.6	24.0	6.0
41	1,500	52.7	45.1	14.4
Mud No. 2				
42	1,000	1.6	1.5	6.0
43	1,250	6.1	6.6	7.6
44	1,500	28.2	26.4	6.6
Mud No. 3				
45	1,000	13.7	12.2	11.0
46	1,250	14.9	13.7	8.1
47	1,500	34.0	37.6	9.6
Mud No. 4				
48	1,000	5.9	6.6	10.6
49	1,250	14.6	13.2	9.6

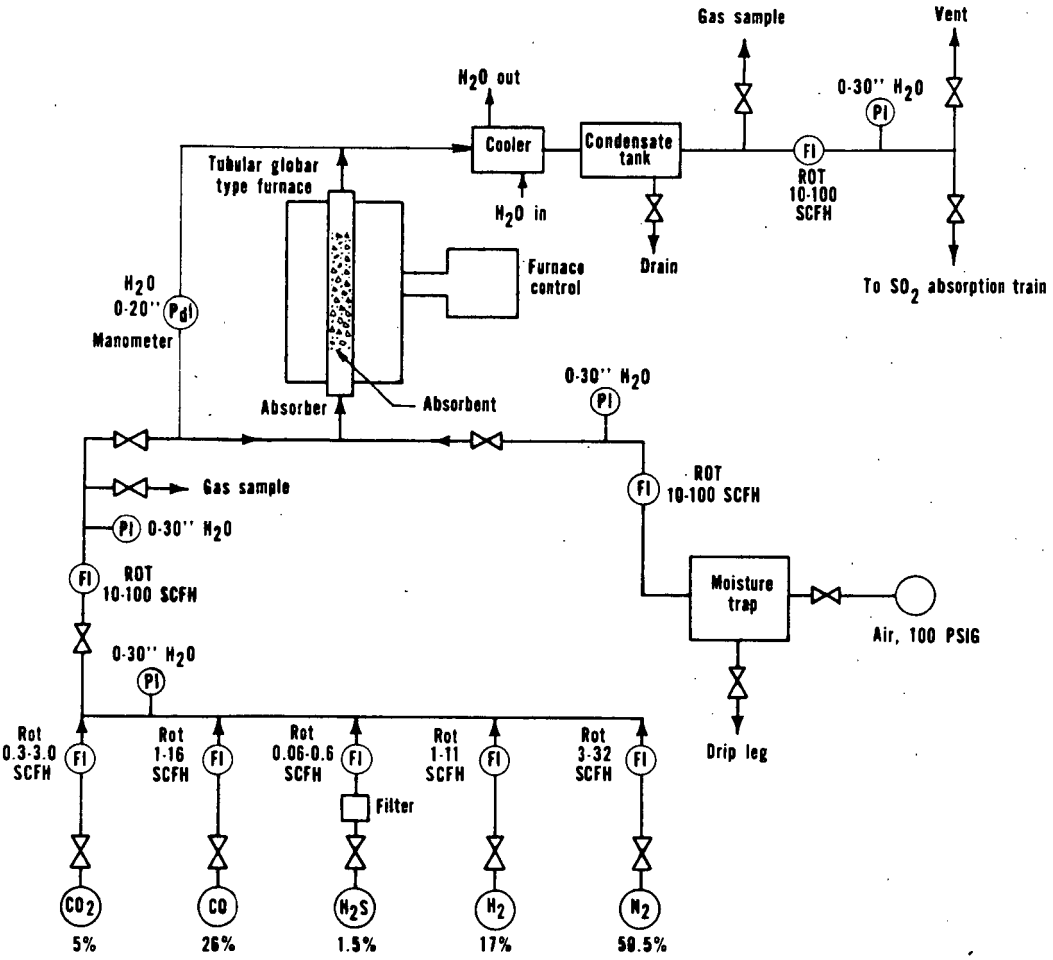

Figure 1. - Flowsheet for Removal of Sulfur from Hot Producer Gas.

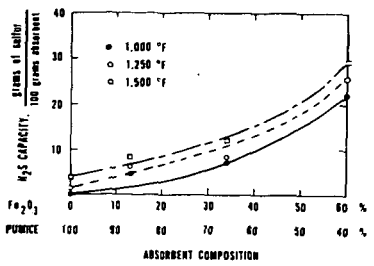

Figure 2. - H_2S Absorption Capacity of Sintered Pumice Stone.

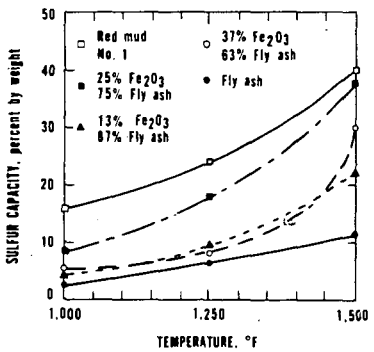

Figure 3. - Sulfur Capacities of Absorbents at 1,000° F to 1,500° F.

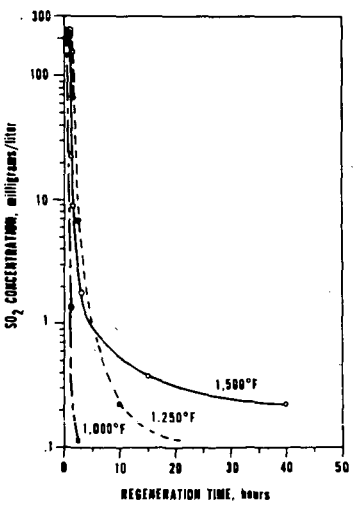

Figure 4. - Typical SO_2 Concentration Versus Regeneration Time.

DISSIMILAR BEHAVIOR OF CARBON MONOXIDE PLUS WATER AND OF HYDROGEN IN HYDROGENATION

Herbert R. Appell, Irving Wender, and Ronald D. Miller

Pittsburgh Coal Research Center, U. S. Bureau of Mines,
4800 Forbes Avenue, Pittsburgh, Pa. 15213

Under certain conditions the conversion of lignite, subbituminous and some bituminous coals to benzene-soluble oils proceeds more readily in the presence of carbon monoxide and water than in the presence of hydrogen (1-4).

The purpose of the work described here was to compare the behavior of carbon monoxide plus water with that of hydrogen under mild coal hydrogenation conditions. Pure compounds and materials having structures resembling those that might exist in coal were the objects of the hydrogenations.

The experimental work was conducted in a 500 ml rocking stainless steel autoclave. Analysis of the pure compounds was by gas chromatography and mass spectrometry. Conversions of lignite, lignin, and cellulose were measured by extracting the products with hot benzene and then weighing and analyzing the benzene-insoluble residues. Pressures referred to in the tables are initial pressures. The maximum pressures were about three times the initial pressure. The time at temperature did not include the time required to reach operating temperature or the cooling off period. The reactants were thus exposed to temperatures where a significant amount of reaction was occurring for approximately an additional hour.

RESULTS AND DISCUSSION

The effectiveness of carbon monoxide and water in solubilizing low rank coal may be due to a number of reasons, including (1) hydrogenation with activated hydrogen produced by the water-gas shift reaction, (2) the introduction of alkyl groups, and (3) the unique ability of carbon monoxide to cleave certain types of bonds or to inhibit condensation reactions leading to benzene-insoluble materials.

Mass spectrometric analysis of the benzene-soluble products from a fresh lignite and a less reactive, rapidly aged lignite, revealed that a major difference in composition was an increase in methylated aromatic compounds in the product from the more reactive lignite. This is in agreement with the observation of Sternberg and Delle Donne of our laboratory that coal may be solubilized by the introduction of alkyl groups (5). The relatively high methyl content of the products suggested that the effectiveness of CO and water in lignite solubilization might be due in part to the introduction of methyl groups.

Table 1 lists the relative peak heights of several of the more prevalent compounds in the products. Inasmuch as the solvent used consisted of equal weights of α-naphthol and phenanthrene, the compounds present in largest concentration were the solvent and products derived from the relatively reactive α-naphthol. (In a solvent free system the cresols usually show the highest mass peaks.) Not only are the aromatic compounds from fresh lignite present in higher concentration, but the methylated derivatives of the parent aromatic compound are also consistently and significantly higher. The large content of methylnaphthol, in both products, indicates that methyl groups are being picked up, either from the lignite, from the carbon oxides, or from traces of formaldehyde. The probable reactions are

carbonylation, carboxylation, and hydroxymethylation, followed by reduction. The presence of relatively large amounts of dinaphthylmethanes suggest that naphthoic acid, hydroxymethylnaphthalene and naphthylmethyl radical may be intermediates in the route from naphthol to methylnaphthalene.

TABLE 1. - Methyl groups in benzene soluble material from hydrogenated lignite
(30 g. lignite, 15 min. at 380°C, 1500 psig CO pressure, 1:1:1 = water:lignite:solvent[a])

Compound	Relative peak heights by M.S. analysis: North Dakota lignite (89% conversion)	Aged North Dakota lignite[b] (54% conversion)
Phenol	12	8
Cresols	18	11
Xylenols	14	5
Naphthalene	50	27
Methylnaphthalene	80	24
Naphthol	900	1070
Methylnaphthol	340	240
Phenanthrene	2500	2500
Methylphenanthrene	14	10
Dinaphthylmethane, dinaphthofuran	60	43
Methylnaphthylnaphthylmethane) Methylnaphthonaphthofuran)	57	26

[a] Equal parts of α-naphthol and phenanthrene.
[b] Heated 24 hr. in air at 105°C, 54% conversion.

Although treatment with hydrogen, with or without water present, gave a smaller total yield of benzene-soluble product, the ratio of methylated to parent aromatic structures were the same, within experimental error, as those obtained in the presence of carbon monoxide and water (4). This result inplies that carbon monoxide or dioxide liberated during lignite hydrogenation was reentering the reaction. In the presence of the alkaline lignite ash, carbon dioxide would be expected to add to phenolic materials readily via a Kolbe type carboxylation. One advantage of the reaction with hydrogen is that in the absence of large quantities of water, the carboxylation reaction may proceed rapdily. Reduction of the carboxyl group to a methyl group also occurs more readily with hydrogen than with carbon monoxide and water.

Although methylation may be a factor serving to increase the solubility of lignite, the effect is similar for carbon monoxide plus water and for hydrogen. Methyl group introduction, therefore, does not appear to be a major reason for the greater effectiveness of carbon monoxide and water in lignite solubilization.

The presence of methoxyl groups in lignite prompted several experiments probing the behavior of anisole at mild coal hydrogenation conditions (approximately 4500 psig maximum pressure at 380°C using low activity catalysts). Table 2 shows that in addition to demethylation to phenol, a significant portion of the anisole is converted to benzene and toluene. The highest yield of benzene was obtained with hydrogen. This demonstrates the greater effectiveness of hydrogen in hydrocracking reactions. The absence of dimethylated products suggests that ring methylation proceeds predominantly by an intromolecular shift. It does not appear likely that methoxy or methyl transalkylation occurs to a major extent during coal hydrogenation.

TABLE 2. - Hydrogenolysis of anisole

(20 ml. anisole, 15 ml. water, 1 g. catalyst, 1500 psig, 2 hr. 380°C)

Catalyst	Gas	Wt. pct. of total products			
		Benzene	Toluene	Phenol	Anisole
None	CO	1.9	7.4	6.5	84
Lignite ash	CO	1.5	4.2	18	76
Charcoal	CO	2.0	7.8	6.5	83
Fe	CO	2.6	8.5	10	77
Fe_3O_4	CO	2.9	8.4	8.3	80
Fe_3O_4[a]	H_2	6.8	7.7	11	74
Fe_3O_4	H_2	4.5	8.2	16.5	70

[a] No water present.

The possibility that methyl groups could be introduced via CO, CO_2, or methyl alcohol was evaluated by treating phenol under mild coal hydrogenation conditions. Table 3 shows that in the presence of iron oxide, methylation occurs to a significant extent with CO_2 and with methyl alcohol. Although small amounts of the latter might be formed by a Fischer-Tropsch reaction, it appears more likely that either formaldehyde or CO_2 adds to reactive phenolic rings and the compound formed is then reduced by the carbon monoxide or by the hydrogen. Even in the absence of added catalysts, small amounts of cresol, toluene, and xylene were obtained with CO_2 plus either CO or H_2. More reactive phenolic materials can be expected to methylate to a greater extent. The formation of dinaphthylmethanes indicated in table 1 is perhaps a result of carboxylation or hydroxymethylation of the α-naphthol followed by condensation with a molecule of naphthol or methylnaphthol. The condensed product apparently loses phenolic OH groups easily; not more than traces of masses corresponding to oxygen containing dinaphthylmethanes were observed. This mechanism may account for the formation of some high molecular weight materials during coal hydrogenation.

TABLE 3. - Methylation of phenol

(20 g. phenol, 1 g. catalyst, 2 hr. 380°C, 1500 psig)

Catalyst	Gas	Water, g.	Reagent, g.	Wt. pct. of total products
$CoCO_3$	CO	15	None	Trace o-cresol
None	CO	15	MeOH, 10	No reaction
Fe_3O_4	CO	15	MeOH, 10	o-Cresol, 6%; anisole, 1.3%; xylenol, trace
None	CO	15	CO_2, 15	Traces of o-cresol, toluene, xylene
None	H_2	None	CO_2, 15	o-Cresol, 0.7%; traces of benzene, toluene, xylenol
Fe_3O_4	H_2	None	CO_2, 15	o-Cresol, 6%; benzene, 2.5%; toluene, trace
Lignite ash	H_2	None	CO_2, 15	o-Cresol, 0.4%; benzene, 0.2%

Although not more than traces of formaldehyde can be expected to be present at operating conditions, the high reactivity of formaldehyde with phenols suggests that the small amounts formed are continuously scavenged from the system by reaction with the phenols.

The major high molecular weight oxygen containing compound appeared to be dinaphthofuran. This is probably formed by cyclization of dinaphthyl ether; but oddly, not more than very small amounts of the mass corresponding to this ether was found by mass spectrometry.

A number of compounds were tested for their ease of hydrogenation with carbon monoxide and water and with hydrogen. The hydrogenation of 1-octene proceeded more rapidly with hydrogen than with carbon monoxide and water at the same total pressure (table 4). However, the rate with carbon monoxide and water was four times as fast as expected based on the partial pressure of hydrogen in the autoclave in the absence of a catalyst. In the presence of potassium carbonate, more hydrogen was formed by the water-gas shift reaction but the rate of hydrogenation was only three times that expected. The rate, however, was approaching that obtained with high pressure hydrogen. It thus appears that hydrogen formed by the water-gas shift reaction is activated and has a beneficial effect on the rate of hydrogenation. The lower total extent of hydrogenation, in this system at least, makes it clear that the hydrogen is not activated sufficiently to reach or surpass the hydrogenation rates obtainable with high pressure hydrogen. It may be that, with the proper choice of catalyst, reactants and operating conditions, the hydrogenation rate with carbon monoxide and water could equal or exceed that obtained with hydrogen.

TABLE 4. - Hydrogenation of octene-1

(1 hr. 400°C, 1000 psig, water:hydrocarbon = 1.5:1)

	H_2	CO[a]	CO-K_2CO_3[b]	H_2[c]
Product (mole pct.)				
Below C_8	8	9	11	8
n-Octane	61	36	50	26
n-Octene-1	21	41	22	49
n-Octene-2	9	11	13	15
Above C_8	1	3.5	4	2.5

[a] 14.6 Mole pct. H_2 in final gas; 36.5% water-gas shift reaction.
[b] 27 Mole pct. H_2 in final gas; 66% water-gas shift reaction.
[c] 400 psig initial pressure.

The reduction of p-methylbenzaldehyde to xylene also proceeded at a more rapid rate with hydrogen than carbon monoxide and water (table 5). The yield of condensation products (tolylxylylmethanes) was also higher when hydrogen was used.

TABLE 5. - Reduction of p-methylbenzaldehyde

(20 ml. aldehyde, 1 g. Fe_3O_4, 2 hr. at 380°C, 1500 psig)

			Products, percent (wt.)			
Gas	Water	Conversion	Toluene	Xylene	Methylbenzylalcohol	Diaryls
CO	15 ml.	50	25	14	6	4
H_2	None	94	14	70	3	7

The possibility that carbon monoxide plus water has a unique ability to cleave certain types of bonds in coal was explored by subjecting a variety of compounds to coal hydrogenation conditions (table 6). Very little hydrogenolysis occurred

except with phenyl sulfide; but here again hydrogen was more effective than carbon monoxide and water. The considerable reduction of sulfur in lignite with carbon monoxide and water (4), and the stability of thiophene at these conditions suggests that thiophenic sulfur is not common in lignites.

TABLE 6. - Conversions of miscellaneous compounds

(20 g. compound, 15 ml. water, 1 g. catalyst, 2 hr. 400°C, 1500 psig)

Compound	Catalyst	Gas	Products, percent (wt.)
Phenyl ether	Na_2CO_3	CO	Very little reaction
3-Methylthiophene	Na_2CO_3	CO	Very little reaction
3-Methylthiophene	Charcoal	CO	Very little reaction
Diphenylmethane	Na_2CO_3	CO	Very little reaction
Diphenylmethane	Charcoal	CO	Benzene 1.0, toluene 1.4
Diphenylmethane	Charcoal	H_2	Benzene 3.1, toluene 3.8
Phenyl sulfide	Charcoal	CO	Benzene 3.6, toluene 2.0
Phenyl Sulfide	Charcoal	H_2	Benzene 61

Lignin and cellulose, the generally accepted coal precursors, were found to be, like coal, more reactive with CO and water than with hydrogen (table 7). Glucose and presumably certain other carbohydrates share this property. Surprisingly, cellulose is most reactive. This order of reactivity is probably caused by the relatively large number of stable aromatic units in lignin and the ease of pyrolysis of glucose. A carbonyl group appears to be necessary for low temperature charring. Glucose and other carbohydrates that contain a carbonyl group or an incipient carbonyl group form chars on being heated at 250 to 300°C with the liberation of considerable quantities of water. Sorbitol and sorbic acid do not form chars at these conditions.

TABLE 7. - Conversion of lignin and carbohydrates to benzene-soluble material

(1500 psig, 40 ml. water, 2 hr. at temperature)

Material, g.	Gas	Temp., °C	Catalyst, g.	Conversion, % of feed (maf)[a]	Benzene soluble product, wt. %[a]
Lignin, 10	CO	250	None	77	29
Lignin, 10	H_2	350	None	33	9
Lignin, 10	CO	380	None	80	N.A.
Lignin, 10	CO	380	Na_2CO_3, 1	92	N.A.
Glucose, 20	CO	350	None	64	6.5
Glucose, 20	H_2	350	None	60	3
Glucose, 20	CO	350	Na_2CO_3, 1	93	35
Cellulose[b], 20	CO	350	None	90	40
Cellulose[c], 20	CO	350	None	63	17
Cellulose[b], 20	H_2	350	None	60	20
Cellulose[c], 20	CO	350	Na_2CO_3, 1	94	46
Cellulose[c], 20	H_2	350	Na_2CO_3, 1	90	27

[a] Based on charge.
[b] Crude cellulose.
[c] Ash free cellulose.

The advantage of carbon monoxide and water over hydrogen in liquefying carbohydrates is reflected not only in the higher yields of benzene-soluble product but also in the composition of the residues (table 8). The atomic ratio of

hydrogen to carbon in the residue from hydrogenation with carbon monoxide and water is close to 1:1, whereas the much larger residue obtained in the presence of hydrogen is only 0.73:1.

TABLE 8. - Composition of benzene-soluble products and residues from cellulose (2 hr. at 350°C, 1500 psig)

	Benzene soluble product ($CO + H_2O$) (40% yield)[a]	Residue ($CO + H_2O$) (10% yield)[a]	Residue (H_2) (40% yield)
C (%)	83.3	71.4	74.9
H (%)	7.8	5.9	4.6
H/C	1.11	.98	0.73

[a] The remaining 50% yield is largely water plus some carbon dioxide.

Sodium carbonate is an effective catalyst for liquefying cellulose, glucose, or lignin in the presence of carbon monoxide and water. Benzene-insoluble residues of less than 5% of the original weight of cellulose and less than 10% of the original weight lignin have been obtained at relatively mild conditions. The product is similar in elemental analysis to that obtained from lignite but is less aromatic.

The ease of conversion of cellulose and glucose to benzene-soluble products with carbon monoxide and water suggests that structural units derived from those found in carbohydrates exist in low rank coals. The reactivity of coals with CO and water may be indicative of the number of carbohydrate-derived structures in the coal. The structure of low rank coals is even less certain than that of high rank coals and it is hoped that this approach will assist in improving our knowledge of low rank coal structure.

REFERENCES

1. F. Fischer and H. Schrader, Brennstoff-Chem., 2, 257 (1921).

2. H. I. Waterman and F. Kortland, Rec. trav. Chim., 43, 258, 691 (1924).

3. H. I. Waterman and J. N. J. Perquin, Proc. Acad. Sci. Amsterdam, 27, 132 (1924); CA, 18, 1903 (1924).

4. H. R. Appell and I. Wender, 156th National Meeting, American Chemical Society, Fuel Division Preprints, vol. 12, No. 3, 220 (1968).

5. H. W. Sternberg and C. L. Delle Donne, 156th National Meeting, American Chemical Society, Fuel Division Preprints, vol. 12, No. 4, 13 (1968).

HYDROCRACKING IN STATIC AND EBULATING BED REACTOR SYSTEMS

S. A. Qader, W. H. Wiser, and G. R. Hill

Department of Mineral Engineering

University of Utah, Salt Lake City, Utah 84112

Abstract

The results of hydrocracking of coal and petroleum oils in static and ebulating bed reactors are presented. The static bed system was found to be more efficient at low space velocities, while the efficiency of both the systems was almost the same at higher space velocities with respect to the yield of naphtha. The gas oil and coal oil hydrocracking severities, respectively, varied from 0.03 to 0.4 and 0.08 to 0.45 in the case of the static bed system and 0.03 to 0.31 and 0.07 to 0.32 in the case of the ebulating bed system. The static bed system affected more desulfurization, denitrogenation, and deoxygenation at lower space velocities, while the ebulating bed system was more efficient at higher space velocities. The static bed system appears to be more suitable for operations designed for the production of naphtha and for the complete removal of heterocyclic compounds.

Introduction

Hydrocracking of fuel oils is mostly carried out in static bed reactor systems which are very versatile for the processing of distillate oils. They, however, pose some problems in the treatment of heavy and residual oils. The residual oils may give rise to excessive deposits in the bed leading to catalyst deactivation, reactor plugging, and pressure drop in the bed. This necessitates frequent regeneration and changing of the catalyst which is an expensive and tedious problem. The heavy feed stocks can easily be processed in an ebulating bed type of reactor system as incorporated in the H-oil process (1, 2). In the ebulating bed system, the catalyst bed expands in excess of the true volume of the catalyst and the catalyst remains always in a state of random motion caused by the velocity of the feed oil, hydrogen, and some internal circulation of the oil. This system has several advantages and can be employed for the processing of different types of feed stocks ranging from vacuum residues to light gas oils (3, 4). It is, thus, evident that the ebulating bed system has the advantage of processing heavy and residual oils over the static system, while both the systems can be employed for the treatment of distillate oils of medium and low viscosities such as some gas oils and coal oils. There are no data available at this time in the open literature on the relative efficiencies of these two reactor systems for the processing of either petroleum or coal oil and is, therefore, difficult to select the proper system for practical adaptation. This communication describes the results of our investigation on the evaluation of the relative efficiencies of the static and ebulating bed reactor systems in the hydrocracking of petroleum and coal oil distillates.

Experimental

Materials.

The gas oil was prepared from a mixed base petroleum crude and the coal oil was obtained by the carbonization of a high volatile, bituminous coal from Utah at 650°C in a laboratory oven (Table I). A dual-functional catalyst containing sulfides of nickel and tungsten on silica-alumina in 1/16th-inch size pellets was used as the hydrocracking catalyst.

Equipment.

The static bed reactor system (Figure 1) contained a tubular 316-stainless steel reactor of 0.75-inch diameter and 40-inch length. One hundred c.c of the catalyst was used in the reactor. The ebulating bed reactor system (Figures 2 and 3) contained a reactor of 3-inch internal diameter and 9-inch height. The ebulation of the catalyst was mainly caused by a magnetic drive stirrer of 1800 r.p.m. The total volume of the catalyst bed was 500 c.c and 250 c.c of the catalyst was used for the experimental work.

Hydrocracking procedure.

Both systems were first flushed and pressurized with hydrogen and heated to the reaction temperature. The pressure was then adjusted to the experimental value and the oil was fed at the desired rate. The hydrocracking reactions were carried out at a constant pressure of 2000 p.s.i. and the hydrogen to oil feed ratio was maintained at about 1000. The data presented were obtained at a reaction temperature of 450°C unless otherwise mentioned. The values of space velocities varied in the range of ±10% and were rounded off. In the case of the static bed reactor, the experiments were carried out at 1 to 6 space velocities (V. of oil/hr./V. of catalyst). In the ebulating bed reactor system, experiments were carried out at 2.5 to 6 space velocities and the results were extrapolated down to 1-space velocity. Experiments could not be carried out at space velocities lower than 2.5 due to practical difficulties. In this system, the catalyst (250 c.c) expands to a total volume of 500 c.c (catalyst bed volume) and, hence, the space velocities were calculated on the basis of 500 c.c of the catalyst volume. The product was cooled in the condenser and the liquid product was collected in the separator. The gaseous product containing some uncondensed oil was passed through an active carbon tower to adsorb the oil and a gas meter to measure the rate and total volume passed. The liquid product was distilled and the fraction boiling up to 200 C was designated as naphtha and the residue as middle distillate. The yield of gas was calculated from the total gas and its composition. All products were obtained in single pass operations. The ratio of naphtha plus gas to the feed is designated as cracking severity. The analyses of the products were done by standard methods.

Results and Discussion

Selection of a suitable processing system mainly depends upon the type of feed stock to be processed and the nature of products desired. Due to the anticipated development of synthetic oil industry in the near future, feed stocks widely varying in physical and chemical properties will be available and

different types of processing systems may have to be employed for their treatment. It is, therefore, necessary to consider the different types of reactor systems available and evaluate their relative efficiencies for the processing of different feed stocks. A realistic evaluation can only be made by processing the same feed stock under similar reaction conditions in different systems. The gas oil and the coal oil used in this work were distillates of medium viscosity and can be easily processed in either static or ebulating bed system without problems, so that a reasonably good evaluation of the two processing systems can be made. The product distribution data obtained in the hydrocracking of gas oil (Figure 4) illustrated that both systems are almost equally efficient at space velocities greater than 4. They yielded almost the same amounts of naphtha and middle distillate at 430° and 450°C. The yield of naphtha, however, was very low and varied between 2 and 3%. Both systems exhibited different efficiencies at lower space velocities with respect to the yields of naphtha and middle distillate. At space velocities between 1.0 and 4.0, the static system yielded more naphtha and, correspondingly, less middle distillate when compared to the ebulating bed system. There was no significant difference in the yield of the gaseous product. The results obtained under the experimental conditions employed, indicate that the static bed system is more suitable for hydrocracking operations mainly designed for naphtha production, while both systems are equally suitable if middle distillate production is desired. This is further illustrated by the similar data obtained in the hydrocracking of a coal oil (Figure 5) which, however, yielded relatively more naphtha and less gas. The latter probably is due to the differences in the boiling ranges and the composition of the two feed stocks. The static bed system exhibited higher cracking severities when compared to the ebulating bed system at lower space velocities (Figure 6). The gas oil and coal oil hydrocracking severities, respectively, varied from 0.03 to 0.4 and 0.08 to 0.45 in the case of the static bed system and 0.03 to 0.31 and 0.07 to 0.32 in the case of the ebulating bed system. The results indicate that the product distribution obtained in the static bed system is being influenced very much by the space velocity, while the latter is not very critical in the case of the ebulating bed system. In any system the efficiency of contact between the catalyst and the reactants is mainly affected by the size of the catalyst and the space velocity. It appears that the space velocity is a more critical factor in the operation of the static bed system, while the size of the catalyst is probably more critical in the case of the ebulating bed system.

The product distribution at different levels of naphtha formation (Figures 7 and 8) indicates that both systems affect the product yields in a similar manner. The actual quantities, however, depend upon the nature of the feed stock. The properties of the naphtha and middle distillate produced by the two systems were found to be quite similar (Tables II and III). The coal oil naphtha was, however, more aromatic in nature than the gas oil naphtha. The composition of the gaseous product was somewhat different and the static system product from gas oil contained more C_4 hydrocarbons while the ebulating system product contained more C_1 and C_2 hydrocarbons. The static system product from coal oil contained more C_3 hydrocarbons, while the ebulating system product contained more C_1 and C_2 hydrocarbons. The production of more C_1 and C_2 gases in the ebulating bed system is indicative of the occurrence of more thermal cracking reactions in this system.

Removal of heterocyclic compounds from fuel oils is one of the major functions of hydrocracking and the extent of such hydroremoval depends upon the nature of the feed stocks, the catalyst, and the experimental conditions. The type of processing system may also have some influence. In gas oil hydrocracking, desulfurization and denitrogenation varied linearly with space velocity in the static bed system, while it was not the case in the ebulating bed system where the desulfurization and denitrogenation leveled off from a space velocity of 2 and down (Figure 9). The static bed system was more efficient for the removal of sulfur and nitrogen compounds at lower space velocities ranging from 1.0 to 3.0, while the ebulating bed system was more effective at higher space velocities ranging from 4.0 to 6.0. The efficiencies were almost the same in the range of 3 to 4 space velocities. Maximum desulfurization of 96% and denitrogenation of 83% were obtained in the static bed system at a space velocity of 1.0. In the case of the ebualting bed system, a maximum desulfurization of about 75% and denitrogenation of about 64% were obtained at a space velocity of 2.0. At space velocities lower than 2, there was no further removal of sulfur and nitrogen from the gas oil. It appears that the ebulating bed system is not very suitable for operations designed for complete removal of sulfur and nitrogen from fuel oils, though it can remove about 70 to 80%. The obvious choice, then, will be to employ the static bed system for such operations. Analogous results were obtained in the hydrocracking of the coal oil (Figure 10) wherein maximum desulfurization and denitrogenation of 97% and 87% were respectively affected by the static system and about 82% and 72% by the ebulating bed system. Oxygen removal from coal oil also followed the same pattern as the removal of sulfur and nitrogen. The rates of hydrocracking of sulfur, nitrogen, and oxygen compounds of gas oil and coal oil appear to be almost the same under conditions of high severities, irrespective of the type of processing system employed. The rates, however, were different under less severe conditions of hydrocracking (Figure 11). The material balance obtained in the two systems with gas oil and coal oil is given in Table IV. A total product recovery of about 102 to 103% was obtained, indicating 2 to 3% of hydrogen consumption in the process. The gas yield was approximated to about 0.5%. The yields of hydrogen sulfide, ammonia, and water were calculated from the extent of removal of sulfur, nitrogen, and oxygen during the process.

Acknowledgement

Research work was supported by the Office of Coal Research and the University of Utah.

Literature Cited

1. Hellwig, K. C., Feigelman, S., Alpert, S. B., Chem. Eng. Progress, 62, No. 8, 71 (1966).

2. Rapp, L. M., Van Driensen, R. P., Hydrocarbon Processing, 44, No. 12, 103 (1965).

3. Chervenak, M. C., Johanson, E. S., Johnson, C. A., Schuman, S. C., Sze, M., The Oil and Gas J., 58, No. 35, 80 (1960).

4. Chervenak, M. C., Johnson, C. A., Schuman, S. C., Petrol. Refiner, 39, No. 10, 151 (1960).

Table I. Analysis of the feed materials.

	Coal oil	Petroleum oil
Gravity, °API	11.5	31.80
Sulfur, wt. %	0.84	0.94
Nitrogen, wt. %	0.92	0.80
Oxygen, wt. %	6.84	-
Distillation data		
I.B.P., °C	200	300
50% distillate, °C	305	340
F.B.P., °C	395	440
Hydrocarbon types, vol. % (neutral oil)		
Aromatics + olefins	68.0	29.0
Saturates	32.0	71.0

Table II. Properties of products of gas oil. Temperature: 450°C, pressure: 2000 p.s.i., sp. vel.: 4.0

Products	Static bed	Ebulating bed
Naphtha		
Aromatics, vol. %	31.0	30.0
Saturates, vol. %	66.0	66.0
Olefins, vol. %	3.0	4.0
Sulfur, wt. %	0.14	0.21
Nitrogen, wt. %	0.18	0.26
Middle distillate		
Aromatics + olefins, vol. %	30.0	31.0
Saturates, vol. %	70.0	69.0
Diesel index	51.0	50.0
Gas, vol. %		
C_1	10.0	15.0
C_2	12.0	14.0
C_3	29.0	28.0
C_4	49.0	43.0

Table III. Properties of products of coal oil.
Temperature: 450°C, pressure: 2000 p.s.i.,
sp. vel.: 4.0

Products	Static bed	Ebulating bed
Naphtha		
Aromatics, vol. %	42.0	44.0
Saturates, vol. %	54.0	53.0
Olefins, vol. %	4.0	3.0
Sulfur, wt. %	0.11	0.13
Nitrogen, wt. %	0.21	0.28
Middle distillate		
Acids, vol. %	8.5	11.0
Bases, vol. %	1.0	1.7
Neutral oil, vol. %	90.0	89.0
Middle distillate (neutral)		
Aromatics + olefins, vol. %	61.0	60.0
Saturates, vol. %	39.0	40.0
Diesel index	41.0	41.0
Gas, vol. %		
C_1	13.0	16.0
C_2	15.0	19.0
C_3	33.0	25.0
C_4	39.0	40.0

Table IV. Material balance.
Temperature: 450°C, pressure: 2000 p.s.i.,
sp. vel.: 4.0

Product yield, wt. %	Static bed system		Ebulating bed system	
	Gas oil	Coal oil	Gas oil	Coal oil
Naphtha	5.0	10.0	4.0	9.0
Middle distillate	96.0	91.0	97.0	92.0
Gas	0.5	0.5	0.5	0.5
Water	-	1.0	-	1.0
Hydrogen sulfide	0.5	0.5	0.5	0.5
Ammonia	0.5	0.5	0.5	0.5

THE DIRECT METHANATION OF COAL

R. L. Zahradnik* and R. A. Glenn

Bituminous Coal Research, Inc.
350 Hochberg Road
Monroeville, Pennsylvania

Introduction

The fact that coal is composed of various fractions with widely varying properties has long been realized. Recent attention to this fact has resulted in a number of proposed staged gasification schemes. In particular, research at BCR has led to the concept of a two-stage super-pressure gasifier to take specific advantage of the varied nature of coal in the production of a gas rich in methane and amenable to conversion to a high Btu pipeline gas. The two-stage super-pressure gasifier utilizes synthesis gas and heat generated in a high temperature stage to convert a portion of fresh coal in a lower temperature stage into a methane-rich gas.(5)

A study of the methane formation occurring at short gas-coal contact times in the low temperature stage is being carried out at Bituminous Coal Research, Inc., for the Office of Coal Research. This program has included batch tests in rocking autoclaves and continuous flow experiments in an externally-heated 5 lb/hr continuous flow reactor (CFR).(8) Tests in this unit have been carried out under a wide variety of conditions using North Dakota lignite, Elkol subbituminous "C" and Pittsburgh high volatile "A" bituminous coals. The program has produced considerable data on the methanation step and has led to the design and construction of an internally-fired 100 lb/hr process and equipment development unit now being placed in operation.(9)

This paper presents a method of analysis of the short contact time methanation step, based on the premise that rapid heating of coal in the presence of hydrogen produces, in addition to gaseous pyrolysis products, an active but transient species which undergoes rapid reaction with hydrogen to produce additional methane. A simplified rate expression is used to derive a relationship between methane yield and hydrogen partial pressure which fits the experimental data obtained by others.(8,13,16)

Background

Until recently, studies of the coal-hydrogen reaction were generally carried out with long gas-coal contact times, and the results are not directly applicable to short contact time methanation. Von Fredersdorf and Elliott (17) have provided an excellent review of the many such investigations through 1963. Although various methods of contacting were tried and a number of mechanisms for the reaction proposed, the general concensus based on these investigations was that the rate of methane production from coal or char is approximately proportional to hydrogen partial pressure, with the constant of proportionality dependent upon temperature, coal type, and percent carbon burnoff.

* Professor, Chemical Engineering Department,
Carnegie-Mellon University, Pittsburgh, Pa.

Recent investigations have indicated that the rate of methane production varies with gas-coal reaction time. In experiments carried out at the U.S. Bureau of Mines, Hiteshue et al., studied the hydrogasification of bituminous coals, lignite, anthracite, and char (10) and high volatile "A" bituminous coal. A packed bed of coal was used in these studies, but because of heating capacity limitations, two minutes were required to raise the system temperature to 800 C. Nevertheless, the Bureau of Mines group was able to demonstrate that the test coals reacted with hydrogen in the initial period at a rate much higher than that observed at longer contact times.

Further indication of the rapid gasification rates during the initial contact period was obtained by Feldkirchner and Linden in their study of high-pressure gasification with hydrogen and steam.(6)

In 1965, Moseley and Paterson (14,15) demonstrated this rapid initial rate more conclusively and reported the results of their experiments on the high-temperature hydrogenation of coal chars at hydrogen partial pressures up to 1000 atmospheres. By means of a specially constructed reactor heating device, Moseley and Paterson obtained rate data for methane production in 15-second intervals. With this resolution, they observed a rapid initial rate, which decreased with time until a final steady value was obtained. The steady-state methane production rate had many of the characteristics of rate data as as reported earlier by others, i.e., it was roughly proportional to hydrogen partial pressure and depended on char type. However, the rapid initial rate necessitated a new explanation and prompted Moseley and Paterson to suggest a three-step mechanism for the solid phase hydrogenation of coal.

The first step is the devolatilization of coal by a process which is activated by hydrogen but whose rate is not affected by hydrogen. In addition to volatile products, a char is produced in this first step with exposed or labile carbon atoms, which is particularly susceptible to reaction with hydrogen. The second step in the proposed mechanism involves the reactions of the labile carbon atoms, either with hydrogen to form methane or with each other in a cross-linking polymerization to form an inactive char. The third step involves the slow reaction of hydrogen with the inactive char.

Blackwood and McCarthy (3) have discounted the three-step process, offering instead a two-step mechanism consisting of a rapid reaction of hydrogen with groupings in the coal which are associated with oxygen followed by a more sedate attack on the residual carbon structure. Blackwood and McCarthy cited their own data (2,3) as well as Hiteshue's data (10,11) to support their claim, but, in fact, the poor initial time resolution of these data makes it difficult to distinguish between a two- or three-step process.

On the basis of their three-step model, Moseley and Paterson (15) projected that contact times in excess of 0.5 second were unlikely to lead to significant gains in the extent of carbon conversion to methane, and

that complete conversion of the carbon in coal to methane should be possible at 1000 C and 500 atm hydrogen partial pressure. In 1967, they published results of rapid high-temperature hydrogenation of bituminous coal, virtually substantiating their claim.(16) The carbon in the coal was gasified to completion at 500 atm and 900 C.

In point of fact, for contact times of a few seconds, only the first two steps of the three-step model are significant, and a satisfactory accounting of the direct methanation of coal may be obtained on this basis. Moseley and Paterson have presented mathematical relationships between methane yield and gasifier parameters, derived on the assumptions that the decomposition of structures in coal to give the active intermediate is a first-order process, and that the intermediate is simultaneously removed by a first-order process. Methane formation is assumed to give no net consumption of the active species. In this paper, alternate rate expressions are proposed for the first two steps, which result in a simple methane yield expression that properly extrapolates to low and high conversion.

The Initial Reaction

Studies of the thermal decomposition of coal have been carried out at BCURA, largely because of the importance of devolatilization in the ignition process of coal particles in pulverized fuel firing.(1,7) Although a large number of complex chemical reactions and physical changes are known to make up the devolatilization process, workers at BCURA were able to represent the grams of carbon lost as methane per gram of starting carbon, ΔW_I, for twelve coals tested as a function of absolute temperature, T, and time of residence at this temperature, t:

$$\Delta W_I = VM\,(1-C)Q\left\{\left(1- \exp - A\,[\exp - (B/T)]\,t\right)\right\} \qquad (1)$$

where VM = volatile matter in coal on daf basis

Q = ratio of weight loss to change in volatile matter

ABC = empirical constants

Their results were obtained for 20μ coal particles heated at rates of 2.5×10^4 to 5×10^4 C/sec. Since the mechanism for thermal decomposition depends upon the rate of heating of the coal particles, the quantitative results of this research may not apply directly to the initial reactions occurring in the direct methanation of coal. However, many of the aspects will undoubtedly remain the same--particularly the rapidity of the overall process.

By using typical values reported for the constants in Equation 1, $A = 1 \times 10^6$ sec; B = 8900 K, a time constant for the devolatilization process of 14 milliseconds is obtained at a temperature of 1750 F.

The significance of this value is its indication that the initial reaction per se should be essentially complete as soon as hot hydrogen-containing gas contacts the coal feed.

The amount of carbon, ΔW_I, released as methane to the gas phase during this initial step may be dependent on temperature and coal type, but should be independent of other gasifier parameters such as residence time and gas composition.

As indicated by Moseley and Paterson, the presence of hydrogen does, without a doubt, activate the initial "breakdown" of the basic coal "molecule" during thermal depolymerization. Because of the rapidity of these reactions, little experimental evidence has been accumulated to indicate the degree to which the presence of hydrogen affects the rate of this initial "breakdown."

It is apparent, however, both from the work data of Moseley and Paterson and of Glenn and co-workers, that a highly active species or intermediate appears to be the principal primary product of this initial breakdown. This may be shown schematically as:

$$\text{Coal} \xrightarrow{(H_2)} C^{**} + CH_4 + (CO,\ CO_2,\ H_2O,\ \text{etc.})$$

$$C^{**} \xrightarrow{R_1} C^{*}$$

$$C^{**} + H_2 \xrightarrow{R_2} CH_4$$

where,

C** = active intermediate produced directly from coal when coal is thermally depolymerized; and

C* = inactive char produced by reaction of the active intermediate with itself.

The Active Intermediate

The specific chemical processes involving the active intermediate are very complex; any attempt to model them must be viewed, as approximate. The approach taken by the present authors, as opposed to that proposed by Moseley and Paterson, is to consider explicitly the competition between the methanation reaction and the inactive char-forming reaction for the active intermediate.

To this end, consider that coal particles containing one gram of carbon are introduced into a reactor, maintained at a constant temperature, T, together with a gas whose hydrogen particle pressure is P_{H_2}. Consider that there is a sufficient supply of hydrogen so that P_{H_2} does not change as methanation proceeds and that the total gas-coal contact time in the reactor is τ. Assume that upon completion of the initial reaction W_o^* gram of active intermediate has been formed; W_o^* may in general be some fraction, f, of the ungasified carbon and that W_o^* may be represented by $f\ (1 - \Delta W_I)$.

The rate of reaction of hydrogen with carbon is generally taken as a linear function of hydrogen partial pressure and expressed per unit of surface area available for reaction.(4) If then, the rate at which the

active intermediate is removed by the char-forming mechanism is assumed to be a first-order process, a similar behavior may be postulated for the active intermediate, and the net rate of change of W*, the grams of active intermediate per gram of carbon fed, will be given by the following:

$$\frac{dW^*}{dt} = k_1' \left[P_{H_2}\right] \quad A^* - k_2 W^* \tag{2}$$

where A* = area associated with active intermediate

k_1', k_2 = rate constants of methane formation and deactivation reactions respectively

There are ways in which A* may be related to W*; however, at the temperatures and rates under which methanation proceeds, it is reasonable to assume that the methane formation reaction proceeds in a topochemical fashion at a shell-like reaction surface surrounding the active species. In this case A* is proportional to $(W^*)^{2/3}$, so that Equation 2 may be written as follows:

$$\frac{dW^*}{dt} = - k_1 \left[P_{H_2}\right] \quad (W^*)^{2/3} - k_2 W^* \tag{3}$$

where the rate constant k_1' and the proportionality constant relating A* to $(W^*)^{2/3}$ have been confined together in the symbol k_1.

The boundary condition on Equation 3 is that of the completion of the initial reaction (essentially t = o), W* = W_o*. Equation 3 may be integrated to find W* at any time t.

$$\int_{W_o^*}^{W^*} \frac{dW^*}{k_1 \left[P_{H_2}\right] (W^*)^{2/3} + k_2 W^*} = - \int_o^t dt$$

or

$$\ln \left[\frac{k_1(P_{H_2}) + k_2 (W^*)^{1/3}}{k_1(P_{H_2}) + k_2 (W_o^*)^{1/3}}\right] = - \frac{k_2 t}{3} \tag{4}$$

Of particular interest is the time t* when all of the active intermediate will have disappeared; i.e., at t = t*, W* = 0. From Equation 4

$$t^* = \frac{3}{k_2} \ln \left[1 + \frac{1}{S}\right] \tag{5}$$

where $S = \frac{k_1 (P_{H_2})}{k_2 (W_o^*)^{1/3}} = \frac{k_1 (P_{H_2})(W_o^*)^{2/3}}{k_2 W_o^*} = \frac{\text{Initial rate of Methanation}}{\text{Initial rate of Deactivation}}$

Notice that S represents a selectivity for the reacting system.

If t* is less than τ, the gas-coal contact time, then all of the available intermediate will be consumed in the reactor and methane yield will be independent of τ.

In order to compute the methane produced during this process, it is necessary to integrate the rate expression for the reaction of hydrogen with the active intermediate. If W_c denotes the weight fraction of carbon in coal which has appeared as methane, the rate expression for W_c is:

$$\frac{dWc}{dt} = k_1 \left[P_{H_2}\right] (W^*)^{2/3} \qquad (6)$$

where t = o corresponds to the end of the initial reaction and where $W_c = \Delta W_I$. Since the expression for W* as a function of time is known from Equation 4, Equation 6 may be integrated to t = t*, at which point the active intermediate has been completely consumed and $W_c = \Delta W_c$, the total yield of methane from the short time methanation process. Continued exposure of the inactive char to hydrogen will result in further methane production, but at a much reduced rate. The expression for ΔW_c is obtained from the integral

$$\int_{\Delta W_I}^{\Delta W_c} dW_c = 3W_o^* S \int_o^{t^*} \left[(1 + S)\, e^{-\frac{k_2 t}{3}} - S\right]^3 \frac{k_2}{3}\, dt$$

When the right hand side of this equation is integrated and the expression for t* substituted from Equation 5, the resultant expression is:

$$\Delta W_c = \Delta W_I + 3W_o^* S^3 \left[\ln\left(1 + \frac{1}{S}\right) - \left(\frac{1}{S} - \frac{1}{2S^2}\right)\right] \qquad (7)$$

If the series expansion for $\ln(1 + \frac{1}{S})$ is invoked, the square bracketed term in Equation 7 becomes equal to

$$\frac{1}{3S^3}\left[1 - \frac{3}{4S} + \frac{3}{5S} - + \cdots\right]$$

which is closely approximated by the rational fraction

$$\frac{1}{3S^3}\left[\frac{1}{1 + \frac{3}{4S}}\right]$$

hence, Equation 7 becomes

$$\Delta W_c = \Delta W_I + \frac{\frac{4}{3} W_o^* S}{1 + \frac{4}{3} S}$$

Again, if W_c^* and S are replaced by their equivalent expressions, the final relationship between methane yield and gasifier parameters is

$$\Delta W_c = \Delta W_I + \frac{\frac{4 F (1 - \Delta W_I) k_1}{3 k_2 (W_o^*)^{1/3}} (P_{H_2})}{1 + \frac{4 k_1}{3 k_2 (W_o^*)^{1/3}} (P_{H_2})} \qquad (8)$$

Equation 8 predicts that in the absence of hydrogen, methane yield is due only to the thermally induced decomposition. At small hydrogen partial pressures, the denominator is approximately one, and methane yield is proportional to hydrogen partial pressure. At high hydrogen partial pressures, methane yield again becomes constant, being given by the expression $\Delta W_c = \Delta W_I + f\ (1-\Delta W_I)$. If $f = 1$, complete methanation of the carbon in coal is possible.

Correlation of Experimental Data

Equation 8 indicates that the methane yield resulting from the direct methanation of coal by gases containing large excesses of hydrogen should be correlated by an equation of the form

$$\Delta W_c = b_1 + \frac{b_2 (P_{H_2})}{1 + b_3 (P_{H_2})} \qquad (9)$$

where b_1, b_2, and b_3 are correlation constants related to the kinetic parameters for the process.

The methane rate data for lignite and Elkol coal previously reported by Glenn and co-workers (8) were obtained in continuous flow experiments which did not employ large excesses of hydrogen. However, the presence of CO and H_2O in the feed gas permitted replacement of consumed hydrogen via the water-gas shift reaction. Comparison of inlet and outlet gas compositions for these continuous flow experiments shows only slight variations in hydrogen partial pressure values, so that the constancy of P_{H_2} is considered a reasonably valid assumption.

Equation 9 was fitted to the CFR data by a non-linear least squares curve fitting routine.(12) The results of the correlation were:

$$\text{Lignite:}\quad \Delta W_c = 0.07 + \frac{0.0062\,(P_{H_2})}{1 + 0.0067\,(P_{H_2})} \tag{10}$$

$$\text{Elkol coal:}\quad \Delta W_c = 0.08 + \frac{0.0054\,(P_{H_2})}{1 + 0.006\,(P_{H_2})} \tag{11}$$

Equation 10 explains 63 percent of the variance in the lignite data; equation 11 explains 52 percent of that in the Elkol coal data. The effect of changes in P_{H_2} on ΔW_c for the two coals is shown in Figure 1. In the operating region for the continuous flow reactor, the hydrogen partial pressures were low enough so that the predicted curve is approximately linear in hydrogen partial pressure.

If the proposed methane-hydrogen relationship is valid, Equations 10 and 11 should extrapolate correctly for methanation experiments carried out at similar temperatures and higher hydrogen partial pressures. In a study of the rapid high-temperature, high-pressure hydrogenation of bituminous coal, Moseley and Paterson gasified coal in pure hydrogen at temperatures of 950 C and pressures as high as 500 atm.(16) Figure 2 presents their experimental data together with typical data points from the CFR experiments of Glenn and co-workers. The curve through the data is Equation 11; the agreement is good over the entire pressure range.

Moseley and Paterson also reported data from a few experiments at 850 C. Since the parameters in the correlating equation depend upon temperature, Equation 11 cannot be applied directly to these lower temperature results. However, an equation of the form of Equation 9 does fit the data quite well, provided the constants are adjusted as indicated in the following equation:

$$\Delta W_c = 0.07 + \frac{0.0033(P_{H_2})}{1 + 0.0035(P_{H_2})} \tag{12}$$

The 850 C data points and Equation 12 are presented in Figure 3.

Lewis, Friedman, and Hiteshue (13) reported data on the direct conversion of untreated bituminous coal into high Btu gas in a dilute-phase concurrent flow apparatus similar to that used by Glenn and co-workers in the CFR experiments, and by Moseley and Paterson in their later work. The residence times used by Lewis *et al* were somewhat longer than those used by Glenn and co-workers and their operating temperature was lower, i.e., 725 C. The data of Lewis *et al* shown in Figure 4 may be correlated by the following equation:

$$\Delta W_c = 0.09 + \frac{0.0016(P_{H_2})}{1 + 0.0017(P_{H_2})} \tag{13}$$

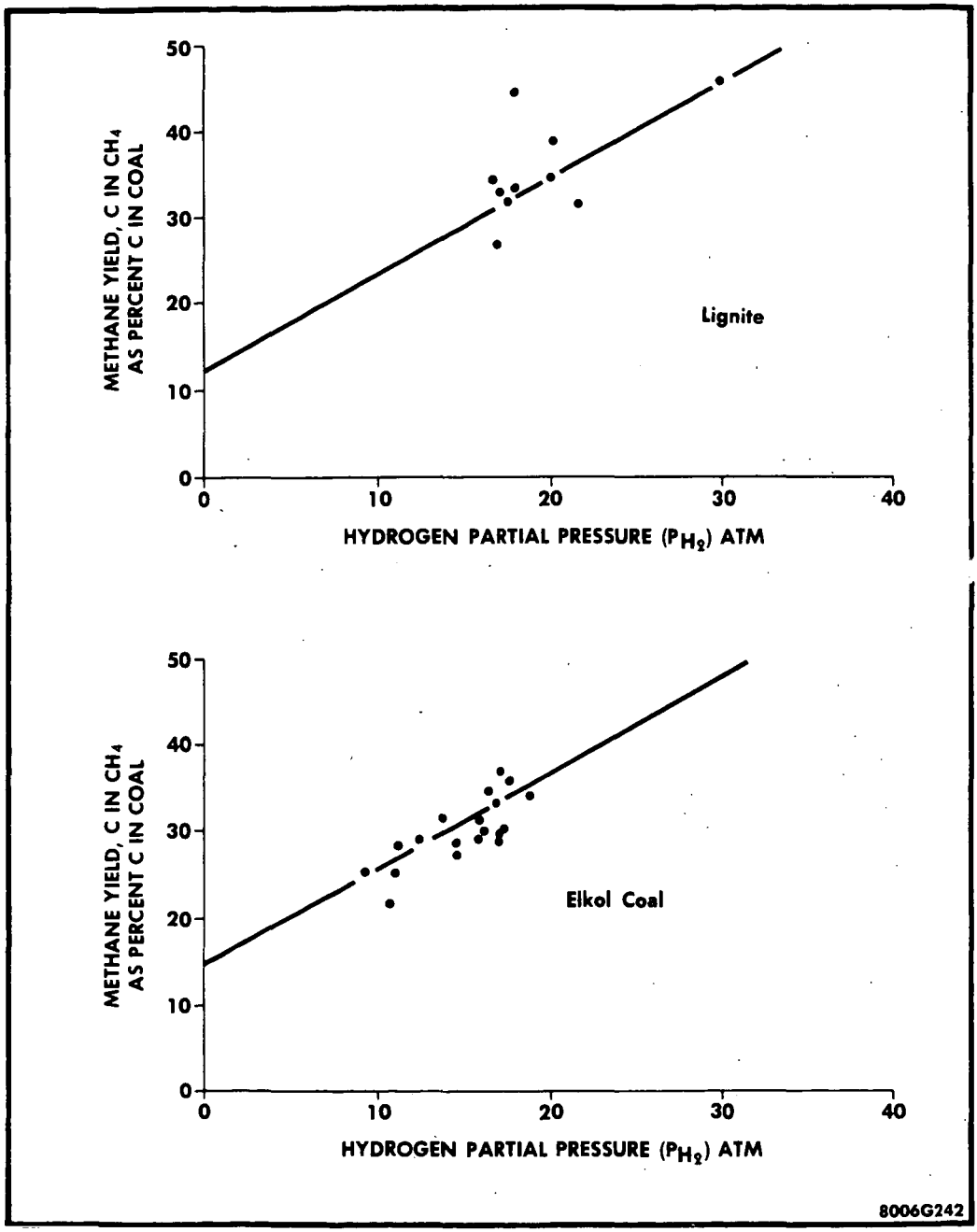

Figure 1. Correlation of Methane Yield with Hydrogen Partial Pressure

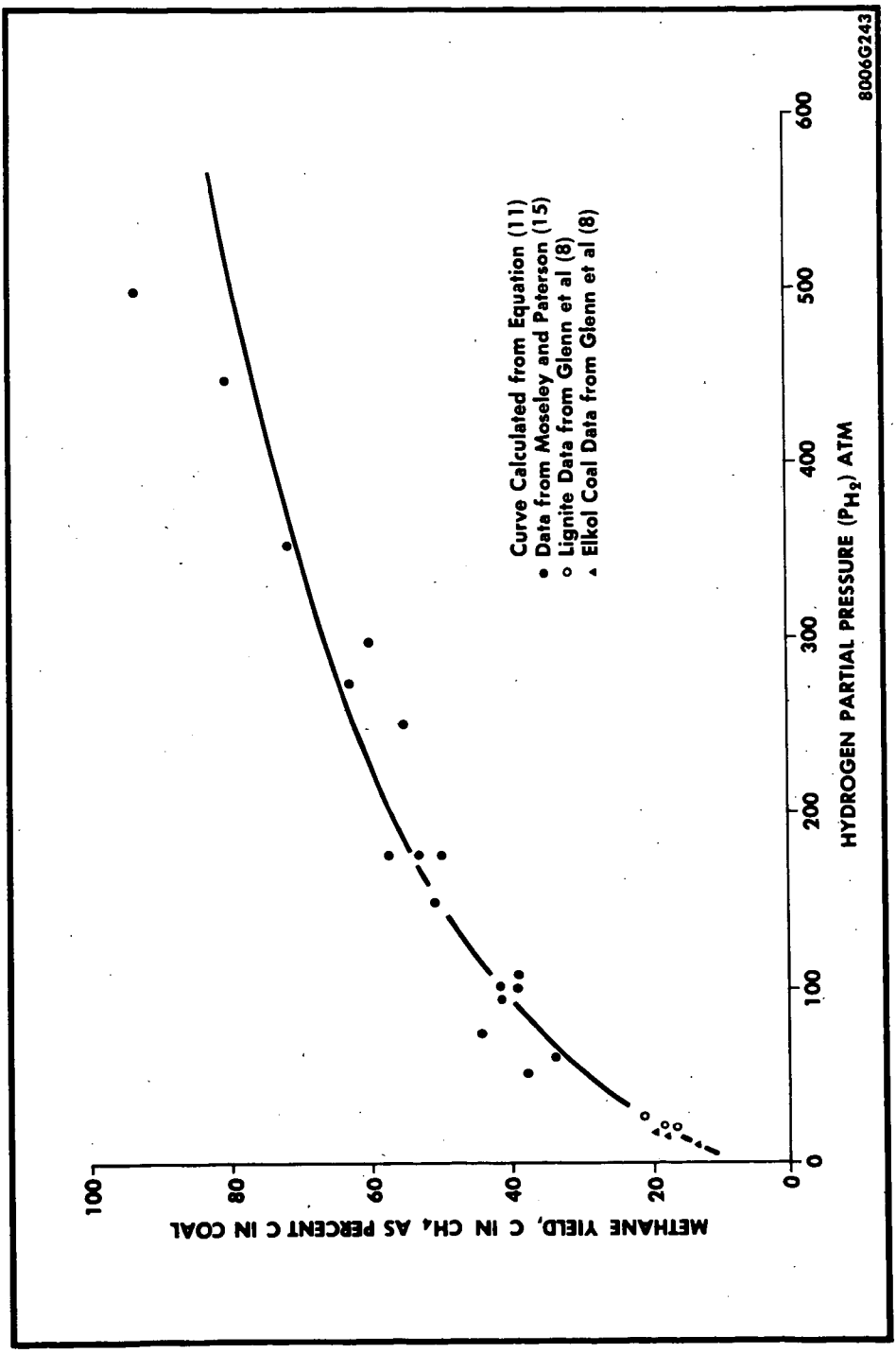

Figure 2. Correlation of Methane Yield with Hydrogen Partial Pressure at 950° C

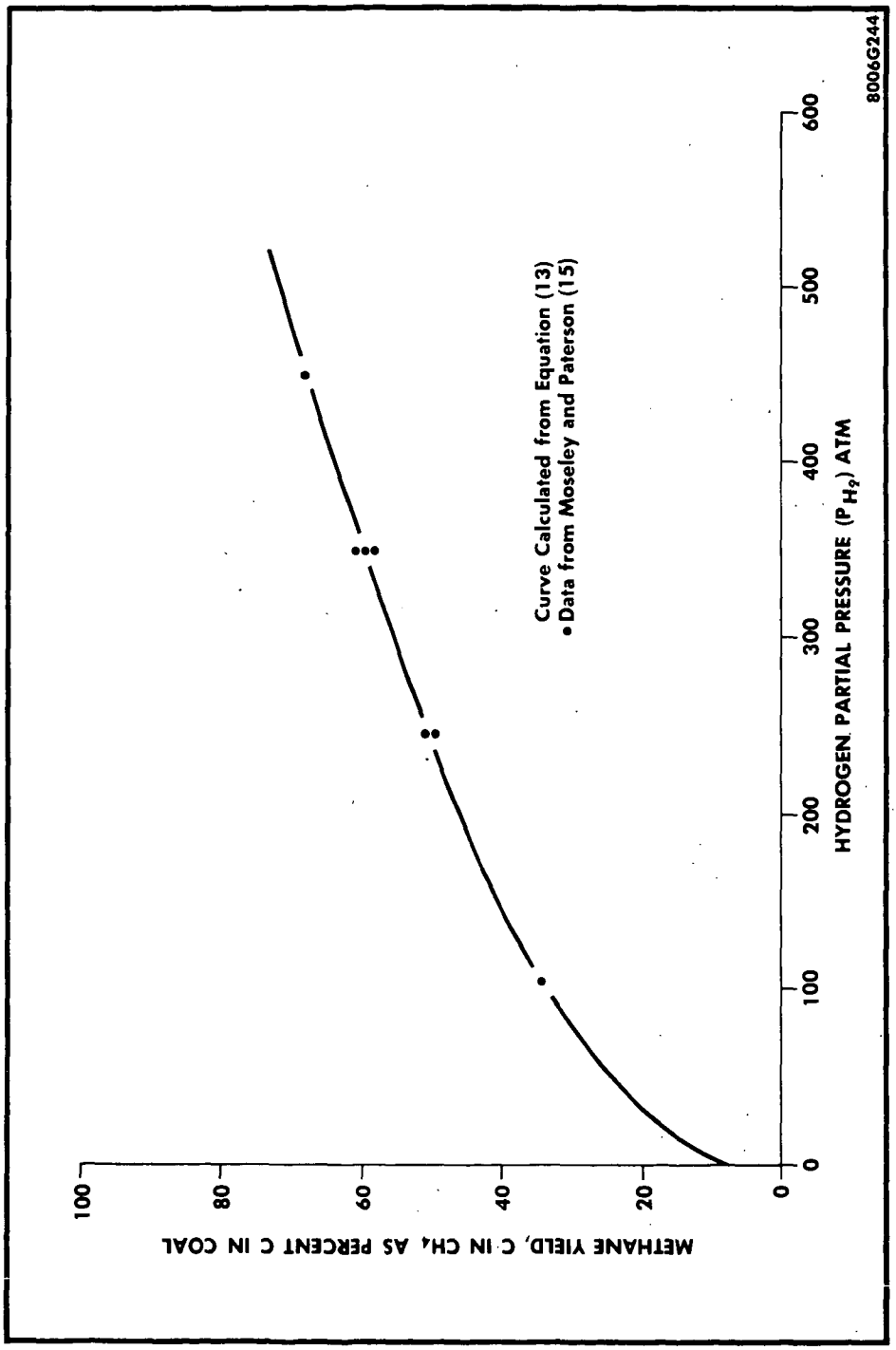

Figure 3. Correlation of Methane Yield with Hydrogen Partial Pressure at 850° C

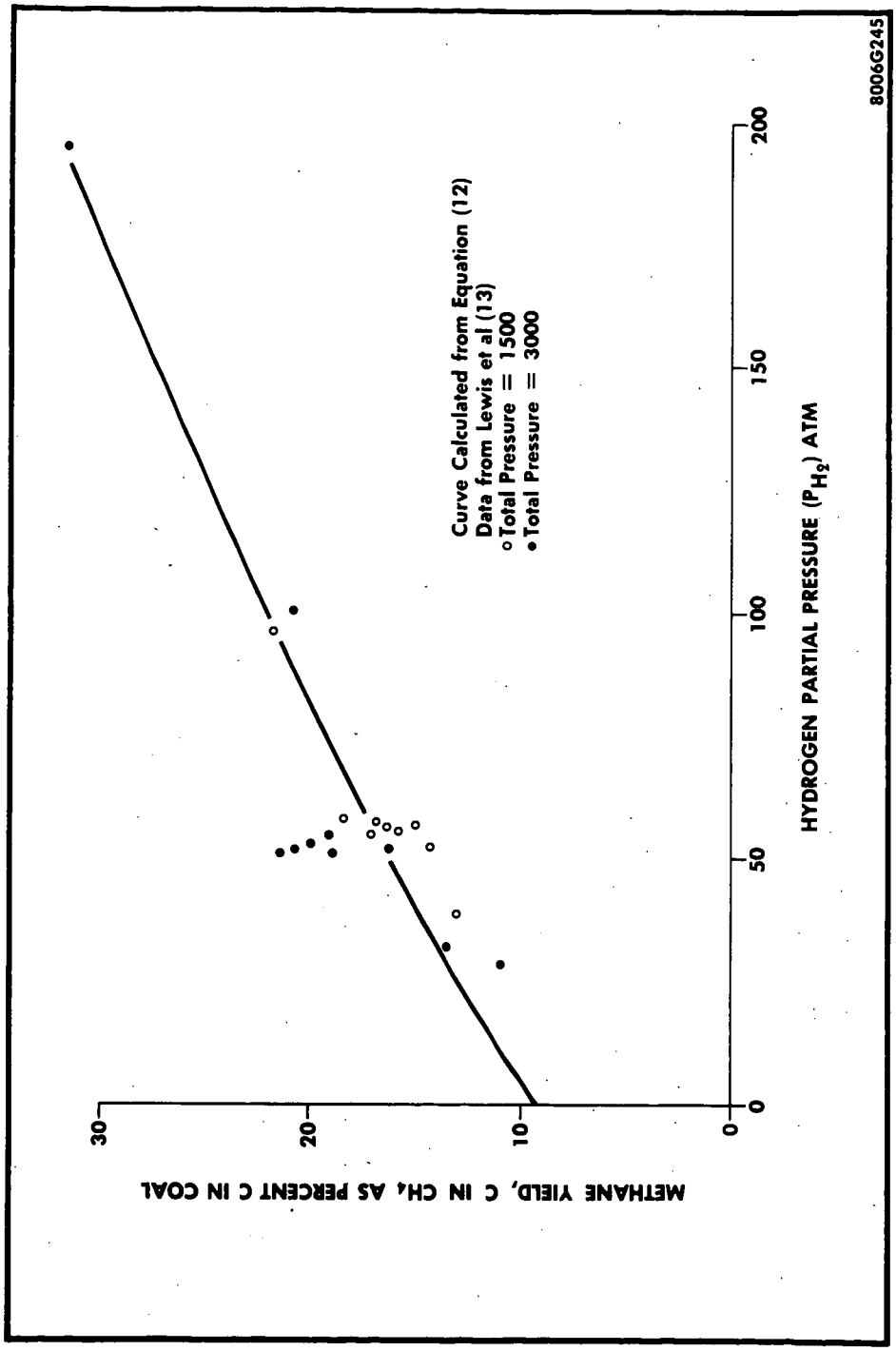

Figure 4. Correlation of Methane Yield with Hydrogen Partial Pressure at 725° C

All of these correlations indicate that methane yield values of one are possible if high enough hydrogen partial pressures are used. Furthermore, it is interesting that an Arrhenius plot of the parameter b_2 (or b_3) gives a reasonably straight line. (See Figure 5.) Since b_2 represents the ratio of k_1 to k_2, one would expect such a fit, and the observed activation energy of 15 Kcal indicates the difference in activation energy between the methanation and the deactivation processes.

The expression for methane yield, as represented by Equation 8, provides a framework for unifying and correlating data on the direct methanation of coal with hydrogen. The fact that the behavior of a variety of coals is consistent with this expression lends support to the hypothesis of the formation of an active intermediate. The fact that the postulated ratio of rate constants for the reactions involving this active intermediate exhibits an Arrhenius behavior further supports this claim and indicates the general validity of the derivation.

It should be pointed out, however, that the rate expressions used to obtain Equation 8 are by no means unique. The unique concept in the analysis is the treatment of the methanation and deactivation steps as being competitive reactions which essentially consume the entire supply of active intermediate in a finite time. For example, if both reactions are assumed to be zero-order with respect to the active intermediate, or if the intermediate concentration at the reaction sites is assumed to be a constant, the equation for the rate of change of W* would be as follows:

$$\frac{dW^*}{dt} = -\hat{k}_1 (P_{H_2}) - \hat{k}_2 \qquad (14)$$

where $\hat{k}_1$ and $\hat{k}_2$ are the rate constants associated with the methane formation and deactivation reactions, now considered zero-order with respect to intermediate concentration.

Integration of Equation 9 in the same manner as before, defines the time to consume the intermediate entirely, t*, to be in this case

$$t^* = \frac{1}{k_2} \quad \frac{W_o^*}{1 + \hat{S}}$$

where $\hat{S} = \dfrac{\hat{k}_1 (P_{H_2})}{\hat{k}_1}$ = selectivity for zero-order assumption.

The methane yield under this condition, ΔW_c, is given as follows

$$\Delta W_c = \Delta W_I + \hat{k}_1 P_{H_2} t^* = \Delta W_I + \frac{f\,(1-\Delta W_I)\,\dfrac{\hat{k}_1 (P_{H_2})}{\hat{k}_2}}{1 + \dfrac{\hat{k}_1 (P_{H_2})}{\hat{k}_2}} \qquad (15)$$

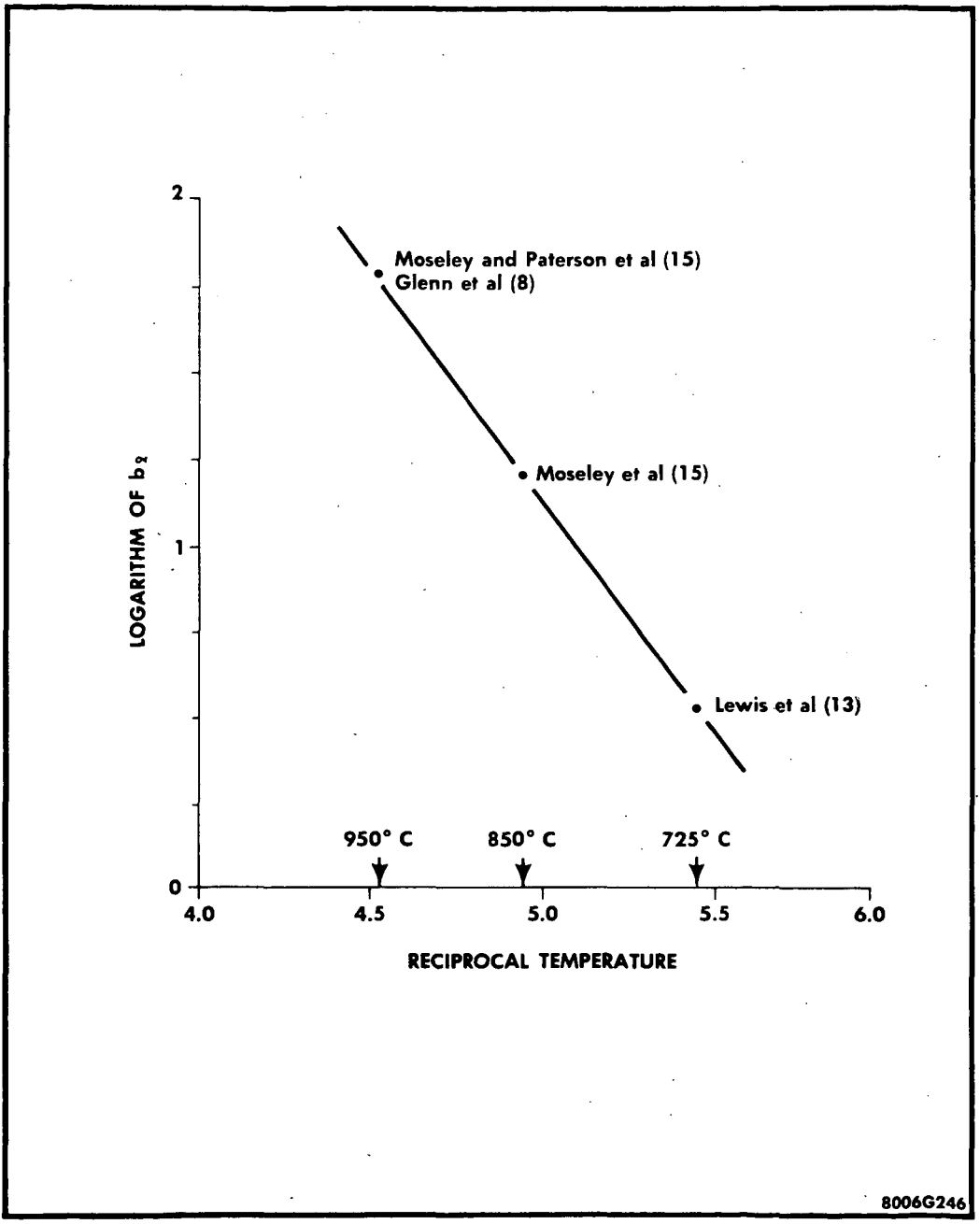

Figure 5. Arrhenius Plot of Parameter b_2

Equation 15 is identical in form to Equation 8 and indicates that there are a number of ways of obtaining the expression which correlates methane yield with hydrogen partial pressure. Thus, even though Equation 8 successfully fits the available data, the nature of the exact mechanism of the reactions involving the active intermediate is still unresolved.

This does not detract from the utility or significance of the yield expression, however. The important point is that the rapid rate of methanation of coal, observed by Moseley and Paterson (16) at high hydrogen partial pressures, has also been shown to be achieved at lower hydrogen partial pressures and in the presence of other gaseous species. Moreover, both conditions are explained by a single equation. The implication, then, is that synthesis gas and steam can be effectively used in a short-contact-time reactor to take advantage of the high activity imparted to coal by rapid heating in the presence of hydrogen. This feature, of course, is the essence of the BCR two-stage super-pressure gasifier.

The specific equations for methane yield, because of their simplicity and independence of most gasifier parameters, can be utilized in the design and engineering evaluation of integrated, multistage gasifiers. This is being done for the BCR two-stage gasifier in order to make better predictions of its ultimate capability as well as to assess effects of process variables and novel operating practices.

Acknowledgment

This paper is based on work carried out at Bituminous Coal Research, Inc., with support from the Office of Coal Research, U.S. Department of the Interior, under Contract No. 14-01-0001-324. Also, the stimulating comments of Dr. E. E. Donath regarding the work are most gratefully acknowledged.

REFERENCES

1. "BCURA annual report 1966," Brit. Coal Util. Res. Assoc., Leatherhead, England, 1967.

2. Birch, T. J., Hall, K. R., and Urie, R., "Gasification of brown coal with hydrogen in a continuous fluidized-bed reactor," J. Inst. Fuel 33, 422-35 (1960).

3. Blackwood, J. D. and McCarthy, D. J., "The mechanism of the hydrogenation of coal to methane," Australian J. Chem. 19, 797-813 (1966).

4. Blackwood, J. D., "The reaction of carbon with hydrogen at high pressure," Australian J. Chem. 12, 14 (1959).

5. Donath, E. E. and Glenn, R. A., "Pipeline gas from coal by two-stage entrained gasification," in "Operating Section Proceedings," New York: Am. Gas Assoc., 1965. pp 65-P-147--151.

6. Feldkirchner, H. L. and Linden, H. R., "Reactivity of coals in high pressure gasification with hydrogen and steam," Ind. Eng. Chem., Process Design Develop. 2 (2), 153-62 (1963).

7. Field, M. A., Gill, D. W., Morgan, B. B., Hawksley, P. G. W., "Combustion of Pulverised Coal." Leatherhead, England: Brit. Coal Util. Res. Assoc., 1967.

8. Glenn, R. A., Donath, E. E., and Grace, R. J., "Gasification of coal under conditions simulating stage 2 of the BCR two-stage super-pressure gasifier," in "Fuel Gasification," Washington: Am. Chem. Soc., 1967. pp 81-103.

9. Glenn, R. A. and Grace, R. J., "An internally-fired process and development unit for gasification of coal under conditions simulating stage two of the BCR two-stage super-pressure process," Am. Gas Assoc., Synthetic Pipeline Gas Symp., Pittsburgh, Pa., 1968.

10. Hiteshue, R. W., Friedman, S., and Madden, R., "Hydrogasification of bituminous coals, lignite, anthracite, and char," U.S. Bur. Mines, Rept. Invest. 6125 (1962).

11. Hiteshue, R. W., Friedman, S., and Madden, R., "Hydrogasification of high-volatile A bituminous coal," U.S. Bur. Mines, Rept. Invest. 6376 (1964).

12. Marquardt, D. W., "Least-squares estimation of nonlinear parameters," Computer Program in Fortran IV Language, IBM Share Library, Distribution No. 3094 (1964).

13. Lewis, S., Friedman, S., and Hiteshue, R. W., "High Btu gas by the direct conversion of coal," in "Fuel Gasification," Washington: American Chemical Society, 1967. pp 50-63.

14. Moseley, F. and Paterson, D., "The rapid high-temperature hydrogenation of coal chars. Part 1: Hydrogen pressures up to 100 atmospheres," J. Ins. Fuel 38 (288), 13-23 (1965).

15. Moseley, F. and Paterson, D., "The rapid high-temperature hydrogenation of coal chars. Part 2: Hydrogen pressures up to 1000 atmospheres," J. Inst. Fuel 38 (296), 378-91 (1965).

16. Moseley, F. and Paterson, D., "The rapid high-temperature high pressure hydrogenation of bituminous coal," J. Inst. Fuel 40, 523-30 (1967).

17. Von Fredersdorff, C. G. and Elliot, M. A., "Coal Gasification," in "Chemistry of Coal Utilization," New York: John Wiley & Sons, Inc., 1963. pp 892-1022.

NOMENCLATURE

A^*	area associated with active intermediate, cm^2
A,B,C	empirical constants in devolatilization yield equation
b_1, b_2, b_3	empirical constants in methane yield correlation equation
C^{**}	active intermediate
C^*	inactive char
k_1', k_1, k_2	kinetic parameters in methanation reactions
P_{H_2}	partial pressure of hydrogen, atm
Q	constant in devolatilization equation representing the ratio of unit change in coal weight per unit change in volatile matter content
S	reaction selectivity
T	reactor temperature, °K
t	time of reaction, sec
t^*	time required to deplete active intermediate, sec
τ	residence time of coal particles in reactor, sec
VM	volatile matter in coal, daf basis, percent
W^*	weight of active intermediate per gram of carbon fed at any time
W_o^*	weight of active intermediate per gram of carbon fed at time zero
ΔW_I	weight of carbon lost by initial devolatilization per gram of carbon fed
W_c	total weight of carbon appearing as methane at any time per gram of carbon fed

EFFECT OF INCREASING FREE SPACE ABOVE THE CHARGE ON THE COMPOSITION AND YIELD OF THE VOLATILE PRODUCTS FROM COAL CARBONIZATION

C. Ortuglio, J. G. Walters, and D. E. Wolfson

U. S. Department of the Interior, Bureau of Mines
Pittsburgh Coal Research Center, Pittsburgh, Pa. 15213

ABSTRACT

The effect of increasing the free space above the charge on the composition and yields of the volatile products from the carbonization of Pittsburgh-bed coal and one industrially used blend from the eastern United States and one from western United States was investigated with the BM-AGA carbonization apparatus.

Increasing the free space above the charge from 1 inch to 3 inches, to 6 inches and to 9 inches resulted in lower tar yields and increased gas and light oil yields. Anthracene and naphthalene yields were increased, quinoline and benzene insoluble fractions of both the tar and pitch increased considerably with increased free space, although the carbon content of the tars and pitches increased only slightly.

Increased cracking, a result of the increase in free space, caused a decrease in the yields of tar acids, tar bases, neutral oils, olefins, aromatics, and paraffins and naphthenes. Gas composition was relatively constant; hydrogen and methane tended to increase and ethane decrease.

Results of the investigation are being used to design a unit to upgrade the volatile products of carbonization by cracking the hot products as they leave the carbonization chamber.

INTRODUCTION

The Bureau of Mines, in cooperation with the American Gas Association, jointly developed a pilot-scale carbonization test apparatus (BM-AGA) to determine the carbonization characteristics of coals and to evaluate the byproduct yields (5).

Although the BM-AGA test apparatus is used primarily to determine the coking characteristics of coals for metallurgical use, the objective of this investigation was to determine the effect of cracking on the quality of carbonization products by varying the free space above the coal charge when the temperature is kept constant.

Carbonization yields are influenced by the rank of coal carbonized, whereas their composition is primarily a function of the temperature and contact time of the evolved vapors with the heated surfaces within the retort or ovens. Decomposition of vapors proceeds in two steps: Primary decomposition of gaseous vapors as they are evolved from the plastic layer at moderate temperatures and then pass through the hot coke surfaces, and secondary decomposition as the vapors pass through the free space above the coal charge with less contact surface. Porter (4) in a study of coal carbonizing equipment has found that the variance of contact time of the gases and vapors passing through the heated spaces in approved industrial ovens may be 100 percent or more.

EXPERIMENTAL PROCEDURES

Procedure and apparatus for BM-AGA carbonization tests have been described in detail in a previous publication (5). Basically, the apparatus consists of a cylindrical steel retort, electrically controlled resistance-type furnace, product

recovery train, gas scrubbers, meters, and sampler. The standard retort used throughout this investigation is 26 inches high and 18 inches in diameter. The results from previous carbonization tests, using standard retorts and 900°C carbonization temperatures have been correlated with industrial (7) and experimental oven (6, 8) data. The coal charges were adjusted in height so as to leave 1-, 3-, 6-, and 9-inches of free space above the coal charge. Duplicate carbonization tests were made at 900°C and the results reported are averages of two determinations.

A single coal (1166) and two commercial coal blends (1161 and 1167A) were used in this investigation. Coal 1161 was carbonized as received so that the size consist would be comparable to that charged at the coke plant. Coals for tests 1166 and 1167A were received separately in lump form and were crushed in the hammer-mill and blended.

In computing yields from BM-AGA carbonization tests, the quantitative yields are based on U. S. gallons (231 cubic inches) and short tons (2,000 pounds). Coke yields are reported as dry coke, weight-percent of coal carbonized. The yield, specific gravity (determined), and gross heating value of the gas are reported as stripped of light oil and saturated with water vapor at 60°F and under a pressure equivalent to 30 inches of mercury. Light oil refers to the crude product stripped from the gas. Liquor includes the fixed ammonia and absorbed free ammonia. Ammonium sulfate is reported in pounds per ton of coal and includes the total free and fixed ammonia. The tar yield, properties, and constituents are reported on a dry basis and includes only that light oil which condenses with the tar, and the specific gravity of the tar is reported at 15.5°C/15.5°C.

The yields of carbonization products are given on the as-carbonized basis (table 1). The latter basis is used to compare coals when the moisture and ash contents differ significantly. Comparisons lose their significance because a high percentage of ash or moisture makes the yield of coke or liquor artifically high and those of other products correspondingly low. The calculation of moisture- and ash-free basis assumes that all ash remains in the coke and that all moisture in the coal is recovered as liquor.

Properties of Tar

The tar yields are affected by coal rank, temperature of carbonization and free space above the coal charge. The temperature of carbonization is the most significant contributing factor in determining tar quality. Increased free space permits the vapors to remain longer at the higher temperature resulting in considerable variations in tar quality.

The effect of free space on tar quality is presented in table 2. Cracking of tar due to increased free space resulted in progressive increases in its specific gravity, naphthalene yield, anthracene yield, except for the 9-inch free space and a reduction in tar acids, bases, and neutral oils. It is interesting to note that unlike naphthalene, the anthracene yield was slightly less at the 9-inch free space for all tests. There was no significant change in the residue yield.

The chemical composition of tars and pitches is presented in table 3. As expected, the carbon content increased and the hydrogen content decreased with progressive increases in the free space.

Quinoline (1) and benzene (free carbon) (5) insoluble values for the tars and pitches, as well as the softening point of the pitches were determined. These are critical factors, commercially important, in determining the suitability of coal tar pitches as electrode binders. The tar values were determined on the whole tar and the pitch values were determined on the +350°C fraction of the tar. The cube-in-air method was used to determine the softening point of the pitches. The results are presented in table 4.

Table 1. - Yields of carbonization products, as-carbonized basis

Coal number	Free space inches	Yields, weight-percent							Yields per ton of coal			
		Coke	Gas	Tar	Light oil	Liquor	Free ammonia	Total	Gas cu. ft.	Tar gallons	Light oil in gas gallons	Ammonium sulfate, pounds
1161	1	65.9	18.2	5.8	1.13	8.8	0.160	100.0	10,450	11.9	2.81	21.3
	3	65.6	16.5	5.5	1.17	10.2	.177	99.1	10,640	11.2	3.25	23.6
	6	65.7	16.2	5.5	1.23	10.3	.180	99.1	10,770	11.1	3.42	22.8
	9	65.5	16.3	5.3	1.13	10.0	.209	98.4	10,790	10.2	3.16	23.1
1166	1	66.3	14.9	7.6	1.28	8.8	.166	99.0	10,400	15.8	3.57	25.3
	3	66.3	15.3	8.1	1.24	8.0	.168	99.1	10,750	16.5	3.45	23.7
	6	66.4	15.3	7.7	1.31	7.6	.173	98.5	10,700	15.2	3.64	22.6
	9	66.4	15.2	7.5	1.37	7.7	.174	98.3	10,850	14.8	3.81	22.1
1167A	1	70.8	13.6	6.7	1.16	7.0	.163	99.4	10,140	13.7	3.23	23.2
	3	70.7	13.9	6.4	1.15	6.2	.161	98.5	10,290	12.9	3.20	20.8
	6	70.7	13.9	6.2	1.24	6.1	.164	98.3	10,350	12.1	3.47	20.0
	9	70.7	14.1	6.1	1.21	6.3	.149	98.6	10,490	11.9	3.36	18.8

Table 2. - Specific gravity and component tar yields

Coal number	Void space inches	Specific gravity of tar	Yields, gallons per ton							Yields, pounds per ton	
							Neutral Oils				
			Acids	Bases	Neutral oils	Residue	Olefins	Aromatics	Paraffins and Naphthenes	Naphthalene	Anthracene
1161	1	1.17	0.52	0.33	3.50	6.82	0.39	2.95	0.16	5.36	2.81
	3	1.19	.35	.27	2.89	6.60	.31	2.52	.06	7.42	3.58
	6	1.20	.20	.22	2.31	7.10	.25	2.04	.02	8.70	5.25
	9	1.23	.11	.15	1.63	7.03	.17	1.45	<.01	9.55	4.71
1166	1	1.16	.78	.32	3.95	10.26	.33	3.52	.10	3.57	1.36
	3	1.18	.55	.28	3.69	10.87	.32	3.33	.04	7.20	2.34
	6	1.20	.25	.24	2.57	10.89	.29	2.26	.02	10.32	3.27
	9	1.21	.20	.22	2.20	10.86	.24	1.95	.01	11.59	2.52
1167A	1	1.17	.69	.27	3.50	8.68	.31	3.14	.09	4.14	1.92
	3	1.19	.37	.26	2.41	8.82	.20	2.19	.03	7.53	3.12
	6	1.22	.21	.18	1.98	8.54	.21	1.76	.01	8.97	3.31
	9	1.22	.17	.17	1.78	8.57	.21	1.57	.01	9.92	2.95

Table 3. - Effect of free space on the chemical composition of tar and pitch

Void space, inches	Tar				Pitch			
	1	3	6	9	1	3	6	9
				Coal 1161				
Hydrogen.....	5.7	5.2	5.0	4.7	4.8	4.4	4.3	3.9
Carbon.....	90.5	91.4	92.7	93.1	92.3	92.8	93.8	94.2
Nitrogen.....	1.1	1.2	1.1	1.0	1.4	1.3	1.2	1.0
Oxygen.....	2.2	1.7	0.7	0.7	1.1	1.1	0.3	0.4
Sulfur.....	0.4	0.4	.4	.4	0.3	0.3	.3	.3
Ash.....	.1	.1	.1	.1	.1	.1	.1	.2
				Coal 1166				
Hydrogen.....	5.4	5.0	4.8	4.7	4.9	4.7	4.6	4.2
Carbon.....	89.7	90.4	90.8	91.1	90.5	91.0	91.9	92.1
Nitrogen.....	1.3	1.3	1.2	1.1	1.5	1.4	1.3	1.3
Oxygen.....	2.5	2.2	2.1	2.0	2.1	2.0	1.3	1.6
Sulfur.....	1.0	1.0	1.0	1.0	0.8	0.7	0.7	0.7
Ash.....	0.1	0.1	0.1	0.1	.2	.2	.2	.1
				Coal 1167A				
Hydrogen.....	5.8	5.4	5.1	5.0	4.9	4.7	4.6	4.4
Carbon.....	90.3	92.0	91.5	92.0	91.1	91.6	92.0	92.2
Nitrogen.....	1.3	1.3	1.3	1.3	1.5	1.4	1.4	1.3
Oxygen.....	1.4	0.4	1.0	0.6	1.7	1.5	1.2	1.3
Sulfur.....	1.0	.8	1.0	1.0	0.7	0.7	0.7	0.7
Ash.....	0.2	.1	0.1	0.1	.1	.1	.1	.1

Table 4. - Effect of free space above coal charge on quinoline and benzene insolubles

Coal number	Void space, inches	Tar[1]		Pitch[1]		Softening point, °C
		Quinoline insolubles	Benzene insolubles	Quinoline insolubles	Benzene insolubles	
1161	1	1.70	6.61	3.85	25.95	119.0
	3	2.73	8.17	3.96	24.25	105.0
	6	4.84	11.29	8.87	28.33	110.0
	9	11.07	17.42	22.03	32.55	138.0
1166	1	2.26	8.64	2.82	22.55	96.8
	3	4.13	11.60	4.78	26.55	101.0
	6	7.29	14.26	9.14	28.33	94.0
	9	11.15	18.76	14.34	30.87	85.8
1167A	1	2.57	7.66	2.86	21.75	94.0
	3	3.87	10.34	4.73	23.70	94.3
	6	6.39	12.47	7.60	25.15	82.3
	9	9.50	15.46	12.15	27.85	85.0

[1]Weight-percent for tar and pitch.

The insolubility values for all tars and pitches increased with increasing free space. There were marked increases at the 9-inch free space for all tests, indicating the formation of insoluble high boiling hydrocarbons.

Properties of Gas

Properties of byproduct gas vary with carbonizing conditions as well as with coal characteristics. An investigation (9) of the gas yielded by coals carbonized by the BM-AGA method at 900°C showed that the physical and chemical properties of the gas depend on the rank of coal.

The yield of carbonization gas increases with increased carbonization temperature; similarly, maintaining the effluent vapors at elevated temperatures by increasing the free space above the coal charge exposes the vapors to high temperatures for a longer time resulting in degradation of the volatile material with a still greater increase in the gas yield. Davis and Auvil (3) have attributed this increase to greater cracking of hydrocarbons in the enlarged free space. Table 1, confirms these results, in that the gas yield increases with increased free space.

The chemical and physical properties of the gas are presented in table 5. Two important properties of gas are its heating value and hydrogen sulfide content. The heating value, generally considered to be the most important property of byproduct gas, is presented on both the cubic foot and pound-of-coal basis. The greatest heat recovery for the longest exposure time of gas in the retort was 112 Btu per pound of coal (1167A) or a gain of 224,000 Btu per ton of coal. Coal 1161 showed a steady decline in heating value with increased exposure time.

The hydrogen sulfide content of the gas, calculated to grains per 100 cubic feet of gas, is becoming increasingly important because of air pollution restrictions, and must be reduced to limited concentrations before disposal. Results indicate that the formation of hydrogen sulfide is related to exposure time; however, the concentration of hydrogen sulfide in the byproduct gas is dependent on the sulfur content of the coal and is not related to coal rank. Although the sulfur content for coal 1167A (1.4 percent) was higher than that for coal 1161 (0.6 percent), the net increase in hydrogen sulfide, attributed to free-space cracking, was only 14.8 percent, compared with 26.0 percent for coal 1161.

Light Oil

The composition of light oil, like the tar, is a function of the carbonizing conditions of which temperature, free space above the coal charge, and the contact time of the gas in the hot free space are the most important; however, the total yield of light oil under normal carbonizing conditions is dependent largely upon the rank of the coal.

Benzene, the principal constituent of the light oil, is a decomposition product whose formation is accelerated under conditions favorable to cracking effluent vapors.

The percent composition of benzene in the light oil, as presented in table 6, progressively increased with an increase in free space, whereas all other constituents of light oil were adversely affected by the free space increases.

The total light oil yield reached a maximum at the 6-inch free space for the coal blends and at the 9-inch free space for the straight coal.

Table 5. - Chemical and physical properties of gas

Coal number	Void space, inches	Composition, dry, volume-percent					Heating value		Hydrogen sulfide grains per 100 cu.ft.
		Hydrogen	Carbon monoxide	Methane	Ethane	Ethylene	Btu per cu.ft.	Btu per lb.coal	
1161	1	60.87	5.98	25.78	2.43	5.03	618	3,235	131
	3	62.13	6.07	24.51	2.15	5.14	608	3,231	157
	6	64.01	5.07	23.79	1.60	5.53	600	3,180	157
	9	63.29	5.91	27.40	1.08	2.32	576	3,121	165
1166	1	59.38	6.49	30.08	1.42	2.63	603	3,133	638
	3	59.37	6.13	30.11	1.56	2.83	608	3,268	714
	6	59.09	6.45	30.97	0.92	2.57	601	3,221	707
	9	61.87	4.52	29.85	.75	2.96	596	3,189	828
1167A	1	63.91	4.31	28.81	1.30	1.67	583	2,956	561
	3	61.94	5.12	30.05	0.85	2.04	587	3,020	600
	6	61.98	5.15	30.08	.70	1.29	581	3,007	606
	9	61.91	4.85	30.94	.56	1.74	585	3,068	644

Table 6. - Composition of light oil, gallons per ton

Coal number	Void space, inches	Benzene	Toluene	m,p-xylene	o-xylene	Ethyl-benzene
1161	1	2.24	0.38	0.12	0.05	0.01
	3	2.65	.42	.14	.04	.006
	6	2.91	.40	.09	.01	.004
	9	2.89	.22	.04	.01	-
1166	1	2.77	.64	.13	.02	.004
	3	2.79	.55	.08	.02	.003
	6	3.13	.45	.05	.01	.001
	9	3.34	.42	.04	.01	.001
1167A	1	3.05	.06	.10	.02	.013
	3	3.05	.05	.07	.02	.003
	6	3.39	.04	.03	.01	.001
	9	3.30	.03	.03	.01	.001

Properties of Coke

The physical properties of the cokes were determined by standard methods of the American Society for Testing Materials (2). The tumbler indices, 1-inch stability and 1/4-inch hardness, are the only coke properties reported as these parameters are most commonly used in evaluating metallurgical coke.

Variations of free space had no effect on the coke yield. The only significant change in the coking properties was for coal 1166 in which the 1-inch stability index was progressively lowered from 33 for the 1-inch free space to 28 for the 9-inch free space. The stability and hardness indices for both coal blends remained essentially the same.

CONCLUSIONS

The yields of carbonization products are influenced by the rank of coal used and the temperature of carbonization. The primary decomposition is influenced by the rate of heating and the secondary decomposition by the time of contact of the vapors while in the hot retort and is dependent on the volume of free space per unit volume of charge.

The cracking of tar due to increased free space resulted in progressive increases in specific gravity, naphthalene yield, anthracene yield (except for the 9-inch free space test) and a reduction in tar acids, bases, and neutral oils.

Free space increases had no effect on the coke yield or coke properties except for the 1-inch tumbler stability for coal (1166) which was progressively lowered with increased free space.

The light oil yield was increased and reached a maximum at the 6-inch free space for the coal blends, and the 9-inch free space for the straight coal.

There was a progressive increase in gas yield, with the greatest variation of 500 cubic feet per ton of coal and the heat recovery for the longest exposure of gas in the retort was 112 Btu per pound of coal.

Increased free space above the coal charge during carbonization, permitted longer residence time of the vapors at a specific temperature and improved the quality of the byproducts. However, since coke is the major and most valuable product of coal carbonization, it would be economically infeasible to decrease the capacity of commercial ovens. In recognition of this, the Bureau of Mines is investigating the upgrading of volatile materials, in a separate cracking unit, outside of the coking furnace. Results of this investigation will be published in a subsequent report.

REFERENCES

1. American Society for Testing Materials. Bituminous Materials, Soils, Skid Resistance, Part II, March 1969, pp. 701-704.

2. American Society for Testing Materials, ASTM Standards on Coal and Coke, 1954, 155 pp.

3. Davis, J. D. and S. Auvil. High Temperature Carbonization of Coal. Ind. & Eng. Chem., vol. 27, April 1935, p. 459.

4. Porter, H. C. Improvement of Design of Coal Carbonization Equipment. Ind. & Eng. Chem., vol. 24, 1932, pp. 1363-1368.

5. Reynolds, D. A., and C. R. Holmes. Procedure and Apparatus for Determining Carbonizing Properties of American Coals by the Bureau of Mines-American Gas Association Method. BuMines Tech. Paper 685, 1946, 35 pp.

6. Staff, Division of Bituminous Coal. Comparative Evaluation of Coking Properties of Four Coals. BuMines Inf. Cir. 8010, 1961, 22 pp.

7. Walters, J. G., and G. W. Birge. Duplicability Studies of the BM-AGA Test Method and Correlation with Industrial Coking. BuMines Rept. of Inv. 5467, 1959, 16 pp.

8. Wolfson, D. E., G. W. Birge, and J. G. Walters. Comparison of Properties of Coke Produced by BM-AGA and Industrial Methods. BuMines Rept. of Inv. 6354, 1964, 19 pp.

9. Wolfson, D. E., and D. A. Reynolds. Yields and Properties of Gases From BM-AGA Carbonization Tests at 900°C. BuMines Tech. Paper 693, 1946, 12 pp.

LIGHT-INDUCED CHEMILUMINESCENCE IN DERIVATIVES OF COAL AND PETROLEUM

Raymond E. Markby, R. A. Friedel, Sidney Friedman, and Heinz W. Sternberg

Pittsburgh Coal Research Center, U. S. Bureau of Mines,
4800 Forbes Avenue, Pittsburgh, Pa. 15213

INTRODUCTION

In connection with work requiring the use of a liquid scintillation spectrometer for the determination of radioactive methyl groups introduced into coal, we discovered that solutions of alkylated coal exhibited chemiluminescence when exposed to light in the presence of air. We subsequently found that solutions of other products derived from coal and petroleum also exhibited chemiluminescence. In this paper we report our observations and suggest a mechanism for this light-induced chemiluminescence in products derived from coal and petroleum.

EXPERIMENTAL

Materials Investigated — The materials investigated are described in table 1.

TABLE 1. - Materials Tested

Material	Description
Coal tar I	High temperature coal tar from Pocahontas No. 3 (lvb) coal prepared in 1% yield by Bm-AGA method.[a/]
Coal tar II	Commercial high temperature coal tar.
Coal asphaltenes	Obtained by combining samples from several coal hydrogenation runs carried out at Pittsburgh Coal Research Center.
Methylated coal Ethylated coal Butylated coal	Prepared by reductive alkylation of Pocahontas No. 3 (lvb) vitrain.[b/]
Petrolenes I	Pentane soluble portion of straight run residual asphalt (Venezualean crude) 85/100.
Asphaltenes I	Pentane insoluble, benzene soluble portion (20%) of above asphalt.
Petrolenes II	Pentane soluble portion of straight run residual asphalt (Californian crude) 85/100.
Asphaltenes II	Pentane insoluble, benzene soluble portion (21%) of above asphalt.

a/ Technical Paper 685, U. S. Government Printing Office, Washington, D. C., 1946.
b/ H. W. Sternberg and C. L. Delle Donne, "Solvation and Reductive Alkylation of Coal via a Coal Anion Intermediate." Preprints of Papers presented at the Division of Fuel Chemistry, Atlantic City, N. J., September 8-13, 1968.

Apparatus — A tensor* lamp with a GE 1133 bulb (rated 32 candle power at 6 V. and 3.9 A.) was used as a light source and a liquid scintillation spectrometer, model 2101 by Packard Instruments Company was used to detect light emission. The quantum efficiency of the instrument was 16% at 3800 Å, 4% at 5500 Å, 1% at 6000 Å, and 0% at 6500 Å.

Procedure — One-tenth to 5 milligrams of the material dissolved in 20 ml. of toluene was placed in a 22 ml. counting vial provided with a screw cap. The vial was irradiated by a tensor lamp at a distance of 1 cm. between light bulb and wall of vial for a period of one minute. The vial was then placed in the cavity of the liquid scintillation spectrometer and counting was started 30 seconds after the irradiation had been completed. To obtain chemiluminescence decay curves, the intensity of light emission (in counts per 0.1 minute) was recorded at 30 second intervals.

RESULTS

Chemiluminescence Decay Rates — The count rate of a sample as determined by the liquid scintillation spectrometer is proportional to the intensity, I, of the emitted light. The decay of chemiluminescence intensity, I, with time was determined for the materials listed in table 1. In all cases straight line relationships were obtained when $I^{-1/2}$ was plotted vs. time. In all cases the straight line relationship held up to at least 85% completion. A typical chemiluminescence decay curve as obtained for butylated coal is shown in figure 1. The arrow marks 92% completion.

Spectral Region of Chemiluminescence — Qualitative information on the spectral region of the light emitted was obtained by wrapping the sample vial after irradiation in various Kodak Wratten Gelatin filters of known transmittance and recording the count rate. A zero count rate indicated complete absorption, a normal count rate no absorption. By this method we established that the light emitted during chemiluminescence was in the 4800-5200 Å region.

Wavelength of Irradiating Light — We were interested in determining whether irradiation with red light, i.e., light in the lower energy region of the visible spectrum is capable of inducing chemiluminescence. A solution of 10 mg. of Petrolenes I (see table 1) in 20 ml. toluene was irradiated for 1 minute with a red filter (transmission in the 6500 Å region) placed between tensor lamp and sample. The irradiated sample emitted light in the same spectral region as a sample irradiated with white light.

Intensity of Chemiluminescence — The chemiluminescence intensities of the various materials listed in table 1 were obtained by determining count rates after irradiation. The results are summarized in table 2.

The chemiluminescence of irradiated solutions can be detected by visual observation. A vial containing 20 mg. of petrolenes I in 20 ml. of toluene emits a greenish-blue light which is clearly visible to the dark-adapted eye. The intensity of the light emitted immediately after irradiation of this sample corresponded to about 10^6 counts per minute. The light remained visible for about 20 minutes after which time the count had dropped to approximately 2×10^4 counts per minute.

---

* Reference to a company or product name is made to facilitate understanding and does not imply endorsement by the U. S. Bureau of Mines.

TABLE 2. - Intensity of chemiluminescence in products derived from coal and petroleum

Material	Intensity, counts/min./mg.	Relative intensity
Coal tar I	1.6×10^3	1.0
Coal tar II	6.2×10^3	3.9
Coal asphaltenes	7.1×10^4	4.4×10
Methylated coal	3.8×10^6	2.4×10^3
Ethylated coal	3.8×10^5	2.4×10^2
Butylated coal	2.0×10^5	1.3×10^2
Petrolenes I	7.9×10^3	4.9
Petroleum asphaltenes I	9.0×10^3	5.6
Petrolenes II	4.3×10^4	2.7×10
Petroleum asphaltenes II	6.5×10^4	4.1×10

DISCUSSION

We believe that the light-induced chemiluminescence we observed involves photosensitized addition of oxygen to acene-type ring systems to form labile endoperoxides followed by decomposition of these endoperoxides with emission of light. This view is consistent with the experimental evidence and is based on the following considerations.

Moureau, Dufraisse and their co-workers[1] have shown that acene-type hydrocarbons such as anthracene react with oxygen under the influence of sunlight or artificial white light to form endoperoxides:

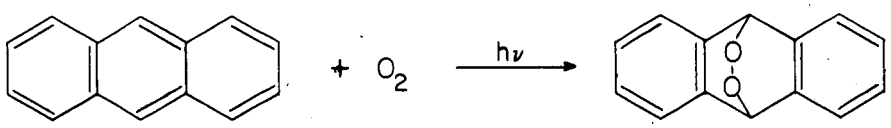

(1)

The mechanism[2] of this light-induced endoperoxide formation involves excitation of ground state triplet $O_2(^3\Sigma_g^-)$ to excited singlet $^1O_2$ ($^1\Delta_g$ or $^1\Sigma_g^+$) by a sensitizer S. The sensitizer ^1S_o absorbs light energy to give an excited singlet state ($^1S_1$) which is converted by intersystem crossing to a triplet state

$$^1S_o \xrightarrow{h\nu} {}^1S_1 \qquad (2)$$

$$^1S_1 \longrightarrow {}^3S_1 \qquad (3)$$

The sensitizer in its triplet state exchanges energy with triplet ground state oxygen to give singlet oxygen which adds to anthracene (A) to form the endoperoxide (AO_2):

$$^3S_1 + {}^3(O_2) \rightarrow {}^1S_o + {}^1(O_2) \qquad (4)$$

$$^1(O_2) + A \rightarrow AO_2 \qquad (5)$$

Decomposition of the acene-type endoperoxides formed in coal and petroleum derived products with emission of light

$$AO_2 \rightarrow A + O_2 + h\gamma \qquad (6)$$

explains the observed chemiluminescence. Rubrene endoperoxide, for example, decomposes at elevated temperature with emission of greenish-yellow light,[3] visible to the dark-adapted eye, to give oxygen and rubrene. On the basis of recent work[4,5] the emission of light observed during the decomposition of peroxides is attributed to transition of excited van der Waals type "double molecules" $[^1O_2 + {}^1O_2]$ to ground state oxygen $^3O_2$. Depending on the state of the $(^1O_2)_2$ double molecule, light of different wavelengths can be emitted. The transition $(^1\Delta_g + {}^1\Delta_g) \rightarrow 2\ {}^3\Sigma_g^-$ produces light of 6335 Å (orange-red), $(^1\Delta_g + {}^1\Sigma_g^+) \rightarrow 2\ {}^3\Sigma_g^-$ light of 4780 Å (blue) and $(^1\Sigma_g^+ + {}^1\Sigma_g^+) \rightarrow 2\ {}^3\Sigma_g^-$ light of 3800 Å (ultraviolet) wavelength. The light observed in our experiments was in the 5000 Å region, corresponding to a $(^1\Delta_g + {}^1\Sigma_g^+) \rightarrow 2\ {}^3\Sigma_g^-$ transition.

The formation of an excited double molecule, $(^1O_2)_2$, resulting from the interaction of two endoperoxide molecules, AO_2

$$2AO_2 \xrightarrow{k} 2A + (^1O_2)_2 \qquad \text{Rate} = k[AO_2]^2 \qquad (6)$$

followed by rapid transition of $(^1O_2)_2$ to ground state with emission of light

$$(^1O_2)_2 \rightarrow 2(^3O_2) + h\gamma \qquad \text{Rate} = I \qquad (7)$$

is consistent with the observed decay rate, i.e., with a straight line relationship between $1/I^{1/2}$ and time. According to (6) and (7), the rate of light emission, I, is proportional to the $[AO_2]^2$ concentration and consequently $I^{1/2}$ may be substituted for the $[AO_2]$ concentration. In the integrated rate equation

$$1/C = 1/C_o + kt \qquad (6a)$$

the instantaneous concentration c is replaced by $I^{1/2}$ and the initial concentration by $I_o^{1/2}$. This leads to the observed straight line relationship between $1/I^{1/2}$ and time

$$1/I^{1/2} = 1/I_o^{1/2} + kt. \qquad (6b)$$

According to equation (5), singlet oxygen (in either the $^1\Delta_g$ or $^1\Sigma_g^+$ state) is required for the formation of endoperoxide, a fact which determines the minimum of irradiating energy required to excite ground state triplet oxygen to excited singlet oxygen. The excitation energies for ground state oxygen ($^3\Sigma_g^-$) to singlet oxygen ($^1\Delta_g$) is 22.5 kcal (12,700 Å) and to singlet oxygen ($^1\Sigma_g^+$) is 37.5 kcal (7620 Å). Consequently, light in the red region (44 kcal, 6500 Å), should contain sufficient energy for the excitation of ground state triplet to excited singlet oxygen, provided that sensitizers are present capable of absorbing this energy (equation 2) and of intersystem crossing (equation 3) to a triplet level whose energy lies above the energy (22.5 resp. 37.5 kcal) required for the $^3O_2$ to $^1O_2$ excitation. That sensitizers meeting these requirements are present in products derived from coal and petroleum follows from the observation that irradiating light in the red region (6500 Å) produces chemiluminescence in the blue-green (5000 Å) region. The formation of endoperoxide by irradiation in the presence of a sensitizer (methylene blue) absorbing in the red (6400 Å) region was recently demonstrated[6] in the case of rubrene. That singlet oxygen is involved in our light-induced chemiluminescence reaction is supported by the fact that addition of an excess of tetramethylethylene (TME) prior to irradiation reduces the chemiluminescence intensity by 98%. TME was shown to act as a captor for singlet oxygen and as an inhibitor in the photosensitized oxidation of rubrene.[6]

Normal acene endoperoxides, containing a 9,10 bridge, are stable at room temperature, while the endoperoxides observed in coal and petroleum derivatives decompose with chemiluminescence at room temperature. This behavior is similar to that reported for the 1,4-endoperoxides formed by certain 1,4-dimethoxyanthracenes,[7] and suggests that the chemiluminescent endoperoxides in coal and petroleum derivatives are also of the 1,4 type and consequently contain activating substituents in the 1,4 positions. These substituents may be ethers present in the starting material, or in the case of alkylated coal, formed from OH groups during the alkylation. Moreover, the substituents undoubtedly need not be ethers, but probably could be any sufficiently electron-releasing groups, such as alkyl groups. This effect is illustrated by the 100-fold greater rate of formation of endoperoxide from 9,10-dimethylanthracene and singlet oxygen than from anthracene and singlet oxygen.[8] The activating effect of alkyl groups is undoubtedly the reason why alkylated coal exhibits chemiluminescence which is 2 to 3 orders of magnitude higher in intensity than that of the other materials examined (table 2).

CONCLUSIONS

Solutions of coal tar, coal asphaltenes and alkylated coal as well as petroleum asphalts exhibit chemiluminescence when exposed to oxygen and light. This chemiluminescence is believed to be due to decomposition of endoperoxides formed by photooxidation of acene-type compounds present in products derived from coal and petroleum.

REFERENCES

1. For a comprehensive review of their work, see W. Bergmann and M. J. McLean, Chem. Rev. 28, 367 (1941) and Yn. A. Arbuzov, Russian Chemical Reviews 34, 558 (1965).

2. Foote, C. S., Wexler, S., Ando, W., and Higgins, R., J. Am. Chem. Soc., 90, 975 (1968).

3. Moureau, C., Dufraisse, C., and Butler, C. L., Compt. Rend., 183, 101 (1926).

4. Khan, A. U. and Kasha, M., J. Am. Chem. Soc., 88, 1574 (1966).

5. Stauff, J. and Schmidkunz, H., Z. Physik. Chem. (Frankfurt), 35, 295 (1962).

6. Wilson, T., J. Am. Chem. Soc., 88, 2898 (1966).

7. Dufraisse, C., Rigaudy, J., Basselier, J., and Cuong, N. K., Compt. Rend., 260, 5031 (1965).

8. Corey, E. J. and Taylor, W. C., J. Am. Chem. Soc., 86, 3881 (1964).

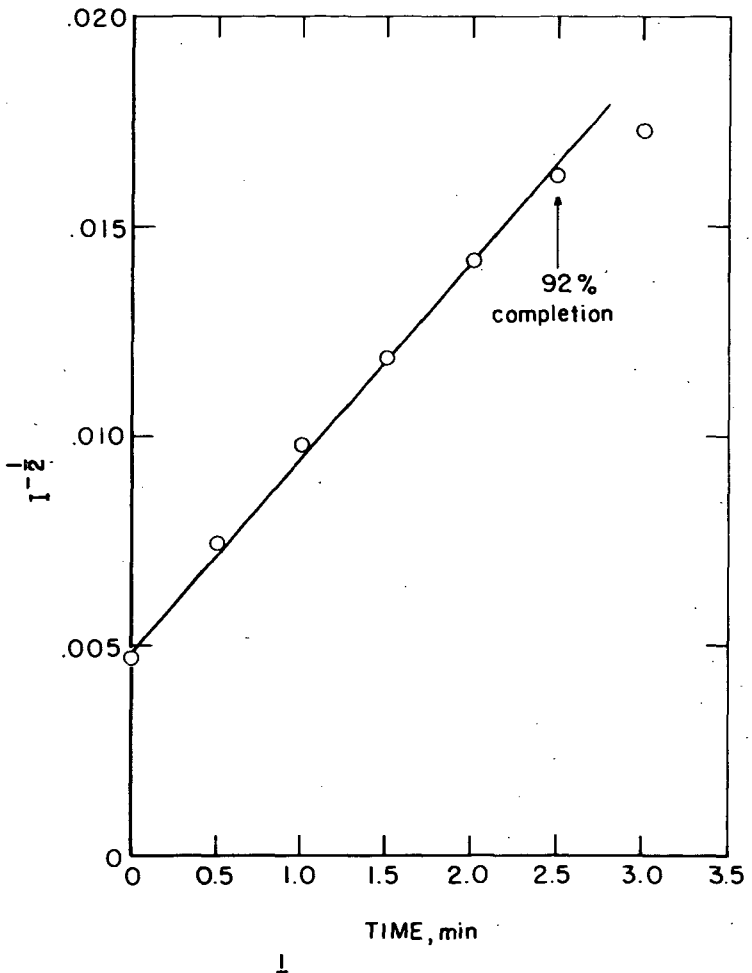

Figure 1- $I^{-\frac{1}{2}}$ vs time curve of chemiluminescence decay for butylated coal. L-11223